DEVELOPMENT OF A PANCREATIC SUBSTITUTE BASED ON GENETICALLY ENGINEERED INTESTINAL ENDOCRINE CELLS

A Dissertation
Presented to
The Academic Faculty

By

Aubrey R. Tiernan

In Partial Fulfillment
of the Requirements for the Degree
Doctor of Philosophy in the
School of Chemical & Biomolecular Engineering

Georgia Institute of Technology

August, 2014

DEVELOPMENT OF A PANCREATIC SUBSTITUTE BASED ON GENETICALLY ENGINEERED INTESTINAL ENDOCRINE CELLS

Approved by:

Dr. Athanassios Sambanis, Advisor
School of Chemical & Biomolecular Engineering
Georgia Institute of Technology

Dr. Julie Champion
School of Chemical & Biomolecular Engineering
Georgia Institute of Technology

Dr. William Koros
School of Chemical & Biomolecular Engineering
Georgia Institute of Technology

Dr. Joe LeDoux
Department of Biomedical Engineering
Georgia Institute of Technology and Emory University

Dr. Peter Thulé
School of Medicine
Emory University

Date Approved: 23rd April 2014

ACKNOWLEDGMENTS

I would first like to acknowledge my advisor, Dr. Athanassios Sambanis, who welcomed me into his laboratory and helped me to become the researcher I am today. I will always be grateful for his optimism and support throughout my Ph.D. experience. I have learned so much from him, especially in designing experiments and writing scientifically. I would also like to wholeheartedly thank Dr. Peter Thulé who has been like a second advisor to me and I am so grateful for his warmth, guidance, and time devoted to helpful discussions. My sincerest thanks also go to Drs. Susan Safley, Julie Champion, Andrés García, Joe Le Doux, Bill Koros, and Cherie Stabler for their constructive feedback, cordiality, and time dedicated toward helping me.

I am so lucky to have had such a wonderful and supportive group in the Sambanis Lab. I would especially like to thank Dr. Kiranmai Durvasula for being such a friendly and patient mentor, Dr. Fernie Goh for her laughter, Dr. Hajira Ahmad for being the best lab encyclopedia, and Stephanie Duncanson for her continuous support and friendship. In addition, I am grateful to Dr. Alison Lawson and Saif Al-Mamari who offered helpful discussions while I was troubleshooting my experiments. I would very much like to thank my two undergraduates, José Antonio Vásquez Porto-Viso and Derrius Anderson, who were the most motivated people I have had the pleasure of mentoring and who significantly contributed to research in the lab. José set up the PCR protocol for others to use in the lab and Derrius helped me investigate effects of histone deacetylase inhibitors.

I must thank the labs of Drs. Nerem, Platt, and Kemp who allowed me to share their equipment for my PCR studies and helped me with troubleshooting my experiments. I am

extremely grateful for the core facilities made available to me in the Institute for Bioengineering & Bioscience (IBB) building. I would especially like to thank Lina Herrera Estrada in Dr. Champion's lab who has given me advice and training in various gene and protein techniques. I am also grateful to Dr. Laura O'Farrell for her training in animal care and use which were critical to my preclinical animal studies.

Finally, my warmest thanks go to my family and friends who have made this experience one of the best in my life. I would generally like to acknowledge the incoming Classes of 2008 and 2009 for making the first year at Georgia Tech so fun and welcoming. More specifically, I am so grateful for my roommates of the last five years, Steph Didas and Katie Vermeersch. We have been through it all together and they have become like family to me. Lastly, but most importantly, I lovingly acknowledge my mom and dad for their unwavering love, guidance, and support. I have realized, as I have grown, that my parents are my true role models. They have taught me the importance of hard work, having a sense of humor, maintaining my mental and physical health, keeping my family close, and valuing myself. Without their presence in my life, I would not have made it this far in the world.

This work was supported by a grant from the National Institutes of Health (R01 DK076801), the GAANN fellowship from the U.S. Department of Education through the Center for Drug Discovery, Development, and Delivery (CD4), the Undergraduate Petit Scholar Program Scholarship, and the Shell Outstanding Teaching Assistant Fellowship. I would also like to thank the Chemical & Biomolecular Engineering Department at Georgia Tech for awarding me the President's Fellowship for my first four years.

TABLE OF CONTENTS

LIST OF TABLES

LIST OF FIGURES

LIST OF SCHEMATICS

LIST OF ABBREVIATIONS

AAV	Adeno-Associated Virus
ACTB	Beta-Actin
APA	Alginate-Poly-L-Lysine-Alginate
BAP	Bioartificial Pancreas
BDNF	Brain-Derived Neurotrophic Factor
BLI	Bioluminescence Imaging
CDC	Center for Disease Control
CMV	Cytomegalovirus
CSII	Continuous Subcutaneous Insulin Infusion
DMEM	Dulbecco's Modified Eagle's Medium
DMSO	Dimethyl Sulfoxide
DPBS	Dulbecco's Phosphate-Buffered Solution
EINS	GLUTag-EINS
FACS	Fluorescence Activated Cell Sorting
Fluc	GLUTag-EINS-Fluc
G	Guluronic Acid
GFP	Green Fluorescence Protein
GIP	Gastric Inhibitory Peptide
GLP-1	Glucagon-Like Peptide-1
H&E	Hematoxylin/eosin
HDAC	Histone Deacetylase

HDACi	Histone Deacetylase Inhibitor
i.p.	Intraperitoneal
i.v.	Intravenous
IACUC	Institutional Animal Care and Use Committee
IDD	Insulin Dependent Diabetes
IRES	Internal Ribosomal Entry Site
ISR	Insulin Secretion Rate
IVIS	In Vivo Imaging System
M	Mannuronic Acid
MH	Meat Hydrolysate
MOI	Multiplicity of Infection
NMR	Nuclear Magnetic Resonance
NOD	Non-Obese Diabetic
PCR	Polymerase Chain Reaction
PTFE	Polytetrafluroethylene
RER	Rough Endoplasmic Reticulum
RFU	Relative Fluorescence Unit
RIA	Radioimmunoassay
ROI	Region Of Interest
RSP	Regulated Secretory Pathway
SI	Stimulation Index
STZ	Streptozotocin
T1D	Type 1 Diabetes

T2D	Type 2 Diabetes
TEPS	Tissue Engineered Pancreatic Substitute
TGN	Trans-Golgi Network
TSA	Trichostatin A
VPA	Valproic Acid

SUMMARY

Cell-based insulin therapies can potentially improve glycemic regulation in insulin dependent diabetes patients and thus help reduce secondary complications. The long-term goal of our work is to engineer autologous insulin-secreting intestinal endocrine cells as a non-β cell approach to alleviate donor cell shortage and immune rejection issues associated with islet transplantation. These cells have been chosen for their endogenous similarity to β cells, but generating cell constructs with sufficient insulin secretion for therapeutic effect has proven challenging. Previous work in our lab showed that a tissue engineered pancreatic substitute (TEPS) based on an engineered insulin-secreting L cell line, GLUTag-INS, was insufficient in affecting blood glucose levels in streptozotocin-induced diabetic mice, but promising since human insulin was detected in the blood. The objective of this project was therefore to fabricate an improved TEPS based on GLUTag-INS cells and evaluate its suitability as a standalone diabetes therapy. To achieve this objective, the following specific aims were (1) to investigate gene incorporation as a strategy to enhance recombinant insulin secretion from GLUTag-INS cells; (2) to develop and characterize a TEPS *in vitro* based on a microcapsule system containing improved GLUTag-INS cells with bioluminescence monitoring capability; and (3) to assess therapeutic efficacy of the graft in a diabetic, immune-competent mouse model and use bioluminescence monitoring to elucidate *in vivo* transplant behavior. This thesis therefore reports on the progression of studies from the genetic and molecular levels for improved insulin secretion per-cell, to the tissue level for enhanced secretion per-graft, and lastly to the preclinical level for therapeutic assessment in a diabetic mouse model.

CHAPTER 1: INTRODUCTION

In 2011, the Center for Disease Control (CDC) reported that 25.8 million people in the United States alone are affected with Diabetes, and 6.7 million of them are dependent on insulin [1]. To prevent long-term complications in patients with insulin dependent diabetes (IDD), blood glucose levels must be tightly regulated with multiple daily insulin injections or continuous subcutaneous insulin infusion (CSII) by pump [2]. Due to the numerous variables that affect blood glucose levels, this task is far from trivial and requires significant time from the patient. Even with diligent monitoring and insulin administration, many patients fail to achieve recommended control of their blood sugars. An IDD patient's quality of life is burdened with dosing calculations, dietary and exercise restrictions, painful needles, and long-term complications. There is a clear need for a diabetes treatment that improves glycemic regulation without further burdening patients, to reduce morbidity and improve quality of life.

Cell-based treatments can potentially address these needs by allowing a one-time administration at the hospital requiring no work from the patient thereafter and providing a perpetual insulin reservoir regulated by physiological cues, similar to blood glucose regulation in a healthy body. Although this approach is indeed promising, there are challenges that must be resolved before a cell-based insulin therapy can become reality for diabetic patients. The most clinically successful cell therapy thus far is islet transplantation, but this approach is limited by human islet donor scarcity and immune rejection resulting

in limited durability [3]. These hurdles have motivated researchers to explore the possibility of using alternative cell sources.

Substantial efforts have been put forth to use pig islets as the donor cell source to alleviate availability problems [4]. Encapsulation of pig islets within an inert biomaterial for xenogeneic transplantation is a strategy that, at least partially, provides protection from immune rejection [5]. Unfortunately, encapsulated pig islets have been shown in multiple cases to cause an immune response, in addition to rarely restoring normoglycemia, in higher order animals including humans [6-11]. They have, however, contributed to improving blood glucose regulation, if only for a short period of time.

A non-β cell source can potentially address both donor cell availability and immune rejection issues by allowing the cell source to be the diabetic patient's own healthy cells. The overarching goal of this approach is to engineer a fraction of the patient's cells into meal or glucose-responsive insulin secretors for transplantation back into the same patient. The most attractive non-β cell candidates are cells that already possess key β cell characteristics and therefore require the least genetic manipulation. There are three enteroendocrine cell types that are inherently glucose or meal-responsive, possess a secretory mechanism like β cells, and express the prohormone convertases necessary for proinsulin to insulin processing: gastric G cells [12], intestinal L cells, and intestinal K cells [13]. The question is whether any of these cells really could be engineered for insulin production and behave similarly to β cells.

The answer to this question is yes; initial proof-of-concept studies showed that mice transgenic for human insulin-secreting K cells were resistant to streptozotocin (STZ)-induced diabetes [12]. Similarly, insulin-secreting G cells significantly reduced mouse

blood glucose levels [14]. However, since this transgenics approach is not viable for humans, the engineering of enteroendocrine cell lines became more popular for preclinical evaluation. Two groups reported therapeutic efficacy of K cell lines that were stably transfected with the insulin gene, selected for the highest insulin-secreting clones, and transplanted in diabetic mice [15, 16]. The problem with this approach is that it allowed for tumor formation due to uncontrollable cell growth and resulted in an insulin overload, i.e. chronic hypoglycemia, generally leading to death. Additionally, mice with no immune system were used as the preclinical model to avoid transplant rejection. Although these studies showed promise for an enteroendocrine cell therapy approach, they lacked clinical relevance. **The question therefore remains whether a practical number of transplanted engineered enteroendocrine cells can safely alleviate diabetes in an immune-competent animal model.**

Encapsulating cells to control cell growth and provide immune protection for transplanting in immune competent diabetic mice began to address these issues. Unniappan et al. found that microencapsulated insulin-producing K cells were unable to control blood sugars until a drug-inducible element was incorporated into the insulin transgene [17]. Alternatively, Bara et al. seeded human insulin-secreting L cells (GLUTag-INS) in a macrocapsule device for transplantation [18-20]. Human insulin was detected in mouse plasma, but blood glucose levels were unaffected. Insufficient insulin secretion and macrocapsule limitations were two likely barriers that prevented these systems from serving as standalone diabetes treatments. Additionally, a lack of understanding regarding what happened to the graft in real-time limited the ability to clarify when or why failure occurred.

The **overall objective** of this thesis was to fabricate an improved tissue engineered pancreatic substitute (TEPS) based on enteroendocrine cells and evaluate its suitability as a standalone diabetes therapy. Improvements were three-fold: 1) insulin secretion enhancement of the previously developed GLUTag-INS cell line, 2) bioluminescence incorporation for direct, minimally invasive survival monitoring, and 3) alginate microencapsulation for higher overall insulin output per unit graft volume relative to the macrocapsule previously developed [19]. The following **Specific Aims** were completed to build the improved TEPS and transfer this project from the stage of development and characterization to preclinical therapeutic efficacy evaluation:

Specific Aim 1: To investigate gene incorporation as a strategy to enhance recombinant insulin secretion from GLUTag-INS cells.

Specific Aim 2: To develop and characterize a tissue engineered pancreatic substitute *in vitro* based on a microcapsule system containing improved GLUTag-INS cells with bioluminescence monitoring capability.

Specific Aim 3: To assess therapeutic efficacy of the graft in a diabetic, immune-competent mouse model and use bioluminescence monitoring to elucidate *in vivo* transplant behavior.

Per-cell secretion improvements began at the genetic and molecular levels and are covered in CHAPTER 3, with a focus on identifying limiting steps in the L cell regulated secretory pathway (RSP) and developing novel methods for enhancing insulin secretion output per cell. A novel enhancement method was developed after studying the short and

long-term effects of additional human insulin transgene incorporation via lentiviral transduction and histone deacetylase inhibitor (HDACi) treatment on recombinant insulin secretion output per cell. To identify limiting steps in the RSP, this enhancement method was also used as a tool to alter intracellular activity and measure effects such as insulin mRNA, intracellular levels of proinsulin and insulin, and secreted levels of proinsulin and insulin. Increasing knowledge of these cells will better guide the field in pursuing the most feasible options for an enteroendocrine cell-based insulin therapy.

Another limitation of the previous TEPS was its agarose disc configuration which resulted in a dramatic drop in the apparent insulin secretion rate per cell relative to secretion from unencapsulated cells grown on tissue culture plastic. Additionally, cell loading densities were limited and *in vivo* breakage may have caused the observed immune response. Alginate microcapsules have been used extensively in islet transplantation, appearing to have good diffusional capacity, to allow for high cell loading densities, and to better evade the immune system [21]. However, the application of this method to intestinal endocrine cells has been challenging, as demonstrated by Unniappan et al., and it is important for researchers to better identify key factors that influence graft survival *in vivo*. The effects of luciferase lentiviral transduction and alginate microencapsulation on the enhanced cell line developed in CHAPTER 3 are reported in CHAPTER 4. Insulin secretion output per unit graft volume and real-time monitoring capabilities were temporally evaluated, and therapeutic cell numbers were estimated to set the stage for therapeutic efficacy studies covered in CHAPTER 5.

After making significant improvements to the TEPS in CHAPTERS 3 and 4, it was necessary to characterize *in vivo* bioluminescence and evaluate therapeutic efficacy in a

preclinical animal model, as reported in CHAPTER 5. The STZ-induced immune-competent diabetic mouse model was chosen for preclinical animal studies. As previously mentioned, the immune-competent, versus incompetent, mouse is more clinically relevant because it allows for realistic testing of the immune protective effects of the alginate microcapsule configuration. This chapter reports on the blood glucose levels, exogenous insulin administration, body weight trends, and bioluminescence signals for 17 days after intraperitoneal injection of the TEPS into diabetic mice. TEPS were retrieved on day 17 for live/dead, histology, metabolic activity, and insulin secretion measurements and analyses.

Finally, CHAPTER 6 summarizes the conclusions drawn from these studies and discusses the practicality of using a non-β cell TEPS as a standalone insulin therapy for diabetes. Additionally, potential future research directions are suggested in the context of supplemental and alternative methods that are the most promising in accelerating the development of a clinically acceptable cell-based insulin therapy.

CHAPTER 2: BACKGROUND

2.1 Diabetes

Diabetes is a group of chronic metabolic diseases characterized by casual blood glucose concentrations above 200 mg/dL due to the loss or impairment of insulin-producing β cells. The long-term impact of the disease is the occurrence of complications such as heart disease, stroke, hypertension, blindness, kidney disease, and nervous system disease [1]. The terms Type 1 and Type 2 refer to two genetically distinct forms of diabetes [22]. Type 1 diabetes (T1D) is considered an autoimmune disease in which changes in certain immune regulatory genes cause T-cell mediated destruction of β cells [23, 24]. On the other hand, lifestyle as well as genetic variations are believed to play roles in the progression of Type 2 diabetes (T2D), causing a significant decline in β cell mass and function [25]. Although insulin resistance is an important factor in T2D, recent reports have shown that β cell dysfunction is the necessary and sufficient cause [26-28].

Diabetes is a major public health issue and the most frequent endocrine disease in industrialized countries [29].The most recent report from the Center for Disease Control (CDC) states that approximately 25.8 million people were affected with diabetes in the United States in 2011 and as of 2007, the economic burden totaled $174 billion. This burden was the result of costs from diabetes management, treatment of secondary complications, and subsequent productivity loss [30]. With the prevalence of diabetes doubling every ten years and an estimated 250 million people afflicted worldwide, better

therapies need to be developed to improve patient quality of life and reduce healthcare costs associated with the disease.

2.2 Insulin and β cells

Insulin is a 5.8 kDa peptide hormone that circulates through blood vessels to instruct the body's cells to absorb glucose and consequently reduce glucose concentrations in the blood. Insulin is exclusively produced by endocrine β cells that make up 65-80% of the islets of Langerhans which reside in the pancreas. Islets are strategically connected to the vasculature and receive ten times more blood than exocrine cells of the pancreas to achieve high nutrient sensitivity. In β cells, the hormone is first synthesized as preproinsulin so it can pass to the endoplasmic reticulum (ER) where the signal sequence is proteolytically removed to form proinsulin. Proinsulin is a polypeptide that consists of the A, B, and C chains, in the order B-C-A, as depicted in Figure 2.1. The C chain is a peptide that connects the A and B peptides to promote proper folding and formation of A-B and intra-chain A disulfide bonds in the rough ER (RER).

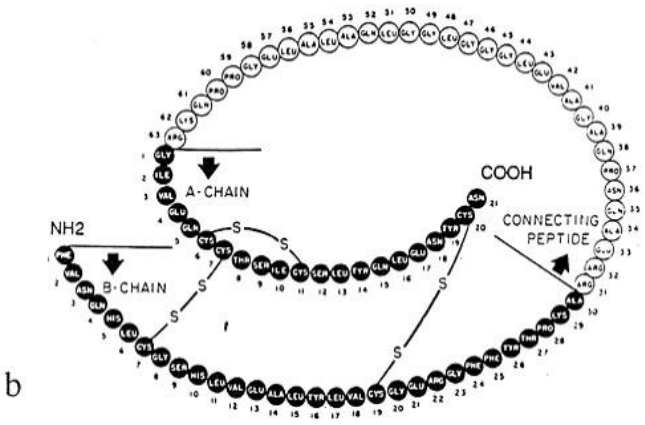

Figure 2.1: Proinsulin hormone structure. Illustration by [31].

From there, proinsulin follows a regulated secretory pathway (RSP) depicted and described in Figure 2.2. In brief, proinsulin gets shuttled via vesicles from the RER to the trans-golgi network (TGN) where the hormone aggregates are eventually packaged into clathrin-coated immature secretory granules for controlled release. Vesicles are also packaged with prohormone convertases PC1/3 and 2 for C-peptide cleavage to form active insulin within the granules. Insulin-containing, mature secretory granules are stored within the cell and fuse with the plasma membrane in response to extracellular glucose stimuli for insulin release. Constitutive vesicles, on the other hand, are immediately shuttled to the plasma membrane for fusion and release. β cells can control proinsulin synthesis rates at the transcriptional and translational levels [32], with insulin synthesis and release corresponding to increases in blood glucose concentrations [33].

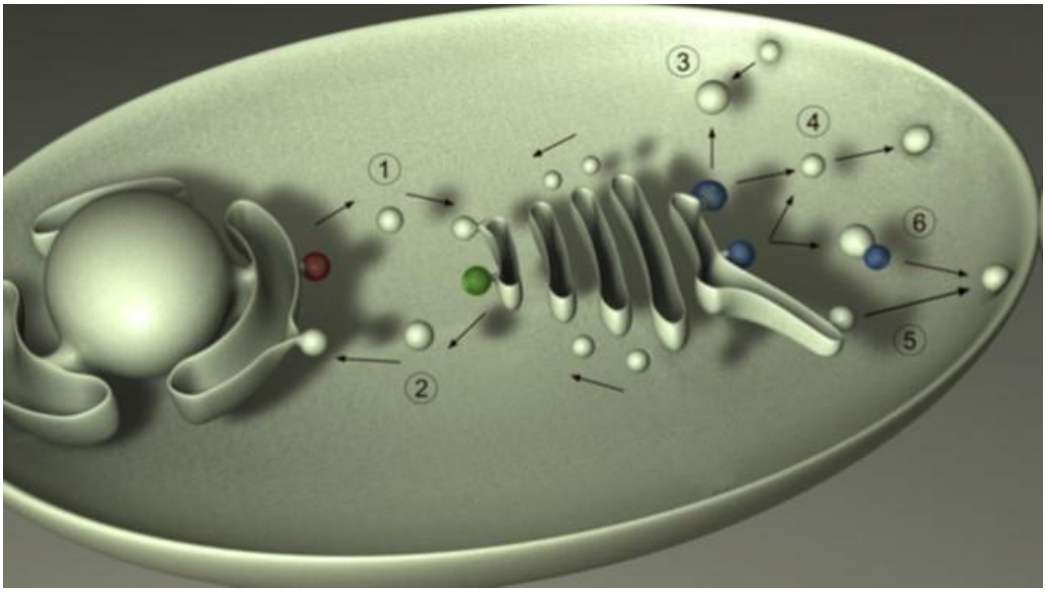

Figure 2.2: The general regulated secretory pathway (RSP). After synthesis, secretory peptides are packed into vesicles (red) derived from the ER membrane. These vesicles are directed to the most-trans cisternae of the Golgi complex. (2) Protein sorting receptors and ER-resident proteins mistakenly directed here are recycled back to the ER within vesicles (green). Once in the trans-golgi network (TGN), proteins are sorted in specific subdomains of this compartment. (3) Lysosomal hydrolytic enzymes are packed within clathrin-coated vesicles (blue) that are transported to and fuse with late endosomes. (4) Other TGN-derived clathrin-coated vesicles are loaded with secretory peptides (immature secretory granules), which undergo further processing and aggregation to form mature secretory granules. Upon extracellular stimulation, these granules fuse with the plasma membrane and release their content in a process referred to as regulated secretion. (5) Peptides packaged within uncoated vesicles are directed towards the cell surface in a constitutive manner (constitutive secretory pathway). (6) Alternatively, it has been proposed the existence of intermediate compartments in which regulated and constitutive secretion diverge based on the capacity of secretory proteins to sort by aggregation. In this case, constitutive secretory proteins would be packed within clathrin-coated vesicles in a process named as constitutive-like secretion. Illustration and modified figure description were taken from [34].

It was first demonstrated by Curry et al. that β cells secrete insulin in a biphasic manner [35]: stimulated (after a meal; postprandial) and basal (after the meal is absorbed; postabsorptive) phases. The first stimulated phase of insulin release, as depicted in Figure 2.3, is characterized by a burst of insulin that occurs within 5-10 minutes after a glucose

load and is followed by the second basal phase of prolonged insulin release at elevated concentrations to bring blood glucose levels back within normal range (70-140 mg/dL).

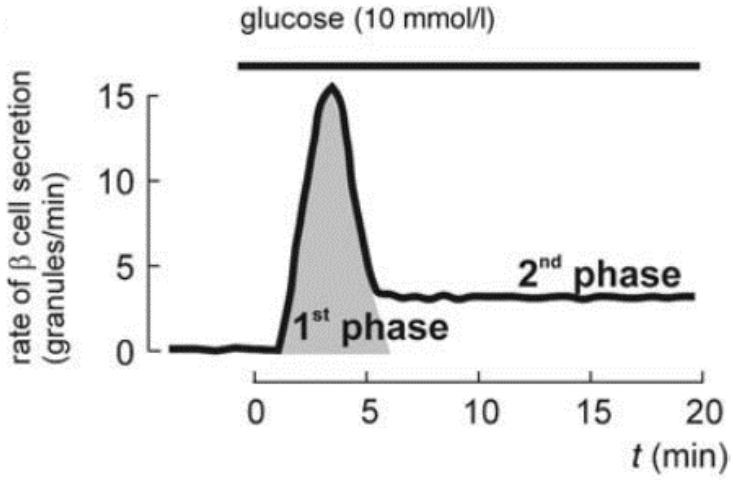

Figure 2.3: Biphasic insulin release from mouse islets subjected to 10 mM glucose. This figure was published in [36].

2.3 Diabetes Treatment Options

T2D patients who have sufficient β cell mass can control their condition with healthy eating and exercise. As β cell mass diminishes, however, patients may need oral medications and/or exogenous insulin to meet target blood glucose levels. On the other hand, exogenous insulin therapy is the only option for T1D patients as they cannot produce insulin endogenously and are therefore also referred to as insulin-dependent diabetes (IDD) patients.

In 1993, The Diabetes Control and Complications Trial demonstrated that intensive insulin therapy improved glycemic regulation and dramatically reduced the frequency and

severity of complications in T1D patients [2]. Since then, novel recombinant human insulins have been developed commercially to better mimic the first and second phases of β cell secretion through the preparation of rapid and long-acting insulin formulations [37]. However, even with intensive therapy, the pharmacokinetics of this approach are limited; the best rapid-acting insulin takes approximately 30 minutes to peak in the blood after subcutaneous administration while a higher peak after just 5 minutes is observed after endogenous β cell secretion. Figure 2.4 is representative of the relative pharmacokinetic differences between various insulin formulations and endogenous secretion.

Regardless of significant improvements in pharmacokinetics, insulin delivery via daily discrete needle injections or continuous subcutaneous insulin infusion (CSII) by pump [38] could never match the precise glucose-sensitive insulin release provided by β cells working at all times. The current insulin therapy approach is therefore limited in its ability to tightly regulate blood glucose levels and intensive application merely delays rather than prevents morbidity and mortality in T1D patients. Al-Tabakha and Arida extensively reviewed the challenges of current (syringes, CSII, jet injectors, and pens) and future (inhalers, mouth sprays, pills, and patches) insulin delivery systems in which they concluded that the ultimate treatment of T1D is likely a cell-based insulin therapy [39].

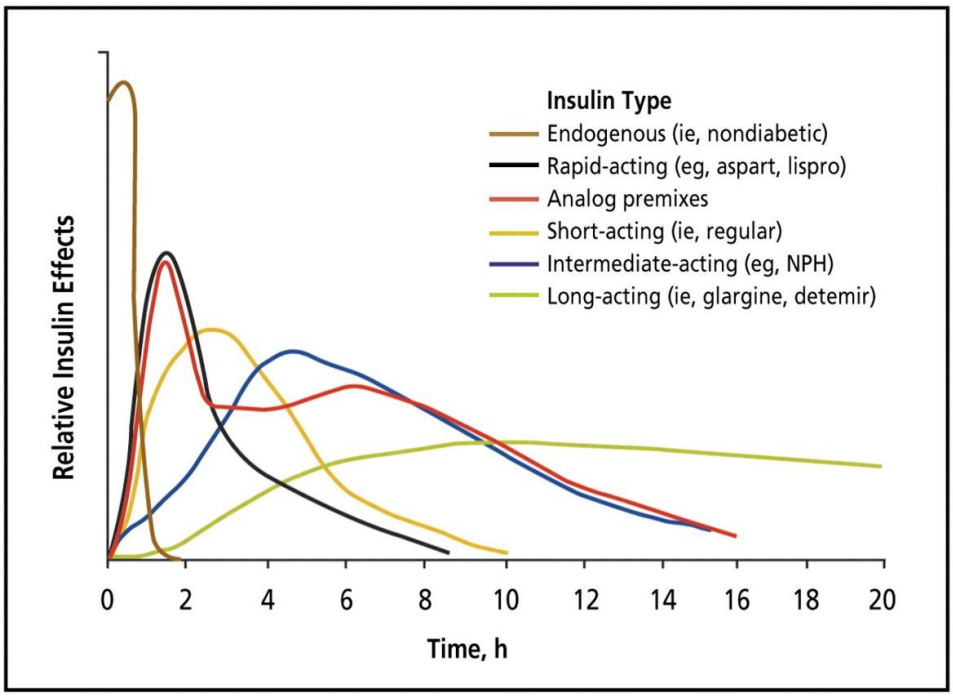

Figure 2.4: Pharmacokinetics of various rapid and long-acting insulin formulations in the blood after subcutaneous injection compared to endogenous, or non-diabetic, insulin secretion kinetics. This figure was published in [40].

2.4 Cell-Based Insulin Therapy

Using cells and encapsulated cells as therapeutic devices for insulin delivery is promising in providing tight and continuous physiologic blood glucose regulation as an alternative to the discrete, daily insulin injection or infusion therapies that are currently used. Such an approach would also minimize patient interaction and thus dramatically improve quality of life. The term cell-based therapy encompasses a broad area of research including whole pancreas or islet transplantation, engineered β cell lines, stem cell differentiation into β-like cells, *in vivo* gene therapy, and genetic engineering of isolated autologous non-β cells (Figure 2.5).

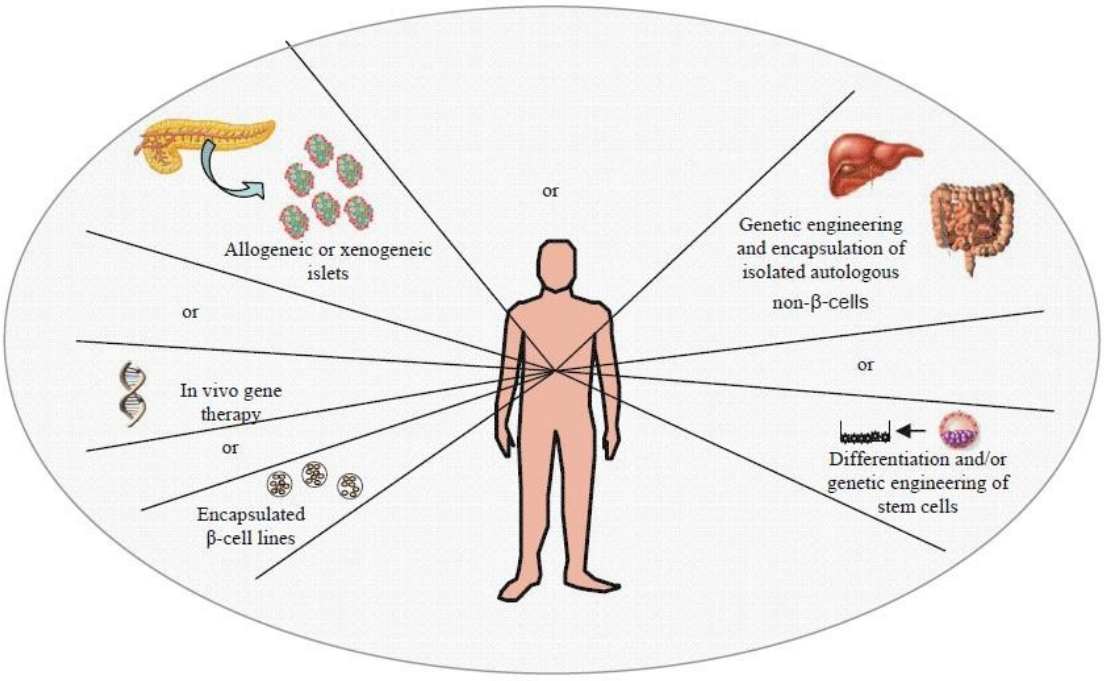

Figure 2.5: Cell-based therapy research avenues for IDD treatment (illustration by [41]).

2.4.1 Islet Transplantation and β Cell Lines

2.4.1.1 Allogeneic Islet Transplantation

Compared to whole pancreas transplantation, islet transplantation (Figure 2.6) is a less invasive procedure and results in a shorter hospital stay with lower morbidity [42, 43]. Both procedures are reserved only for patients with severe cases of T1D due to cadaveric islet donor shortage, graft failure in the long-term, and the need for lifelong immunosuppressive treatment. Immunosuppression drugs increase patient susceptibility to opportunistic infections and incidence of malignancy; adverse effects of these drugs toward the transplanted graft itself have also been observed [44-46].

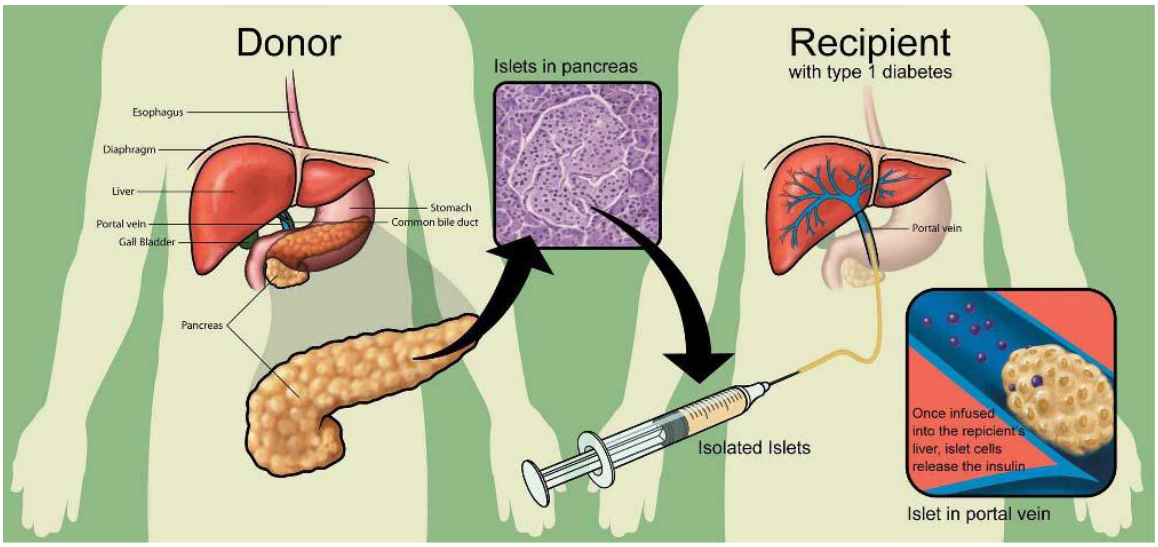

Figure 2.6: Process of islet transplantation. Islets are isolated and purified from a cadaveric donor and later infused into the portal vein of the diabetic recipient. Illustration by [47].

In 2000, the Edmonton Protocol was established with an improved immunosuppressive regimen [48] that resulted in an increase from 8 to 44% patients with insulin independence one year after transplantation [49]. However, 76% already required insulin again at two years and most returned to insulin dependence by the fifth year. Areas for improvement in allogeneic islet transplantation are outlined in [50] as enhancing the quantity and quality of the pre-transplant material and prolonging post-transplant graft survival.

In an effort to improve the quantity and quality of pre-transplant material, researchers aim to improve the islet isolation procedure by making gentler enzyme cocktails that yield more intact islets, minimizing islet culture time pre-transplant, and optimizing purification methods [51]. On the side of improving post-transplant islet survival, researchers are either trying to come up with less toxic immunosuppressive

regimens [52] or enhance immune isolation technologies to obviate the need for immunosuppression drugs [53].

2.4.1.2 Xenogeneic Islet Transplantation

In an effort to address the human islet supply issue, pig islets are being investigated as an unlimited, alternative cell source due to the close similarity in insulin and secretion kinetics between pig and human islets [54, 55]. To use this xenogeneic approach clinically requires encapsulation for partial immune protection [56] and has shown some promise in large animal models and humans, but the rate of insulin independence is highly variable and short-lasting [6-11]. There is also concern of the possibility of transmitting porcine endogenous retroviruses (PERVs) to humans after transplantation, which some studies have demonstrated as possible [57, 58] and others as impossible [59-61]. One of the suspected challenges to the success of this approach may be in evading the host inflammatory response after xenograft transplantation, as large animal and human studies have consistently reported fibrotic or inflammatory responses [6-11].

2.4.1.3 β Cell Lines

Insulinoma-derived β cell lines have been pursued to provide an ample supply of alternative donor cells due to their proliferative capacity and ability to maintain function at high passage numbers; an additional benefit is the ease with which β cell lines may be genetically engineered for effects such as improved function and survival [62]. However, in the past 30 years, generating and using human β cell lines have proven complicated [63-

66]. Generation of the NAKT-15 human β cell line in 2005 appeared promising, but no reports of its utility have been published since then [67]. Only in the past couple of years has a new promising human β cell line named EndoC-bH1 been developed with potential as a tool for replacement cell therapy [68]. For these reasons, much of the literature consists of experimental studies on rodent β cell lines that have been successfully generated.

Commonly used β cell lines for research are based on the mouse βTC cell line that was originally derived from transgenic mice carrying a hybrid insulin-promoted simian virus 40 tumor antigen gene [69]. The early variant, βTC-3, can process proinsulin and store insulin (20-30% of normal islets) similarly to normal β cells, but responds to subphysiological glucose ranges (0.15-16.7 mM glucose) and proliferates uncontrollably [70]. The genetically engineered variant, βTC-tet, has more normal glucose responsiveness (0.5-16 mM glucose) [71] and a bacterial tetracycline operon regulatory system that can be triggered with tetracycline to inhibit cell proliferation [72]. Table 2.1 compares insulin secretion rates from the two βTC cell line variants against mouse islets, in which the best to worst secretors are ranked as follows: islets > βTC-tet > βTC-3.

Table 2.1: Comparison of insulin secretion rates from βTC-3 insulinomas [73], βTC-tet cells [74], and mouse islets [75]. The range of insulin secretion rates per cell from mouse islets was approximated from graphical data in [75] and based on the assumption that each islet contains roughly 1,000 cells.

			Insulin secretion rate (pmol/(10^6 cells · h))
Mouse βTC-3 Insulinomas	Basal	0 mM Glucose	0.4
	Stimulated	16.7 mM Glucose	3.9
Mouse βTC-tet Cells	Basal	0 mM mM Glucose	5
	Stimulated	15 mM Glucose	24
Mouse Islets	Basal	1 mM Glucose	12-36
	Stimulated	20 mM Glucose	156-288

2.4.2 Stem and Progenitor Cells

A number of studies have indicated that stem cells could be an alternative donor cell source for T1D treatment. This approach could allow for an autologous cell therapy and would eliminate donor cell scarcity and possibly immune rejection issues. Differentiation of human pluripotent stem cells to generate pancreatic progenitor cells has shown promise [76], but fully functional β cells have not yet been produced *in vitro* [77]. The major drawbacks of using embryonic stem cells (ESCs) to generate insulin-producing cells are that they are difficult to differentiate into only insulin-producing cells, there are ethical and religious issues to deal with, and ESC transplantation has led to teratoma formation [78, 79]. Other studies have reported that mesenchymal stem cells (MSCs) can be differentiated into insulin-producing cells [80, 81] and some have even shown efficacy in diabetic rodent models [82, 83]. The overall major challenges to a stem cell approach

are that stem cells are still not well understood, they can form teratomas, differentiated insulin-producing cells secrete very low levels of insulin, and only short-term graft survival *in vivo* has been attained [79]. In addition, there is a possibility that the stem-cell derived β cells will be recognized by T1D patients for autoimmune destruction.

2.4.3 Non-β Cells

Like stem cells, non-β cells can potentially serve as an autologous cell source to alleviate donor cell scarcity and immune rejection issues. Contrary to stem cells, the non-β cell approach does not require extensive differentiation protocols and eliminates the risk of unintended differentiation post-transplant. Non-β cells may also better avoid autoimmune destruction in T1D patients; a study by Lipes et al. showed that, unlike β cells, insulin-secreting non-β cells in nonobese diabetic (NOD) mice were not targeted or destroyed by the immune system [84]. The overall goal of this approach is to engineer the patient's own healthy, non-β cells into meal or glucose-responsive insulin secretors for transplantation back into the patient. Many non-β cell sources and genetic engineering strategies have been investigated, each with their own challenges and none so far with complete preclinical success.

2.4.3.1 Gene Therapy Strategies

The gene therapy method is an important consideration when engineering non-β cells for sustained insulin expression over time. The two different strategies are *ex vivo* gene therapy in which cells are isolated from the patient to be genetically engineered and

transplanted back into the patient, and *in vivo* gene therapy which involves the genetic modification of cells as they reside in the patient. In either of these cases, there are two general gene delivery methods: viral and non-viral. The former is referred to as transduction and the latter as transfection. Viral transduction is generally the most efficient means of gene introduction, but carries with it some safety concerns. On the other hand, transfection is safer, but has been inefficient at transferring genes.

Viral Transduction

The most widely studied viruses for gene transfer systems are retrovirus, lentivirus, adenovirus, and adeno-associated virus (AAV). AAV and lentivirus have been successfully used to deliver the genes necessary to generate insulin-secreting hepatocytes and enteroendocrine cells [85-87]. AAVs are human parvoviruses that can transduce cells through both episomal transgene expression and random chromosomal integration for permanent expression [88]. Lentiviruses are RNA-viruses based on human immunodeficiency virus-1, non-human immunodeficiency, or feline immunodeficiency viruses. By integrating into the host genome, they could lead to long-lasting and stable transgene incorporation. Although gene silencing has been identified as a challenge in achieving long-lasting transgene expression after viral transduction [89-91], recent studies have shown that inhibiting histone deacetylases (HDACs) in virally transduced cells may reverse gene silencing and reactivate transgene expression [92-95]. HDAC inhibitors (HDACi) may therefore play a role in enhancing viral transduction methods in the future.

Non-Viral Transfection

Transfection in mammalian cells with plasmids of naked DNA containing the gene of interest is another viable method for gene delivery, where selection via antibiotic resistance is normally performed in *in vitro* applications. This is an approach that has been used the most in engineering non-β cells for insulin secretion [15, 16, 18, 96-100]. It has also received attention as a safer alternative to viral transduction for *in vivo* gene therapy. However, even if delivery is efficient, transfection *in vivo* is only transient which precludes its application in treating diseased states like diabetes in which sustained transgene expression is required [101].

2.4.3.2 Cell Sources

The ideal non-β cell candidate should be glucose or meal-responsive, express prohormone convertases PC1/3 and PC2 for proinsulin processing, and use a regulated secretory pathway (RSP) for quick hormone release. Proinsulin processing is important for both the secretion of active insulin as well as the cleavage product, C-peptide, which has shown to be beneficial in preventing hyperglycemia-induced vascular and neural dysfunction in animal and clinical diabetes models [102-105].

The first target non-β cells to be studied were monkey kidney cell lines [106, 107], fibroblasts [108], and Chinese hamster ovary cells [109], all of which were transfected with the insulin gene. However, since these cells were unable to process proinsulin, they released biologically inactive insulin. Next, researchers showed that modifying the insulin gene for cleavage by the ubiquitous enzyme, furin, in NIH 3T3 fibroblasts, led to biologically active insulin secretion [110]. When applied to muscle in diabetic mice, basal

insulin levels were comparable to those observed from normal mice [111, 112]. This approach is limited, however, and only allows for basal secretion due to the lack of exocytotic systems for first phase secretion kinetics. In addition, these cells are not glucose-sensitive.

Neuroendocrine Cells

Neuroendocrine cells are appealing since they have an RSP and the enzymatic machinery required to process proinsulin. AtT20, a mouse corticotropic cell line derived from the anterior pituitary, has been engineered to express active insulin, but they lack glucose-responsiveness [84, 113-115]. Hughes and Motoyoshi et al. managed to engineer AtT20 cells for glucose-sensitivity via co-transfection with genes encoding the glucose transporter (GLUT2) and glucokinase, but stimulated insulin release was lower by more than 2-fold relative to release rates after stimulation with 8-bromo-cyclic AMP, a cAMP analog [97-99]. In 2003, Wu et al. demonstrated that engineered primary rat pituitary cells co-expressing human insulin and the GLP-1 receptor, co-secreted pituitary hormones and human insulin after oral glucose tolerance testing in mice [116]. The major limitation of this approach, however, is that over-secretion of adrenocorticotropic hormone as a result of glucose-sensitivity could severely disrupt the metabolic state of the patient.

Liver Cells

Hepatocytes have glucose-sensitive molecules such as GLUT2 and glucokinase, and several promoters that can be used for *in vivo* liver-targeted insulin gene therapy [117]. Lack of proper enzyme machinery, however, requires the introduction of a furin-cleavable

proinsulin gene [118]. Intraportal gene delivery of furin-cleavable insulin via adenovirus or AAV under the control of a liver-specific, glucose-responsive promoter resulted in nearly normal blood glucose levels in diabetic rats [119]. Lack of an RSP for glucose-responsiveness can be addressed by making modifications to the promoter driving insulin transgene expression [120] and secretion kinetics can be improved through insulin mRNA destabilization [121] but regulation at only the transcriptional level still results in slower insulin dynamics compared to β cells [119].

Intestinal Endocrine Cells

Enteroendocrine cells are appealing as non-β cell candidates due to their close similarity to β cells: post-prandial response system, insulin-processing proteases, and secretory granules for quick release [13, 122]. After a meal, enteroendocrine release of incretin hormones follows similar kinetics to insulin secretion from β cells (Figure 2.7). A subpopulation of enteroendocrine cells is K cells which are mainly located in the stomach, duodenum, and jejunum and they secrete gastric inhibitory peptide (GIP). Initial proof-of-concept studies showed that mice transgenic for human insulin-secreting K cells were resistant to streptozotocin (STZ)-induced diabetes [12]. Similarly, insulin secreting enteroendocrine G cells significantly reduced mouse blood glucose levels [14]. The engineering of K cells isolated from the heterogeneous immortalized STC-1 cell line [15, 16] and stable transfection with an insulin transgene, have permitted preclinical evaluation without resorting to transgenics. Insulin-secreting K cell clones were selected and tested for efficacy after cell transplantation into diabetic mice. Both studies reported restoration of normoglycemia, but mice became hypoglycemic as unrestricted cell proliferation

increased insulin production beyond therapeutic levels. In a K cell study that employed controlled cell growth methods, no effect was observed on blood glucose levels in diabetic mice until a drug-inducible element was incorporated into the insulin transgene [17].

Yet another subpopulation of enteroendocrine cells called L cells is located in the jejunum, ileum, and colon where they secrete glucagon-like peptide-1 (GLP-1) after a meal. GLP-1 plays an important role in potentiating glucose-mediated insulin secretion from β cells, in supporting β cell proliferation and regeneration, and in protecting β cells against apoptotic cell death [123, 124]. In 2003, Tang et al. transduced the heterogeneous human L cell line, NCI-H716, via recombinant AAV (rAAV)-mediated transfer of the human insulin transgene, after which 2% (wt/vol) meat hydrolysate (MH) simultaneously stimulated GLP-1 and insulin secretion in a similar manner and co-localization of both hormones were observed in secretory granules [125]. In 2008, Bara et al. used the GLUTag L cell line to stably transfect with the human B10 insulin transgene and generated the GLUTag-INS cell line [18].

B10 human insulin differs from wild-type human insulin by a single amino acid residue on the B-chain due to a single point mutation in the proinsulin gene substituting aspartic acid for histidine. It has been shown to be 4-5 times greater in potency than that of the natural hormone and is called superactive insulin [126]. GLUTag cells are immortalized murine L cells which make up a homogeneous population with comparable function to primary L cell cultures and various *in vivo* models [127]. For this reason, GLUTag cells provide a useful model for L cell regulated secretion studies and they can serve as an allogeneic donor source for experimental studies in mice. Extensive studies of GLUTag-

INS *in vivo*, however, showed that insulin secretion was likely insufficient in affecting blood glucose levels in diabetic mice [20].

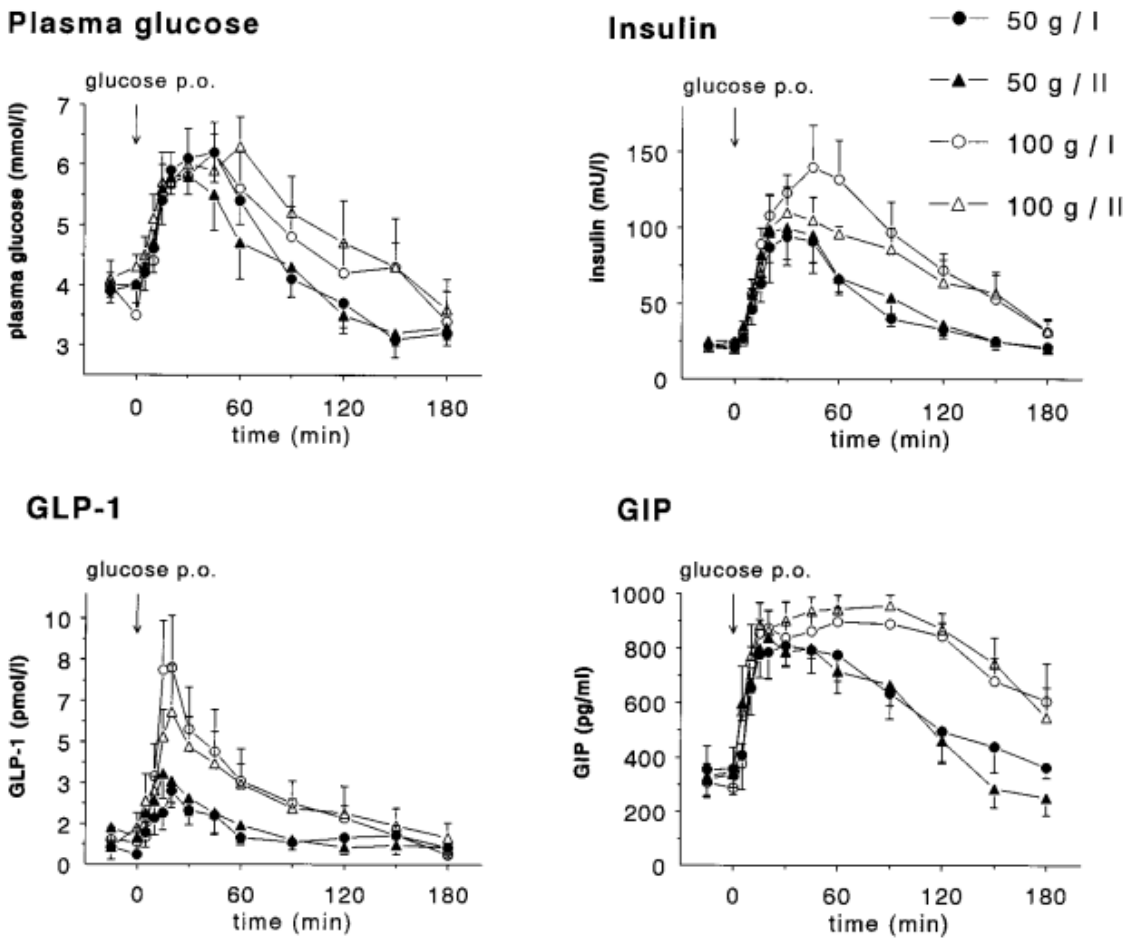

Figure 2.7: Plasma insulin, GLP-1, and GIP responses to oral ingestion (arrows) of 50 and 100 grams of glucose, published in [13].

The highest reported range of secreted insulin from intestinal endocrine cells *in vitro* is only 5-22% of βTC-3 cell line secretion [18, 73]. This may suggest that insulin transgene expression is low and better gene delivery techniques should be investigated.

2.5 Construct Technologies for a Tissue Engineered Pancreatic Substitute

Contrary to a mechanical artificial pancreas, the bioartificial pancreas (BAP) is defined as a cell-based construct that can be easily transplanted with little or no immunosuppression, is capable of long-term blood glucose regulation, and is retrievable for biopsy or replacement if necessary [128]. The construct should serve as an immune isolation device to prevent rejection and eliminate the use of immunosuppression, and/or provide an optimal environment to support long-term cell function. The encapsulation material and device configuration are important considerations in fabricating a successful BAP for biocompatibility, immune protection, optimal cell loading density, and good diffusional capacity. Since the term BAP is often used to describe islet-containing devices, the more general tissue engineered pancreatic substitute (TEPS) terminology will be used herein and defined as a BAP that contains any of the previously outlined insulin-secreting cell types.

2.5.1 Choice of Materials

The material must serve as a semi-permeable membrane which physically separates the graft from host antibodies and immune cells, but also allows for the influx of glucose and nutrients, and the efflux of insulin and waste products. There are two very general categories that biomaterials fall into for cell encapsulation devices: rigid and flexible [21].

Fairly rigid biomaterials with rough surfaces are often used to elicit a host response such as neovascularization at the transplant site for increased oxygen supply. Unfortunately, this also normally elicits an immune response followed by host cell adhesion and fibrotic overgrowth [129]. Such rigid devices are usually formed using synthetic polymer membranes like polytetrafluroethylene (PTFE), poly acrylic acid, polyethylene oxide, poly vinyl alcohol, polyphosphazene, and poly lactic and glycolic acids [130-132]. The latter two form synthetic hydrogels, but since they are designed to erode, are unappealing options for a long-lasting TEPS.

Flexible biologic polymers with smooth surfaces can be the best at evading detection by the host immune system and the most popular materials are naturally occurring hydrogels like collagen, gelatin, hyaluronate, fibrin, alginate, agarose, and chitosan. The difficulty with using natural materials such as these is in achieving high purity and identity of starting materials, as is the case with alginates [133]. Alginates have low interfacial surface tension (reports range from 56-76 mN/m) which aids in the avoidance of host protein adsorption and cellular adhesion [134]. This and the *in vivo* stability of alginates to oxidative damage have attracted much attention to its use as a material for developing TEPS [21].

Alginates, derived from brown algae, are a family of unbranched anionic polysaccharides arranged in homo- or hetero-polymeric block structures of mannuronic (M) and guluronic (G) acid. Stiffness and flexibility of the material can be tuned by varying alginate composition. A high M:G ratio increases the elasticity and flexibility of the material compared to a low M:G ratio which increases the stiffness. The composition affects alginate viscosity and influences its mechanical stability, permeability, swelling

properties, and surface roughness. A potential limitation is the large-scale isolation and purification of alginates from natural sources.

2.5.2 Device Configuration

The purpose of encapsulation is to provide a physical barrier against host immune cell and antibody infiltration, and allow nutrient and oxygen influx as well as insulin and waste efflux. Unfortunately, small toxic molecules such as cytokines and nitric oxide can also pass through semi-permeable membranes such as these and damage encapsulated cells. Protection methods are being developed to address this issue and are discussed in Section 2.7: *In Vivo* Construct Integration.

Three major approaches to encapsulation have been studied in developing a TEPS: intravascular macrocapsules, extravascular macrocapsules, and extravascular microcapsules (Figure 2.8). Macrocapsules provide one immune isolation barrier for all transplanted cells and are normally on the millimeter scale compared to micrometer sized microcapsules surrounding smaller cell numbers that together make up a larger transplant volume.

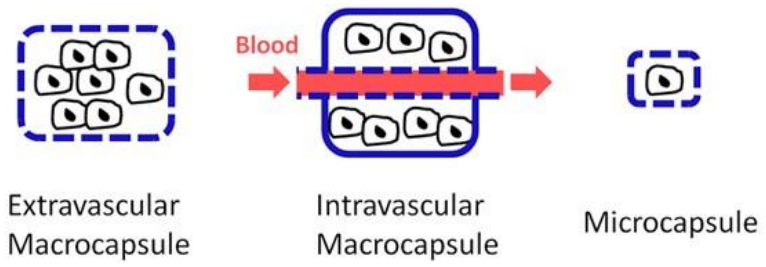

Figure 2.8: The three major configurations for a tissue engineered pancreatic substitute, published in [135].

Intravascular macrocapsule devices are implanted by vascular anastomoses into the host blood vessels for close contact between insulin-producing cells and blood, similar to islets *in vivo*. This was accomplished by fabricating a microporous tube or capillary bundles for blood flow through the lumen and cell attachment to the outer tube, similar to the intravascular diffusion chamber shown in Figure 2.9. The most extensively studied diffusion chamber was based on the one developed by Chick et al. [136] and was found to restore normoglycemia in diabetic rats [137], dogs [138], and monkeys [137]. However, the major problem was the occurrence of blood clotting as a result of insufficient material biocompatibility and small tube diameters. Modifications to device materials and tube diameters have reduced blood clotting, but only for a short time [139]. The intravascular macrocapsule configuration therefore receives less attention due to the major transplant surgery involved and high risk for vascular complications.

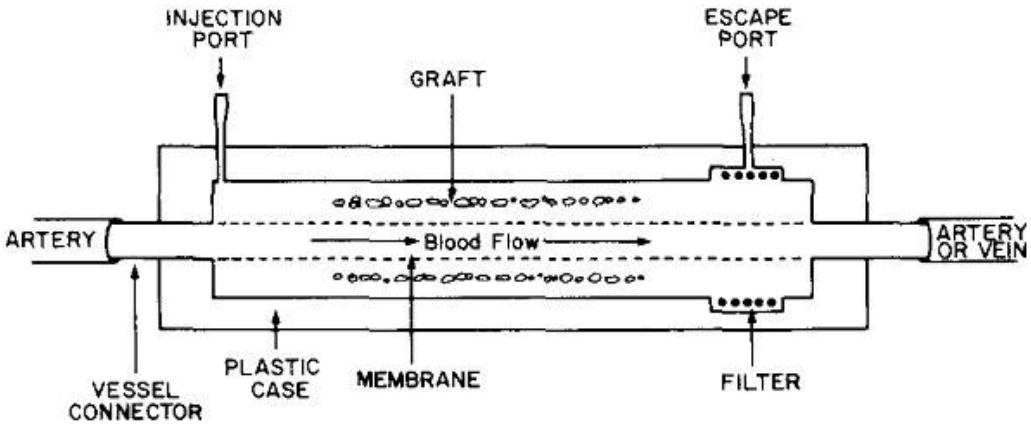

Figure 2.9: Schematic of an intravascular diffusion chamber, published in [135].

A major advantage to using an extravascular rather than intravascular approach is that the risks are much lower since biocompatibility issues with the former normally affect the graft instead of the recipient. Additionally, multiple transplant sites such as the peritoneal cavity and subcutaneous site are available, simplifying the transplant and retrieval processes and better qualifying as a clinically acceptable TEPS. The macrocapsule geometry can vary from planar to tube-like, hollow-fibers (Figure 2.10) and can get as large as 3 cm by 8 cm [19]. Large devices like these, however, result in poor graft nutrition and oxygenation due to increased diffusional distances between the cells and the surrounding environment [140]. In addition, since islet viability is substantially reduced by increasing cell numbers, the loading density is kept quite low. Another disadvantage is that macrocapsules tend to break more easily *in vivo* due to physiological stress [41, 141, 142].

A commercially available macrodevice containing islets, Theracyte^{TM}, is comprised of a double membrane of PTFE where the inner selective membrane prevents immune cell contact with the graft and the outer, less selective membrane, facilitates angiogenesis (Figure 2.10D). Preclinical studies, however, have shown poor results using this device which causes fibrosis and in one case, tumor formation [143, 144].

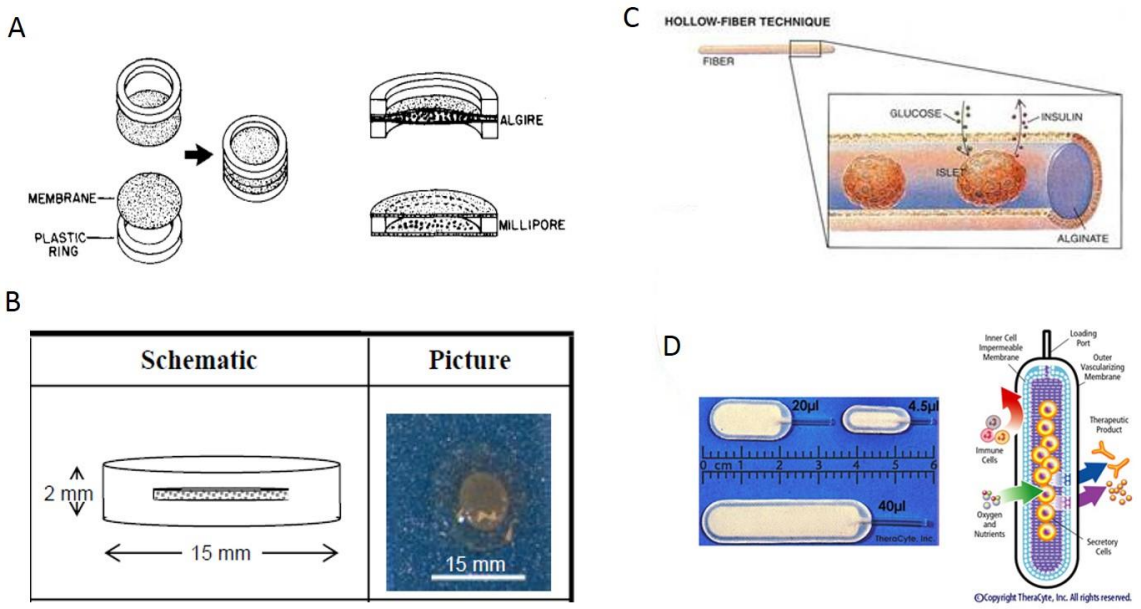

Figure 2.10: Extravascular macrocapsules. Algire and Millipore diffusion chambers with cell-containing membranes in the middle or outside of plastic rings, illustration by [145]. B) Agarose disc construct containing insulin-producing cells encased in cell-free agarose, taken from [41]. C) General schematic for a tube-like macrocapsule device, illustration taken from http://www.isletmedical.com/pages/company_competition, D) TheracyteTM device, illustration from [135].

Microencapsulation involves the formation of a spherical semi-permeable membrane around therapeutic cells (Schematic 2.1). One of the main advantages of the microcapsule configuration is its high surface area to volume ratio, allowing for better diffusion capacity and higher cell loading density relative to a macrocapsule device. Small microcapsule diameters ranging from 150-700 µm are fabricated for optimal oxygen diffusion to prevent cell necrosis, particularly in the case of islets [140, 146]. Out of the three encapsulation approaches mentioned, the microcapsule configuration presents the easiest and least invasive surgical procedure for transplantation since just one simple injection is required. The downside, however, is that full graft retrieval is not possible but

may be necessary in the case of a host inflammatory response. As far as materials, hydrogels are preferred for cell microencapsulation because the procedure for fabrication is milder relative to those for water-insoluble polymers that have been shown to impair cell function [147].

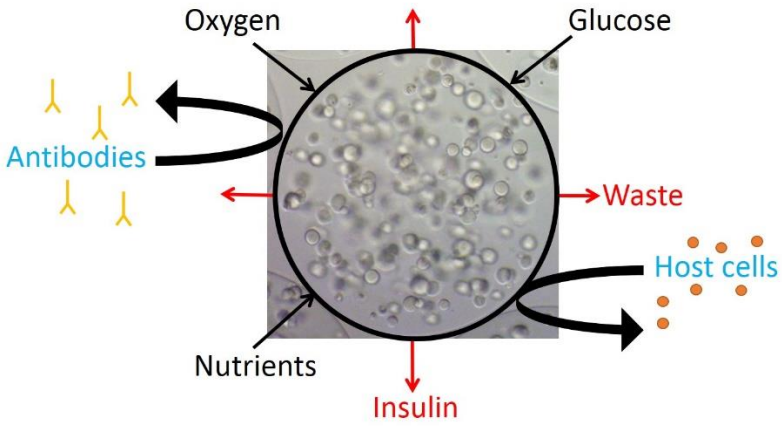

Schematic 2.1: A microcapsule with a semi-permeable membrane surrounding insulin-secreting single cells for protection against host cells and antibodies.

Alginate microcapsules are popular because their fabrication techniques have consistently shown preservation of cell function. A common technique is to use an electrostatic droplet generator in which cells mixed with alginate are passed through a needle to form droplets charged with high static voltage that fall into a collecting vessel containing a cross-linking solution with opposing polarity for gelation (Schematic 2.2). The size of the microcapsules can be varied by changing the needle height, voltage magnitude, and the pumping rate of the alginate solution.

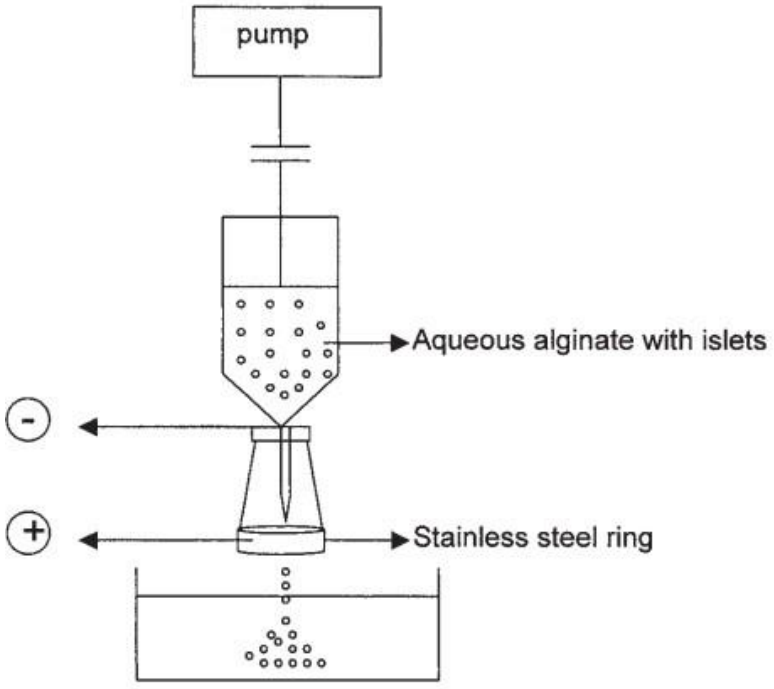

Schematic 2.2: An electrostatic droplet generator, illustration published in [148].

The most commonly studied ionic cross-linking solutions are calcium chloride and barium chloride. Duvivier-Kali et al. reported that microcapsules fabricated with 3.3% (wt/vol) sodium alginate characterized by high mannuronic acid and cross-linked in barium chloride solution yielded better biocompatibility and mechanical stability in rodent models (STZ-diabetic BALB/c and nonobese diabetic (NOD) mice) compared to those of low mannuronic acid cross-linked in calcium chloride solution [149]. Additionally, Safley et al. showed better biocompatibility and prolonged survival of porcine islets encapsulated in barium alginate in NOD mice [150] compared to the commonly employed alginate-poly-L-lysine-alginate (APA) microcapsule configuration [151]. Transplanting islets or β cells encapsulated in barium alginate in this way has also been successful in restoring

normoglycemia in diabetic rodent models [149, 152, 153]. There is some concern, however, that the release of barium ions from transplanted microcapsules may cause toxicity [154], but more studies need to be performed to confirm this.

2.6 Preclinical Diabetes Models

Choosing the best preclinical animal disease model for studying new therapies is important in determining the translatability of the approach to humans. For this reason, the animal model should reflect the human disease well. There are three general preclinical T1D models that are often used to evaluate a TEPS *in vivo*: the streptozotocin (STZ)-induced diabetes model, pancreatomized models, and spontaneous diabetes models induced by an autoimmune response. The first and third methods will be covered here since pancreatomized models are less common.

STZ, an N-nitroso derivative of glucosamine, was discovered in 1963 as a convenient drug for inducing diabetes [155]. STZ is a toxic glucose analogue that preferentially accumulates in β cells via the GLUT2 glucose transporter, leading to DNA fragmentation and β cell destruction [156]. The STZ-induced diabetes model can be applied to any experimental animal, most commonly mice, rats, pigs, and monkeys. The administered dose of STZ depends on the animal species and strain. Mouse strains used for this model are normally BALB/c or C57BL/6 with different optimal doses for each [157]. Researchers have the choice of administering a single high STZ dose or multiple smaller STZ doses to induce diabetes. The former is often chosen for convenience in rodent models, but can be unstable in terms of the diabetic condition and result in approximately 10-20% death. The latter method can achieve hyperglycemia with no, or few, animal deaths [158] and is

considered superior to the single injection model. In small rodent models, STZ is usually administered intraperitoneally (i.p.) because it is easier to manage than an intravenous (i.v.) injection. In the case of larger animals, however, i.v. may be preferable because a lower STZ dose can be used. The STZ-induced diabetes model is useful in testing therapeutic efficacy of a TEPS in terms of sufficient insulin production for normoglycemic restoration, but the effects of a T1D-like autoimmune response cannot be evaluated.

There are two models that come the closest to mimicking T1D etiology: the nonobese diabetic (NOD) mouse and biobreeding rat established by [159] and [160], respectively. These rodent models spontaneously become diabetic due to an autoimmune attack by T cells, B cells, macrophages, and natural killer cells, leading to insulitis and islet loss. These models are used to better understand the mechanism of T1D and to evaluate autoimmune effects on a promising TEPS. However, NOD mice also have inflammation of the thyroid, submandibular glands, and lacrimal glands which increases the complexity of the model. It is therefore important to first identify the research objective and then choose the most appropriate preclinical animal model to achieve valuable results.

2.7 *In Vivo* Construct Integration

Once a TEPS shows promise *in vitro*, the next step is to evaluate its *in vivo* potential in a carefully chosen diabetes animal model. Some key considerations when transplanting a TEPS are what surgical method will be employed and where the TEPS is to be transplanted. A common transplant procedure for microencapsulated cells is to simply inject the microcapsules into the peritoneal cavity, but this may not always be the optimal site. The peritoneal cavity is limited by low oxygenation, limited capacity for

revascularization, and delayed glucose-responsiveness due to the large diffusional distances between the graft and blood vessels [161]. However, the reason for its appeal is that it can hold large volumes and thus allows for high transplanted cell numbers. This becomes important when donor cells secrete low levels of insulin per cell. Ideally, one would choose a site with vascular density for facilitated interchange of nutrients, oxygen, and insulin between the graft and the blood. In addition, that site should provide a less inflammatory microenvironment. Other clinically relevant (intramuscular, subcutaneous, omentum, and venous sac) and immuno-privileged (lymph node and anterior chamber of the eye) transplant sites are discussed in [161].

A major challenge to successful TEPS integration is developing a biocompatible construct that causes little or no host inflammatory response upon transplantation. Even with pure, flexible, and smooth alginate microcapsules, donor cells can shed antigens that diffuse out of the semi-permeable membrane and activate macrophages that cause the release of cytokines, nitric oxide, and oxygen radicals that destroy the donor cells [152, 162]. For this reason, some researchers are investigating ways to tether bioactive agents to the construct that protect transplanted cells from inflammation. For example, one group showed improved protection of encapsulated islets exposed to pro-inflammatory cytokines by functionalizing hydrogels with the anti-inflammatory peptide, interleukin-1 (IL-1) [163].

Another important factor to consider is the diffusional distance between the graft and the blood supply *in vivo*. One of the prime reasons for failure of cell-based constructs is insufficient oxygen tension leading to cell death. Since this issue is observed in most

transplant sites, researchers are working on engineering ways to provide oxygen either by *in situ* oxygen generation or revascularization guidance [161].

Although these are likely limitations, the major obstacle in developing an optimal TEPS is the lack of understanding regarding graft behavior *in vivo*. The *in vivo* environment is essentially a black box in which the construct resides and only indirect and endpoint measurements are made to evaluate progress. These measurements give no indication of the time-scale to failure, thus limiting the ability for researchers to delineate critical factors that contribute to graft failure. An appropriate imaging technology should therefore be employed for minimally invasive, real-time graft tracking *in vivo*. Real-time imaging, alongside end physiologic measurements, can lead to the identification of key factors for construct failure and accelerate the development of a successful TEPS.

2.8 Imaging Technologies

Biomedical imaging is critical to the development of optimal TEPS technologies because it allows researchers to gather physical and physiological information about the engineered tissue *in vivo* without disturbing or damaging the graft. This information is able to be gathered in real-time rather than after important events have caused graft failure, as is the case when measuring indirect effects like blood glucose and C-peptide levels. Imaging technologies are therefore important in the prediction and possible prevention of construct failure. Optical imaging, radiation based imaging, ultrasound, infrared imaging, and nuclear magnetic resonance (NMR) methods are described extensively in [164]. Here, only optical imaging and NMR methods will be discussed, as they are the most prevalent in the research and development of TEPS.

2.8.1 Optical Imaging

Using an optical technique involves the measurement and imaging of visible light emitted from the graft. This can occur either as the result of an enzymatically catalyzed chemical reaction or in response to an excitation wavelength. An example of the former is the firefly luciferase enzyme which catalyzes the oxygenation of the substrate luciferin using ATP and oxygen to yield oxyluciferin and a photon. The photon emission from this reaction can be measured using a charge-coupled device camera. When the luciferase reporter gene is successfully incorporated into the cells of interest, the measured photon flux is proportional to the number of living cells, allowing for the quantitative tracking of cell mass and survival. Bioluminescence imaging (BLI) is a popular method for direct monitoring of cell fate in animals due to its low cost, high sensitivity, ease of operation, near background-free imaging conditions, and reduction of inter-animal variability [165, 166]. The downside of this approach is that it is normally only applied to small animal models due to a short penetration depth (the signal is attenuated 10-fold for every centimeter of tissue depth).

The first proof-of-concept BLI study with free islets offered encouraging results, as it demonstrated that islets transduced *in vitro* with a luciferase lentivirus could be quantitatively monitored long-term after transplantation in the kidney capsule of diabetic mice [167]. Subsequent studies investigated the use of BLI in early detection of islet graft rejection [168], islet survival immediately post-transplantation [169], and guided timing for corrective interventions [170]. Just a few studies have reported the use of BLI for tracking cell constructs [171-173], and only one for tracking a TEPS [174]. BLI incorporation could be an easy and inexpensive way to track a TEPS in diabetic rodents,

but more research needs to be done to investigate the advantages and limitations of this approach.

Fluorescence is another popular optical imaging method, but the mechanism for emission is different. Instead of a chemical reaction, an excitation wavelength of 400-600 nm is required for photon absorption by the fluorescence reporter protein which triggers an emission wavelength of 450-650 nm that can be measured. Tissues or cells can be tagged in a variety of ways like incorporating fluorescent reporter genes, using dyes, microspheres, or nanoparticles. The downsides of this approach are the short penetration depth, autofluorescence emitted from natural tissues, and high protein stability which precludes its use in tracking dynamic cellular processes. Protein degradation rates can be increased to address the latter issue, but this requires genetic manipulation [175]. For these reasons, BLI incorporation has become a more popular optical technique for *in vivo* cell tracking technologies.

2.8.2 Nuclear Magnetic Resonance

NMR techniques like Magnetic Resonance Imaging (MRI) and spectroscopic methods are frequently used in a variety of applications, both preclinically and clinically. MRI has been identified as a suitable tracking method for *in vivo* graft monitoring [176, 177], with its own advantages and limitations [178]. Some studies have investigated the application of ^{19}F NMR spectroscopy to measure the oxygen concentration at the graft site in mice post-transplantation of microencapsulated β cells [179, 180]. This method, however, only allowed for indirect graft monitoring. Alternatively, ^{1}H NMR has been applied for direct monitoring of encapsulated β cells, but the macrocapsule construct design

that allowed for such monitoring was not optimal for cell function [181]. To preserve construct design, perfluorocarbons (PFCs) can be used as imaging contrast agents for computed tomography, ultrasonography, and MRI [182]. However, this only allows for spatial tracking of the capsules rather than the monitoring of living cell mass within the microcapsules. Ideally, the monitoring method should allow for minimally-invasive *in vivo* real-time tracking of the viable TEPS while preserving construct design for optimal graft function.

2.9 Significance

Previous work in our lab reports on the promise of using engineered, insulin-secreting intestinal L-cells as a non-β cell source to circumvent donor cell availability and autoimmune rejection issues associated with islet transplantation [18-20, 87, 125]. A major challenge in the field, however, has been in engineering cells with sufficient insulin secretion to lower blood glucose levels in preclinical diabetes animal models. In CHAPTER 3 of this thesis, a novel secretion enhancement method was applied to the GLUTag-INS cells previously developed in our lab to generate engineered L cells that significantly surpass reported insulin secretion from other enteroendocrine cells in the literature.

Preclinical efficacy studies of engineered enteroendocrine cells are primarily studied as uncontrollable growth systems that lead to tumor formation [15, 16]. Encapsulation is a strategy for controlling cell growth, but has precluded therapeutic efficacy, perhaps partially due to suboptimal construct design. As reported in CHAPTER 4 of this thesis, a barium alginate microcapsule configuration was investigated as an

appropriate construct design to allow for controlled cell growth, retained insulin secretion, and high cell loading densities. Compared to the previous macrodevice developed in the lab, the microcapsule configuration enabled insulin secretion rates that were 100-fold higher per graft volume.

In most cases, graft efficacy is assessed by endpoint measurements from the animal model, but this has offered limited information into what happens to the graft within a clinically relevant timescale. In CHAPTERs 4 and 5, application and characterization of bioluminescence *in vitro* and *in vivo* are reported. This was the first study to show that injectable, free-floating microencapsulated cells could be tracked in real-time using bioluminescence imaging.

Preclinical reports of transplanted controlled-growth systems containing insulin-secreting enteroendocrine cells have been unable to show a lowering effect of blood glucose levels in diabetic rodents [17, 20]. CHAPTER 5 reports the therapeutic efficacy of the improved TEPS design containing the enhanced recombinant intestinal L cells. This study was the first to find a beneficial effect of such a construct on blood glucose levels in STZ-induced diabetic mice, but significant challenges remain to be addressed in an effort toward developing a clinically acceptable cell-based insulin therapy.

CHAPTER 3: NOVEL METHODS FOR INSULIN SECRETION ENHANCEMENT FROM RECOMBINANT L-CELLS

3.1 Abstract

Genetically engineering intestinal endocrine cells for recombinant insulin secretion constitutes a promising cell-based approach for insulin dependent diabetes therapy. Generating cells with sufficient insulin secretion using conventional gene delivery methods, however, has proven challenging. In this work, we applied two enhancement methods to an already engineered L cell line with insulin secretion capabilities named GLUTag-INS. The first method, lentiviral transduction, increased insulin mRNA and secretion by 10- and 2-fold, respectively. After several passages, enhanced secretion was lost but cells still retained 3.5 times more insulin mRNA. Therefore, in itself, additional transgene incorporation was insufficient in generating therapeutic, insulin-secreting L cells. The second method, histone deacetylase inhibition (HDACi) with Trichostatin A, significantly revived transgene mRNA production and concurrently enhanced downstream steps in the regulated secretory pathway (RSP). With these methods combined, recombinant basal and stimulated insulin secretion rates of 655 and 888 fmol/(10^6 cells·h), respectively, significantly surpassed reported secretion from previously engineered intestinal endocrine cells by over 6-fold. In addition, some HDACi enhancement effects in engineered cells were able to be sustained for as long as seven days within a 3D, alginate microcapsule configuration. We concluded that therapeutic insulin production from L cells

(384 and 3930 fmol/(10^6 cells·h) for basal and stimulated, respectively) may be attainable by both increasing transgene incorporation and RSP efficiency. Furthermore, HDACi treatment is promising as a novel approach for enhancing graft secretion function from cells with an RSP, such as β and L cells. The findings from this study have allowed us to isolate promising research avenues in an attempt to accelerate the development of a non-β cell-based diabetes therapy with real clinical potential.

3.2 Introduction

Daily insulin injections and infusion by a pump are the current treatment options for insulin dependent diabetes (IDD) patients, neither of which are continuously regulating, closed-loop systems. As a result, the patient's glycemic state is difficult to control and often leads to long-term complications like heart disease and stroke, hypertension, blindness, kidney disease, nervous system disease, and amputations [1]. Cell-based options like pancreas or islet transplantation are clinically used, but only for extreme, brittle cases of diabetes due to donor cell scarcity and adverse effects of immunosuppression treatment [183]. An alternative cell-based therapy approach is being explored with the overall goal of genetically engineering autologous non-β cells for insulin secretion to fulfill donor cell demand and avoid autoimmune destruction [184].

Many non-β cell sources and genetic engineering strategies have been investigated, each with their own challenges and none so far with complete preclinical success. The ideal non-β cell candidate should be glucose or meal-responsive, express prohormone convertases PC1/3 and PC2 for proinsulin processing, and use a regulated secretory pathway (RSP) for quick hormone release. Muscle [96, 112, 185], skin [186, 187], and

fibroblast [76, 110] cells have been engineered for constitutive insulin secretion, but do not naturally process proinsulin and require modification of the insulin gene for cleavage by the ubiquitous enzyme, furin, to produce biologically active insulin [110]. This approach is further limited since these cells do not possess nutrient-responsive elements nor do they have an RSP.

Pituitary cells can process proinsulin and have an RSP, but do not naturally respond to nutrients. Sambanis et al. showed that insulin secretion rates from engineered AtT20 pituitary cells [114] were induced 6-fold after stimulation with 8-bromo-cyclic AMP (BrcAMP), a cAMP analog [113]. Hughes and Motoyoshi et al. managed to engineer AtT20 cells for glucose-sensitivity via co-transfection with genes encoding the glucose transporter (GLUT2) and glucokinase, but insulin secretion induction was more than 2-fold lower than that observed from secretion stimulated by BrcAMP [97-99].

Hepatocytes express glucose-sensitive molecules GLUT2 and glucokinase, but have no RSP and cannot process proinsulin [117]. Delivery of plasmids containing partially bioactive insulin transgenes for simple cleavage by furin in hepatocytes has improved glycemia in preclinical diabetes models [118]. Furthermore, intraportal insulin gene delivery via adenovirus or adeno-associated virus (AAV) under the control of a liver-specific, glucose-responsive promoter [120] resulted in nearly normal blood glucose levels in diabetic rats [119]. However, recombinant hepatocytes, due to the secretion lag time resulting from transcriptional regulation, are unable to match the tight glucose regulation achieved by β cells after an intraperitoneal glucose load [119].

Enteroendocrine cells may be the best non β-cell candidates due to their nutrient-responsiveness, proinsulin processing abilities, and use of an RSP for fast hormone release

[13, 122]. Proof-of-concept studies in mice transgenic for insulin-secreting gastric G or gut K cells have shown promise in this approach [14, 122], but engineering intestinal endocrine cell lines for sufficient insulin secretion has proven challenging. The highest reported range of secreted insulin from intestinal endocrine cells is only 5-22% of the β cell line, βTC-3 (384-3930 fmol·10^6 cells^{-1}·h^{-1}) [18, 73]. βTC-3 secretion is used here as the standard for comparison because a reasonable cell number (3-4x10^7 cells) could be transplanted to achieve a secretion output comparable to that from βTC-tet cell grafts that restored normoglycemia in diabetic mice (19-92 pmol·h^{-1}) [74, 180].

In two preclinical studies, blood glucose was reduced after transplanting engineered K cells, but uncontrollable cell growth and tumor formation likely contributed to this success by providing excessive amounts of insulin which eventually led to severe hypoglycemia [15, 16]. On the other hand, controlled growth preclinical studies that eliminated the chance of tumor formation have failed so far in achieving normoglycemia [17, 20]. Engineering a cell line to produce therapeutic quantities of recombinant insulin is therefore needed to transplant reasonable cell numbers under controlled growth conditions for a safe cell-based insulin therapy.

Up to now, the focus of engineering enteroendocrine cell lines for insulin expression has been primarily on genetic incorporation using various viral or non-viral gene delivery systems. These, however, have led to inadequate insulin secretion. Little emphasis has been placed on gene expression enhancement or targeting other steps downstream of transcription in the RSP and novel methods should be developed along this line to enhance secretion. Without a better understanding of the RSP in enteroendocrine cells, however, it is difficult to target the right mechanisms for improved secretion. For

these reasons, it is necessary to also identify potential limiting steps that can be targeted to improve the enteroendocrine RSP for insulin production.

Some recent findings have shown that treating islet or β cell lines with the histone deacetylase inhibitors (HDACi) Valproic Acid (VPA) or Trichostatin A (TSA), caused an increase in insulin secretion output [188, 189]. In another study, TSA was shown to increase Brain-Derived Neurotrophic Factor (BDNF) release from neuronal cells by acting on HDAC6 and increasing acetylated tubulin levels which increased vesicular transport [190]. In this work, TSA was used as a tool to better understand recombinant insulin production and secretion from intestinal L cells by evaluating its effects on insulin mRNA levels and various steps of the RSP. In addition, the longer-term effects of a one-time TSA treatment were evaluated to investigate its use as a novel method for hormone secretion augmentation.

Our lab previously engineered the murine GLUTag L cell line for insulin secretion by stable transfection with a vector containing the B10 human insulin gene and neomycin resistance [18]. The highest secreting clones were selected and used thereafter as the GLUTag-INS cell line and these have remained one of the highest reported insulin-secreting enteroendocrine cells. Although GLUTag-INS had a higher insulin secretory capacity (86-180 fmol·10^6 $cells^{-1}$·h^{-1}) than Zhang et al.'s normoglycemia-achieving K cells (32-70 fmol·10^6 $cells^{-1}$·h^{-1}) [16], transplanting GLUTag-INS within a controlled-growth system had no effect on blood glucose levels in streptozotocin (STZ)-induced diabetic mice [20]. Human insulin, however, was detected in the blood of treated mice.

The overall objective of this work was to improve secretion from the GLUTag-INS cell line and identify promising research avenues for closing the gap between insulin

secretion from recombinant L cells and endogenous β cells. Here we report the short- and long-term effects of two novel enhancement methods involving additional insulin transgene incorporation and TSA treatment. Limiting steps within the RSP of the engineered L cell lines, possible targets for enhancement, and the broad application of a novel HDACi treatment for hormone secretion augmentation are discussed.

3.3 Materials and Methods

3.3.1 Cell Culture

GLUTag-INS and further genetically engineered GLUTag-INS cells were cultured as in [191] using Dulbecco's modified Eagle's medium (DMEM) with 25 mM glucose, without L-glutamine (Corning cellgro, Manassas, VA, Cat. #15-017), and supplemented with 10% fetal bovine serum and 1% penicillin/streptomycin. Cultures were propagated in a humidified incubator at 37^{o}C/5% CO_2.

3.3.2 Secretion Enhancement via Lentivirus Transduction

The enhanced, GLUTag-eINS cell line, was generated by transducing GLUTag-INS at passages 15-17 with the wild-type human insulin lentivirus (LV-WT-INS; Emory University; Dr. John Shires). The lentiviral vector, as shown in Schematic 3.1, contained the wild-type human insulin gene driven by a cytomegalovirus (CMV) promoter for constitutive gene expression. The Internal Ribosomal Entry Site (IRES), positioned between the human insulin and green fluorescence protein (GFP) reporter genes, provided an additional site for ribosomal binding during translation so that human insulin and GFP

proteins could be separately synthesized. Two days after seeding in 12-well plates at $1x10^5$ cells/cm^2, lentivirus was added at a multiplicity of infection of 30 to fresh medium containing 8 μg/mL of polybrene (Sigma, St. Louis, MO). After 24 hours, the medium in wells was changed to fresh, cells were expanded and passaged twice, and insulin secretion rate (ISR) tests were performed 13 days post-transduction.

Schematic 3.1: Lentiviral vector containing the wild-type human insulin gene driven by a CMV promoter for constitutive expression followed by the GFP reporter gene. An IRES between the two genes allows for the translation of GFP separately from insulin gene translation.

3.3.3 Fluorescence Activated Cell Sorting

Since only transduced cells expressed GFP, fluorescence served as an indicator of transduction efficiency measured by fluorescence activated cell sorting (FACS). FACS was also performed on GLUTag-eINS cells to generate a pure, GFP-positive population. Using the BD FACS Aria cell sorter (BD Biosciences; San Jose, CA), GFP-positive and GFP-negative cells were sorted into separate tubes and percentages of each were estimated by FACSDiva software after 10,000 events. The negative control, non-transduced GLUTag-INS cells, was used to set the fluorescence threshold under which cells were sorted as GFP-negative and above which cells were sorted as GFP-positive. This threshold was determined for each experiment and representative images of the setup and software analyses are shown in Figure 3.1. The GFP-positive population of GLUTag-eINS cells was

collected and seeded as a monolayer culture in 12-well plates for expansion, passaging, and ISR testing. After three passages, cells were conventionally frozen as the new cell line, GLUTag-EINS (EINS). Post-thaw, ISR tests and relative insulin mRNA quantitation were performed on EINS over eight passages to evaluate stability.

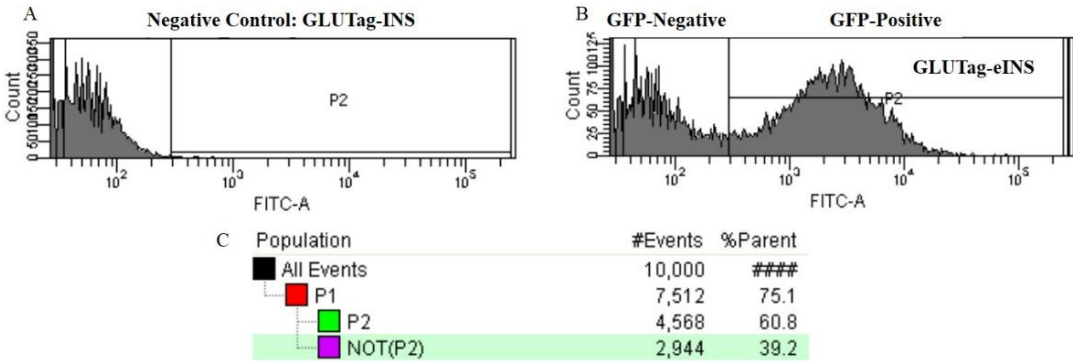

Figure 3.1: Representative setup and analysis screen using FACSDiva software for GFP cell sorting. P1 is the total sorted population of GLUTag-eINS cells, P2 is the GFP-positive population, and NOT(P2) is the GFP-negative population. A) Frequency plot of detected fluorescence from non-transduced GLUTag-INS cells, the negative control. B) Frequency plot shown during cell sorting in which GFP-negative cells below the set threshold were sent to one tube and GFP-positive cells above the set threshold were sent to a different tube. C) Population statistics chart indicating the percentages of each sorted population out of 10,000 sorted cells.

3.3.4 Human Insulin mRNA Quantitation

Cells were harvested for RNA isolation using the E.Z.N.A Total RNA Kit I (OMEGA bio-tek, Norcross, GA) followed by cDNA synthesis using the High Capacity cDNA Reverse Transcription Kit (Applied Biosystems, Grand Island, NY). cDNA was synthesized from 1μg of RNA following manufacturer's protocols. Real-time, relative

quantitation of insulin mRNA was accomplished using the SYBR Select Master Mix (Applied Biosystems) and the StepOnePlus Real-Time PCR System (Life Technologies) for measurement and comparative C_T method analysis. Human insulin primers were designed using National Center for Biotechnology Information's (NCBI's) Primer-BLAST design software and mouse beta-actin (ACTB) primers were used as endogenous controls. Primer sequences were as follows: forward human insulin 5'-CTA CCT AGT GTG CGG GGA AC-3', reverse human insulin 5'-AGC TGG TAG AGG GAG CAG AT-3', forward mouse ACTB 5'-GCA CAG CTT CTT TGC AGC TC-3', reverse mouse ACTB 5'-CTT TGC ACA TGC CGG AGC C-3'. All primers were used at 300 nM concentrations.

3.3.5 Secretion Enhancement via Histone Deacetylase Inhibition

A dose-response curve was constructed to determine the effect of varying TSA concentrations on insulin secretion and viable cell numbers. This study was performed on GLUTag-INS cells to determine an optimal TSA concentration for the remainder of the study, assuming GLUTag-INS and EINS trends were similar. Serial dilutions of TSA were made in dimethyl sulfoxide (DMSO; Sigma) starting at 2500 nM (six concentrations were tested: 0 nM, 156 nM, 313 nM, 625 nM, 1250 nM, and 2500 nM). After a 24 hour incubation at these varying TSA concentrations, cells in wells were washed twice in Dulbecco's Phosphate-Buffered Solution (DPBS; Corning cellgro) containing calcium and magnesium and then changed to 5mM glucose basal medium for a two hour incubation period, at which point samples were collected for insulin measurement. After collecting insulin samples, cells were trypsinized and viable cells were counted using trypan blue (Sigma).

For short-term studies, GLUTag-INS or EINS cells were seeded in 12-well plates at densities of $1.3x10^5$ cells/cm^2 two days before TSA treatment. On day 0 of the experiment, culture medium was changed to fresh in each well and TSA was added to a final concentration of 625 nM or 0 nM, the latter serving as the non-treated control group for direct comparison. After 24 hours of incubation, cells were washed twice with DPBS. ISR tests were then performed and cells in parallel wells were incubated for one hour in 5 mM glucose basal medium to be harvested for intracellular insulin and total RNA collection. To collect intracellular proteins, TSA and non-treated cell pellets were lysed using the Mammalian Cell Lysis Kit (Sigma). Proinsulin and insulin concentrations were then measured from the same secreted or intracellular sample by ultra-sensitive human insulin and human proinsulin radioimmunoassays (RIA; Millipore, Billerica, MA).

3.3.6 Long-Term Effects of a 24h TSA Treatment

Long-term effects of TSA were evaluated in microencapsulated EINS cells for 14 days in culture. EINS cells were grown in T-75 tissue culture treated flasks to approximately 90% confluency and treated for 24 hours with TSA at a 625 nM concentration. Cells were then washed twice with DPBS, trypsinized, microencapsulated in LVM alginate (LVM; Novamatrix, Drammen, Norway), and cross-linked in 30 mM $BaCl_2$ solution using an electrostatic droplet generator (Nisco Engineering, Zurich, Switzerland) as previously described [180]. ISR tests were performed on 0.1 mL microcapsule volumes 1, 7, and 14 days after microencapsulation. Microcapsules were also solubilized in ethylenediaminetetraacetic acid disodium salt dihydrate solution (ED2SS; 0.2 M; pH 9) to harvest cells for intracellular protein collection and total RNA isolation.

3.3.7 Insulin Secretion Rate Test

ISR tests performed on cell monolayers and microencapsulated cells involved subjecting cells to basal conditions (DMEM with 5mM glucose) for two hours followed by a two hour step-up period under stimulating conditions (DMEM with 5 mM glucose and 2% meat hydrolysate (MH); Sigma). Media samples were taken at 0 and 2 hours (t0, t2-) after adding basal medium and 0 and 2 hours (t2+, t4) after changing to stimulating medium (Schematic 3.2). To normalize secretion rate data to viable cell numbers, monolayers were trypsinized after ISR tests and trypan blue viable cell counting was performed using a hemacytometer. Secretion data from microcapsules were normalized to metabolic activity measured by alamarBlue™ (Life Technologies, Grand Island, NY) as in [192] using a one hour incubation period. Metabolic activity was used as a measure of viable microencapsulated cell number because, over time, cell remodeling and aggregation in microcapsules significantly reduced the accuracy of trypan blue cell counting.

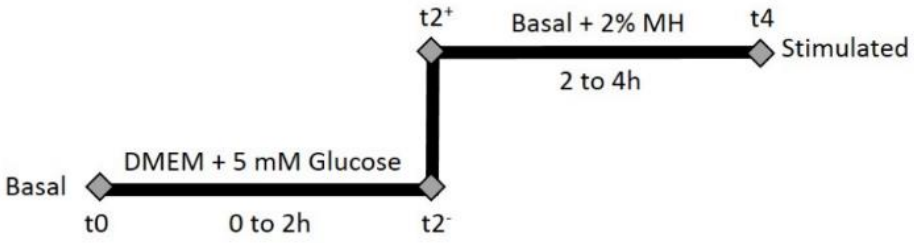

Schematic 3.2: ISR tests involved two hour incubation periods in basal and stimulating media with samples taken at times t0, t2-, t2+, and t4.

3.4 Results

3.4.1 Secretion Enhancement via Lentiviral Transduction

GLUTag-INS cells were transduced with LV-WT-INS and passaged twice, resulting in a 3-fold enhancement in both basal and stimulated insulin secretion rates (Figure 3.2A). A 61% transduction efficiency was achieved and FACS led to a 97% pure EINS population. EINS cells were then passaged three times and conventionally frozen. At early passages post-thaw ($p<8$), EINS produced 10-fold more insulin mRNA than GLUTag-INS, but secretion was only 2-fold higher (Figure 3.2). Then after several passages ($p>7$), EINS produced 3.5 times more insulin mRNA than GLUTag-INS, but secretion was no longer higher. While there was a general trend of decline, possibly due to gene silencing, in both insulin mRNA and secretion over passaging, fold-increases in EINS secretion responded disproportionately to changes in insulin mRNA. Additionally, higher mRNA production did not necessarily lead to more secretion. This implies that one or more steps between transcription and secretion could be limiting the fold-increase in EINS secretion.

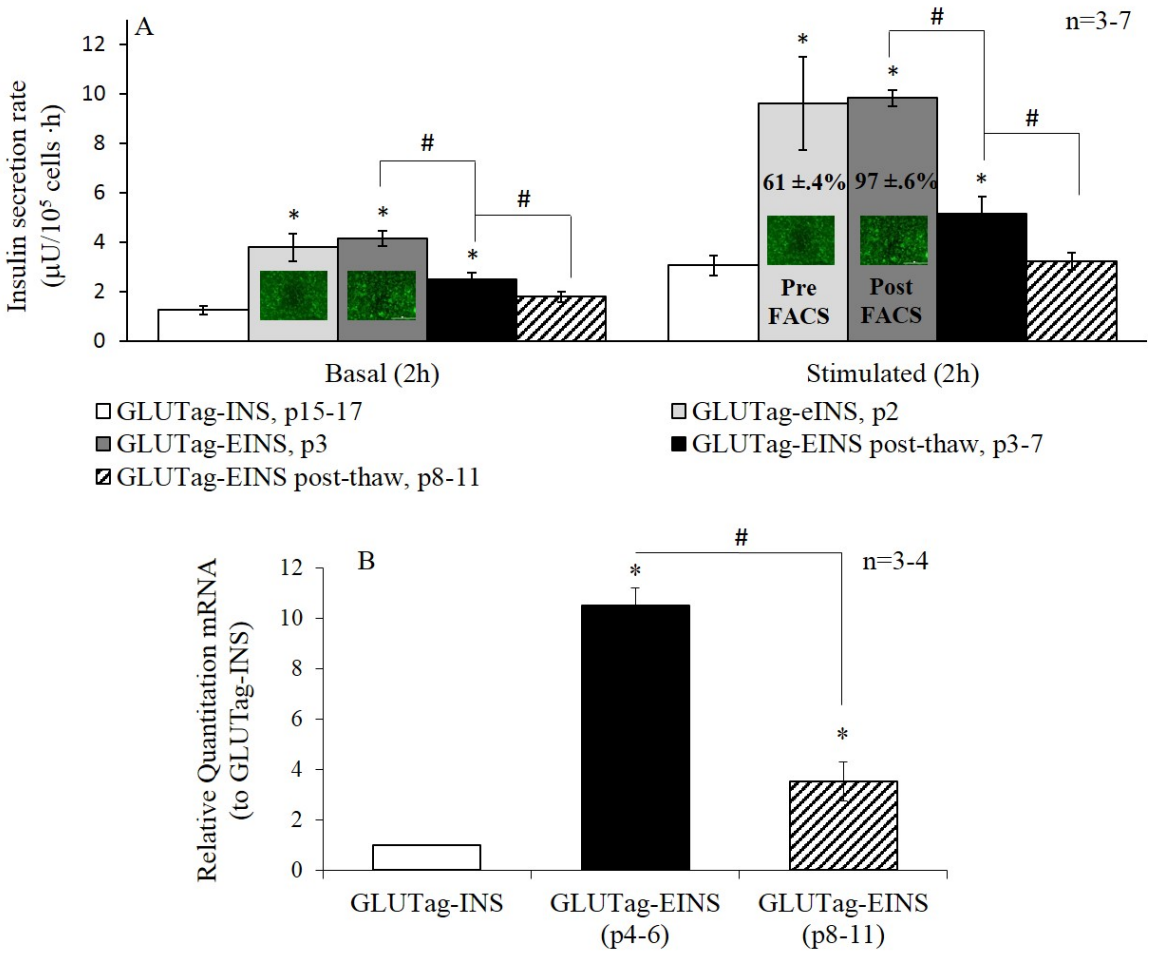

Figure 3.2: Long-term stability of human insulin mRNA and secretion after lentiviral transduction of GLUTag-INS. A) After transduction, eINS were passaged twice and purified to a 97% GFP-positive population to be conventionally frozen as the EINS cell line after three passages. ISR tests were performed on non-transduced GLUTag-INS (n=6), eINS passaged twice (n=3), EINS passaged three times (n=3), EINS at low passage numbers 4-7 post-thaw (n=7), and EINS at high passage numbers 8-11 post-thaw (n=6). From left to right, the average stimulation indices (SIs) ± standard error were 2.5 ± 0.2, 2.5 ± 0.3, 2.4 ± 0.1, 2.0 ± 0.1, and 1.8 ± 0.1. SIs were determined by dividing stimulated by basal secretion. B) Human insulin mRNA levels from early and late passages of EINS post-thaw were quantified relative to GLUTag-INS. Asterisks indicate a statistical difference from GLUTag-INS either under basal or stimulated conditions in graph A, or GLUTag-INS insulin mRNA in graph B (*$p<0.05$). # indicates statistical differences between EINS passages (#$p<0.05$).

3.4.2 Short-Term HDACi Studies

The dose-response curve in Figure 3.3 depicts the effects of varying TSA concentrations on the secretion and viable number of GLUTag-INS cells. TSA treatment resulted in significant cell death dependent on dose. However, TSA had an enhancing effect on insulin secretion per viable cell, with an initial 2 to 2.4-fold increase at low TSA concentrations (0.157-0.625 μM) increasing to 3.5 times higher than non-treated cells at concentrations of 1.25-2.5 μM. Based on these data, a TSA concentration of 0.625 μM was chosen for the remaining studies to evaluate cells with significantly enhanced insulin secretion without excessive loss of cell viability.

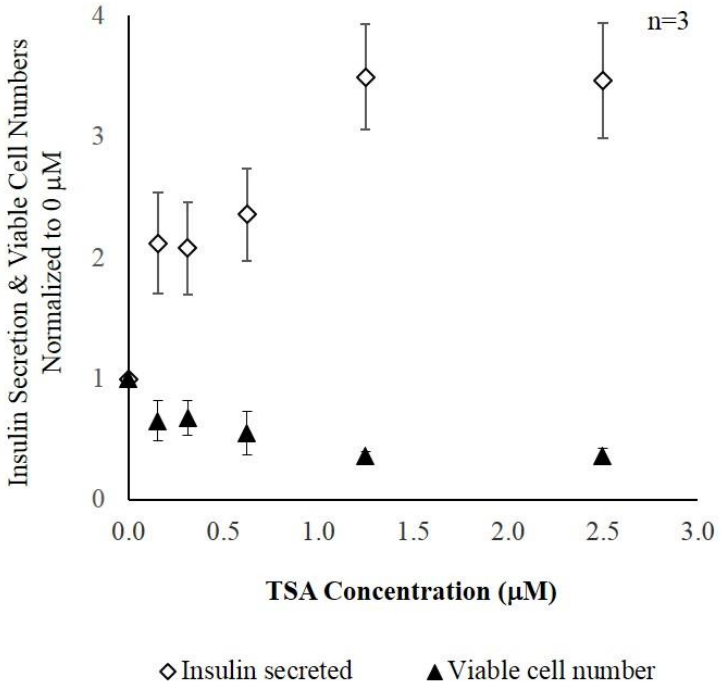

Figure 3.3: TSA dose response curve with data normalized to GLUTag-INS treated with 0 μM TSA. TSA concentration effects on viable GLUTag-INS cell number and insulin secretion normalized to viable GLUTag-INS cell number were evaluated. All data points were statistically different from GLUTag-INS treated with 0 μM TSA.

Insulin mRNA from high-passaged EINS increased 6.6-fold after a 24h treatment with 0.625 μM TSA, whereas no difference (p=0.9) in GLUTag-INS mRNA levels was detected after treatment (Figure 3.4). If indeed the lentivirus-incorporated insulin transgene had been silenced, it is possible that TSA treatment revived its expression in EINS but had no effect on the stably transfected insulin transgene in GLUTag-INS. Due to a difference in only one amino acid, however, distinguishing between B10 and wild-type human insulin is highly complex, making lentivirus-incorporated transgene silencing and reactivation difficult to confirm.

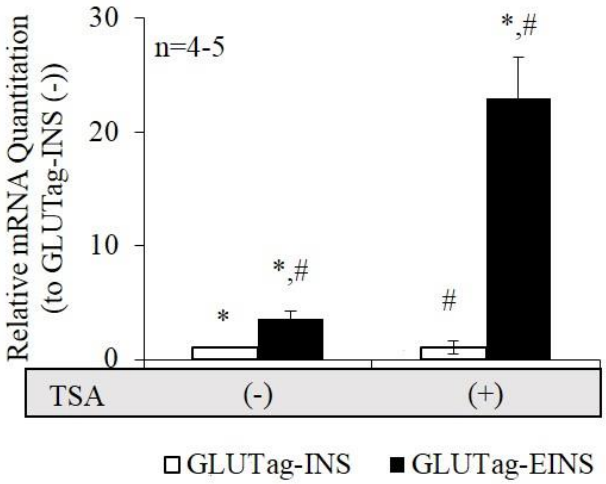

Figure 3.4: TSA effects on insulin mRNA levels in GLUTag-INS and EINS, relative to non-treated GLUTag-INS. Bars sharing symbols are statistically different (*, # $p<0.05$).

Similar to EINS insulin mRNA, EINS proinsulin storage was initially 2-fold higher than GLUTag-INS and increased 5.5-fold after TSA treatment (Figure 3.5B). Interestingly, TSA induced a 2-fold increase in GLUTag-INS proinsulin storage even though mRNA had

been unaffected, suggesting a possible effect of TSA on proinsulin independent of transcription. Surprisingly, both GLUTag-INS and EINS stored the same amount of insulin under either TSA or non-treated conditions (Figure 3.5A), regardless of the fact that proinsulin storage was higher in EINS. This was the first discrepancy observed in the EINS RSP, in which more stored proinsulin did not result in more stored insulin. Therefore, a step between proinsulin and insulin synthesis may have been limiting.

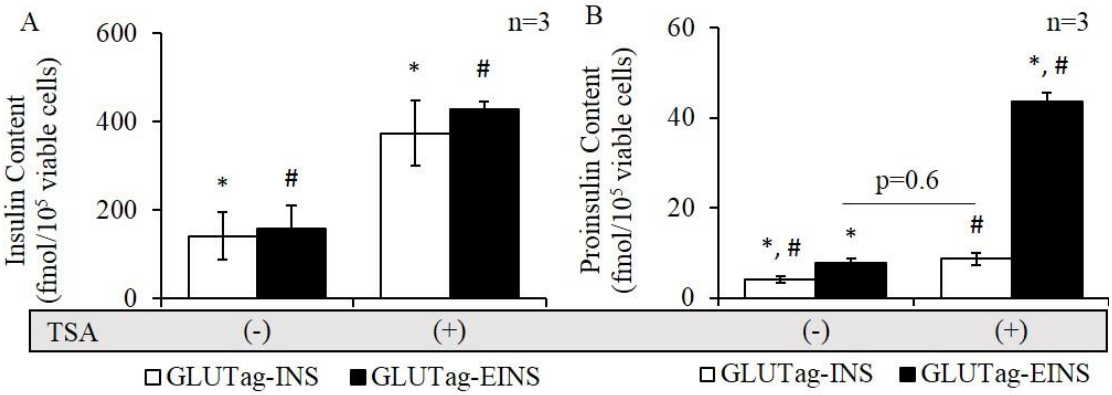

Figure 3.5: TSA effects on GLUTag-INS and EINS intracellular A) insulin and B) proinsulin content normalized to viable cell number. Bars sharing symbols are statistically different (*, # $p<0.05$).

While proinsulin storage was higher in EINS versus GLUTag-INS, EINS basal proinsulin and insulin secretion were not higher (Figure 3.6). This may suggest that the intracellular surplus of proinsulin in EINS was neither converted to insulin for storage nor was it secreted. TSA treatment appeared to at least partially alleviate this issue, causing a significant increase in EINS proinsulin secretion rates with 50-70% more secreted relative to GLUTag-INS. However, the fold-increase in basal proinsulin secretion was higher than

the fold-increase in insulin secretion in both cells, implying that conversion in secreting vesicles may be another limiting step in the RSP.

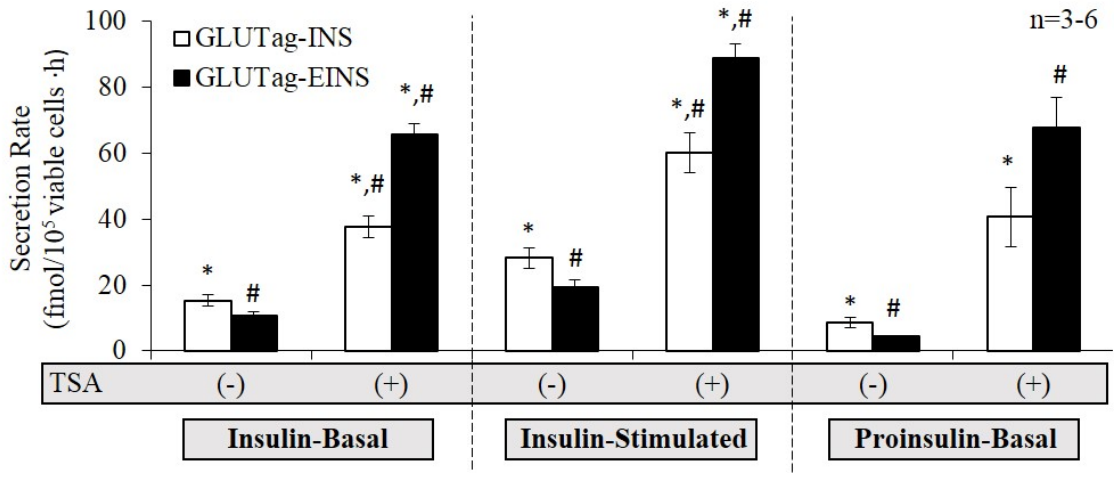

Figure 3.6: TSA effects on GLUTag-INS and EINS insulin and proinsulin secretion rates normalized to viable cell number. Statistical comparisons are indicated between groups under each condition (insulin-basal, insulin-stimulated, proinsulin-basal) and bars sharing symbols are statistically different (*, # $p<0.05$). Statistical comparisons were also made between basal and stimulated insulin secretion groups, indicating that stimulated secretion was significantly higher than the corresponding basal secretion ($p<0.05$).

In support of storage results, EINS appeared less efficient in converting intracellular proinsulin to insulin under either TSA-treated or non-treated conditions (Table 3.1). Additionally, EINS intracellular processing efficiency declined from 95% to 91% after TSA treatment while GLUTag-INS processing efficiency remained the same. Perhaps prohormone convertases were able to keep up with the 2-fold increase in GLUTag-INS proinsulin, but were unable to remain as efficient after the 5.5-fold increase in EINS proinsulin. In support of secretion rate results, secretion processing efficiencies in

GLUTag-INS and EINS were comparable under both conditions, with both declining significantly after TSA treatment. This could again suggest that low proinsulin conversion in secreting vesicles limited basal insulin secretion.

Table 3.1: Mean proinsulin to insulin conversion efficiencies ± standard deviation with and without TSA treatment were determined separately for intracellular and secreted steps in the RSP of GLUTag-INS and EINS cells. Secreted protein measurements were made from samples of basal medium (5 mM glucose) that were taken after a two hour incubation period. Percentages were calculated by dividing the insulin quantity by the total quantity of insulin and proinsulin. Statistical comparisons were made separately for intracellular and secreted processing efficiencies (each column). An asterisk identifies efficiencies that are statistically different from non-treated GLUTag-INS and efficiencies sharing a # symbol indicates that they are statistically different from one another (*, # $p<0.05$).

	TSA	Intracellular	Secreted
GLUTag-INS	(-)	97 ± 0.9%	67 ± 3.0%
	(+)	98 ± 0.2%	52 ± 6.3% *
GLUTag-EINS	(-)	95 ± 0.6% *,#	70 ± 3.6% #
	(+)	91 ± 0.9% *,#	50 ± 6.2% *,#

Overall, TSA-treated EINS had the highest insulin secretion rates, highest proinsulin secretion and intracellular content, and highest insulin mRNA levels (Table 3.2). Interestingly, TSA-treated GLUTag-INS were the second highest insulin secretors even without insulin mRNA enhancement, suggesting that TSA can also act on mechanisms other than insulin transcription to augment secretion. However, since the only difference between GLUTag-INS and EINS was the additional lentivirus-incorporated insulin transgene in EINS, mRNA enhancement likely played some role in secretion improvement.

Table 3.2 displays the intracellular and secreted proinsulin buildup, especially under TSA-treated conditions. Further studies should be pursued to investigate methods that relieve these bottlenecks in the RSP.

Table 3.2: Effects of TSA on insulin mRNA levels and various stages of the RSP of GLUTag-INS and EINS, represented as a fold-difference from non-treated GLUTag-INS. Basal secretion results are represented under the proinsulin and insulin secreted column. Average non-treated GLUTag-INS values were mRNA-1.0, intracellular proinsulin-4.2 fmol/10^5 cells, intracellular insulin-142 fmol/10^5 cells, basally secreted proinsulin-8.6 fmol/10^5 cells·h, and basally secreted insulin-15.3 fmol/10^5 cells·h.

			Intracellular Content		Secreted	
TSA	Cells	mRNA	Proinsulin	Insulin	Proinsulin	Insulin
(-)	GLUTag-EINS	3.5	1.9	1.1	0.5	0.6
(+)	GLUTag-INS	1.1	2.1	2.6	4.8	2.4
	GLUTag-EINS	23	10.9	3.0	8.0	3.8

3.4.3 Long-Term Effects of a 24h TSA Treatment

EINS were chosen for the long-term TSA study because they were the most promising insulin secretors in short-term studies. A 3D environment was chosen because it was better at sustaining viable cell numbers over time than the 2D monolayers (data not shown) and alginate microcapsules have shown promise as a pancreatic substitute configuration in preclinical studies [21]. After a 24h TSA treatment, cells were microencapsulated and cultured *in vitro* for fourteen days. Insulin secretion was 70-80% higher after TSA treatment one day post-encapsulation (two days after TSA treatment) and was sustained for seven days in culture (Figure 3.7). By day 14, however, secretion was no

longer enhanced; insulin mRNA and intracellular insulin had also significantly declined by day 14. Even on day 7, a dramatic decline in insulin mRNA was observed, but this appeared to have no effect on secretion. It was only until day 14 that intracellular and secreted insulin significantly declined to pre-treatment levels. This further strengthens the short-term study findings that suggest human insulin mRNA levels do not always correlate with insulin secretion.

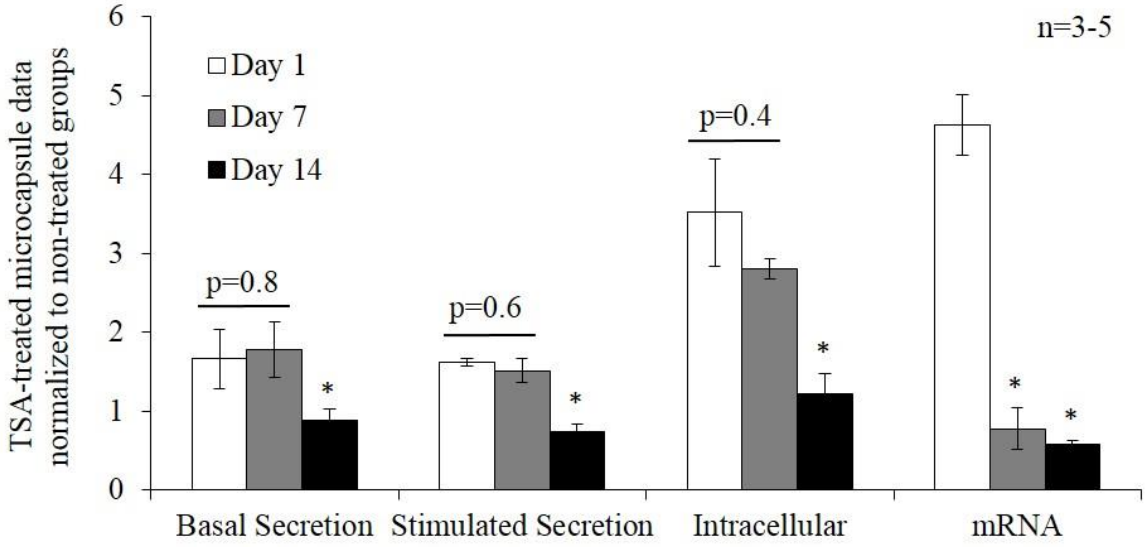

Figure 3.7: Long-term TSA effects on basal and stimulated ISR normalized to alamarBlue™, intracellular insulin content normalized to alamarBlue™, and insulin mRNA from alginate microencapsulated EINS cells over 14 days. To make TSA fold-increase comparisons among secreted, intracellular, and mRNA groups, all data were normalized to non-treated microencapsulated EINS cells cultured and tested in parallel to treated groups. Asterisks indicate a statistical difference from day 1 within each respective measurement (*$p<0.05$). See APPENDIX G for the table of values from non-treated groups that were used to normalize the data.

3.4.4 Effects of HDAC6 Inhibition On Insulin Secretion

Effects of tubacin on secretion were investigated to determine the role of HDAC6 in the enhancement observed from TSA treatment (Figure 3.8). Tubacin treatment experiments were identical to TSA monolayer treatments, except a final concentration of 4 μM was used instead of 0.625 μM. The tubacin concentration was estimated based on cytoblot analyses of TSA and tubacin effects on acetylated tubulin levels in A549 cells in which a tubacin concentration of roughly 4 μM caused a similar increase in acetylated tubulin levels as a TSA concentration of approximately 0.625 μM [193]. Interestingly, a 24 hour tubacin treatment had no effect on basal or stimulated secretion from either cell line, suggesting that HDAC6 had played no role in secretion enhancement. Tests such as this one, with other specific HDACi, may provide more insight into the main mechanisms for the observed enhancements after TSA treatment.

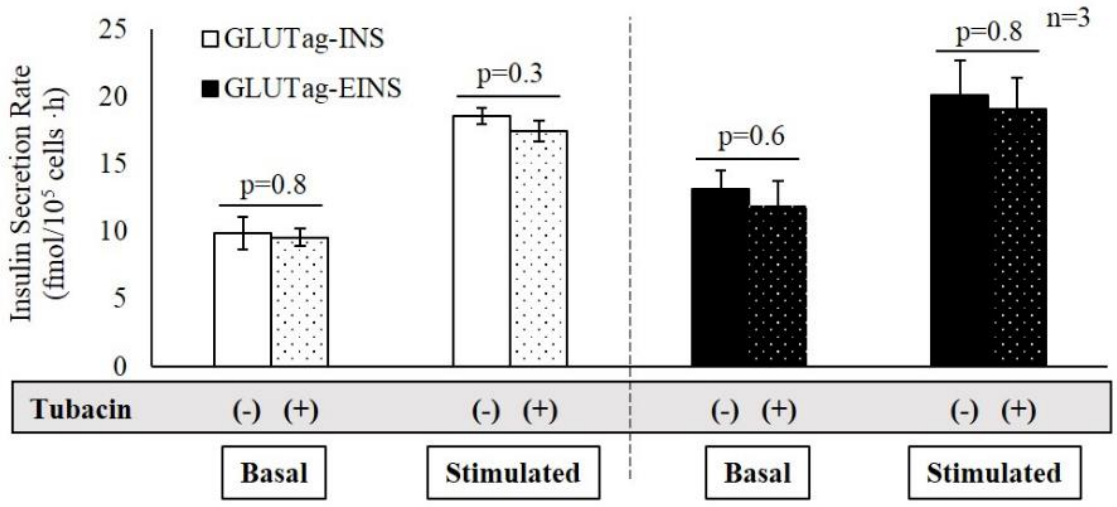

Figure 3.8: Tubacin effects on basal and stimulated insulin secretion from GLUTag-INS and EINS cells. GLUTag-INS and EINS were treated with tubacin at a final concentration of 4 μM for 24 hours, washed twice with DPBS, and tested for ISR.

3.5 Discussion

Enteroendocrine cells are promising as non-β cell sources for diabetes therapy, but novel engineering methods need to be developed to generate cells that are capable of secreting therapeutic quantities of recombinant insulin. Two enhancement methods, lentiviral insulin transgene incorporation and TSA treatment, were applied to GLUTag-INS cells in this study to generate secretion rates ranging from 655-888 fmol/10^6 cells^{-1}·h^{-1} compared to the range of 384-3930 fmol/10^6 cells^{-1}·h^{-1} reported from βTC-3 cells [73]. These have come the closest to murine β cell line secretion, significantly surpassing secretion rates reported from previously engineered enteroendocrine cells that ranged from 32-204 fmol/10^6 cells^{-1}·h^{-1} [16, 18, 125]. In long-term studies, partial secretion enhancement effects were sustainable for seven days in alginate microcapsules, suggesting

HDAC inhibition as a possible drug therapy for weekly enhancement of transplant function. Finally, discrepancies between steps in the RSPs of GLUTag-INS and EINS cells have helped to identify proinsulin conversion as a potential target for optimizing insulin production. Although insulin mRNA enhancement is probably not essential to insulin secretion augmentation, evidence from EINS studies showed that it still contributes to an extent.

Basal secretion rate (75 fmol/10^6 cells·h), stimulation index (2.4), and proinsulin conversion (67%) results from GLUTag-INS cells in this study were similar to those reported in initial studies by Bara et al. (86 fmol/10^6 cells·h; 2.2; 70%). Lentiviral transduction of GLUTag-INS cells resulted in a transduction efficiency of 61%, higher than in previous studies using plasmid transfection [18] or AAV [125] gene delivery methods.

It was surprising to find, however, that after FACS, the purified population of EINS cells did not exhibit higher secretion rates. Perhaps insulin expression began to decline during and after the process of FACS so that the pure EINS population appeared no different from eINS. Another possibility is that the fluorescence intensity from some transduced eINS cells was lower than the set threshold for FACS and were not accounted for during transduction efficiency measurement. The original efficiency, therefore, may have been higher than 61% and purifying to 97% had no measurable effect. The difficulty in pinpointing the exact cause lies in the separate translation of the insulin and GFP genes, enabled by the IRES in the lentiviral vector. For this reason, fluorescence intensity did not correlate with insulin expression.

After lentiviral transduction and minimal passaging, EINS cells were secreting high quantities of insulin. Table 3.3 compares the average secretion rate, SI, and proinsulin

conversion of βTC-3 insulinoma [73] cells, engineered AtT20 [113] cells, engineered NCI-H716 [125] cells, engineered STC-1 [16] cells, GLUTag-INS [18] cells, and GLUTag-EINS cells (4-7 passages post-thaw).

Zhang et al. engineered the mouse STC-1 cells presented in Table 3.3 via stable transfection of K cells with the human insulin gene driven by a gastric inhibitor peptide (GIP)-specific promoter. Two of 22 isolated clones showed promise: one had decent basal insulin secretion (120 fmol/(10^6 cells·h)) but a low SI (1.4), and the other had a better SI (2.2), but basally secreted less insulin (32 fmol/(10^6 cells·h)). In our study, the ISR from EINS cells was 25% higher than the best secreting K cell clone and the SI was comparable to the more responsive K cell clone. We were therefore able to engineer one L cell line with both a good SI and high secretion capacity.

Variable, and sometimes conflicting results have been reported among groups using the heterogeneous STC-1 cell source to genetically engineer enteroendocrine cells. This is likely due to the additional complexity involved in engineering a mixed cell population since it requires the use of cell-specific promoters for targeted genetic incorporation. Using this approach, some groups have generated satisfactory insulin-secreting [15, 16], glucose-sensitive K cells [15-17] while others could not engineer glucose-responsiveness [194] or gain secretion above 2-11 fmol/(10^6 cells·h) [100, 195]. In the present study, using the homogeneous GLUTag L cell line has eliminated the need for cell-specific promoters, thereby simplifying the approach and allowing us to use a strong CMV promoter to drive transgene expression while also achieving meal-responsive insulin secretion.

Table 3.3: Comparisons of average basal and stimulated secretion rates, stimulation medium conditions, SI, and proinsulin conversion of βTC-3 insulinoma [73, 196]* cells, engineered AtT20 [113] cells, engineered NCI-H716 [125] cells, engineered STC-1 [16] cells, GLUTag-INS [18] cells, and GLUTag-EINS cells (4-7 passages post-thaw).

			Insulin secretion rate (fmol/(10^6 cells · h))	Stimulation Index (Stimulated/Basal)	% Proinsulin Conversion ((Insulin/Total) x 100)
Mouse βTC-3 Insulinomas	Basal	0 mM Glucose	384	10	*84 %
	Stimulated	16.7 mM Glucose	3930		
Engineered Mouse Pituitary AtT20 Cells	Basal	0 mM BrcAMP	60	6	N/A
	Stimulated	5 mM BrcAMP	360		
Engineered Human NCI-H716 Cells	Basal	0% MH	79	2.6	80 %
	Stimulated	2% MH	204		
Engineered Mouse STC-1 Cells	Basal	1 mM Glucose	32	2.2	N/A
	Stimulated	10 mM Glucose	70		
GLUTag-INS	Basal	0% MH	86	2.2	70 %
	Stimulated	2% MH	189		
GLUTag-EINS (p4-7)	Basal	0% MH	150	2.1	70 %
	Stimulated	2% MH	315		

Although transgene incorporation via lentivirus into GLUTag-INS was highly efficient, ten times more insulin mRNA in early passages of thawed EINS cells was only accompanied by a 1.7 to 2-fold increase in secretion. Transcriptional enhancement was therefore beneficial, but not in itself sufficient to significantly boost secretion to therapeutic levels. Furthermore, lentiviral-mediated transgene delivery was not a suitable method for stable gene expression in GLUTag-INS cells since secretion enhancement was eventually lost over passaging. Gene silencing can be an issue when using AAV, retroviruses, and lentiviruses for transgene delivery and even the presence of a CMV promoter has been associated with gene silencing [89-91]. As in other studies, inhibiting HDACs in lentivirally transduced EINS cells with TSA may have reversed gene silencing and reactivated transgene expression [92, 93].

Although HDACs were originally named for their action on histone proteins, recent findings have shown that they also play a role in 875 other classes of proteins [197]. Our findings indicated that TSA treatment did not solely affect transgene transcription, but it also had effects on downstream steps in the RSP. This was most clearly seen after TSA treatment of GLUTag-INS cells when intracellular and secreted proinsulin and insulin levels increased even though no difference was observed in insulin mRNA levels. Additionally, long-term studies showed that secretion enhancement effects were still present even after insulin mRNA declined back to original levels.

The approximate half-maximal effective concentration range (EC_{50} = 156-625 nM) of TSA on insulin secretion in this study was similar to a study with cytoblot assay images indicating an EC_{50} range (200-1000 nM) of TSA on α-tubulin acetylation in the human alveolar epithelial A549 cell line [193]. Dompierre et al. reported that TSA increased α-

tubulin acetylation in neuronal cells, leading to an increase in the vesicular transport of BDNF, and enhanced BDNF secretion [190]. Treatment with tubacin, a specific HDAC6 inhibitor, had the same effects as TSA and HDAC6 was identified as a potential target for Huntington's disease. In this work, tubacin treatment of GLUTag-INS and EINS cells had no effect on secretion, suggesting that HDAC6 inhibition did not play a role in the secretion enhancement observed from TSA treatment. Further studies with specific HDACi may help to identify the key mechanisms for secretion augmentation to develop novel, targeted treatment options.

Out of all the non-β cell sources that have been investigated, enteroendocrine cells appear to be the most promising because their endogenous functions are so similar to natural β cells. This study has narrowed down promising research avenues for developing a successful enteroendocrine cell-based diabetes therapy. Cellular engineering studies can focus on relieving bottlenecks in the RSP such as those identified in this work. HDACi can be investigated as a novel drug therapy for enhanced transplant function since long-lasting effects of HDAC inhibition by TSA were observed for seven days in culture. Future work should include long-term *in vitro* and *in vivo* studies to optimize the HDACi treatment protocol. Perhaps periodic treatment in small doses will better augment secretion in a sustained manner. As TSA acts on ten different HDACs, an in-depth mechanistic study should be pursued to identify specific HDACi that augment L cell secretion to develop targeted therapies with reduced side effects for clinical use.

CHAPTER 4: DEVELOPMENT AND IN VITRO CHARACTERIZATION OF A BIOLUMINESCENT PANCREATIC SUBSTITUTE BASED ON MICROENCAPSULATED, ENHANCED RECOMBINANT L-CELLS

4.1 Abstract

Cell-based insulin therapies can potentially improve glycemic regulation in insulin dependent diabetes patients. Enteroendocrine cells engineered to secrete recombinant insulin have exhibited glycemic efficacy, but are primarily studied as uncontrollable growth systems that lead to tumor formation. Encapsulation is a strategy for controlling cell growth, but has precluded therapeutic efficacy, possibly due to suboptimal construct designs. In addition, critical factors that influence graft outcome *in vivo* are difficult to delineate. In this study, tissue engineering strategies were applied to design an optimized encapsulation configuration for enhanced recombinant insulin secretion on a per-graft basis. To provide a growth-controlled and immune protective environment without affecting secretion, cells were microencapsulated in barium alginate. We were able to observe an approximate 100-fold increase in secretion relative to a macrocapsule construct previously fabricated in our lab. In addition, with the goal of enhancing graft fate understanding, stable bioluminescence was incorporated via luciferase lentivirus transduction and microencapsulation effects on signal and tracking capabilities were studied. Although it has been popular in tracking survival of free cells, little is known of

the ability for bioluminescence to track encapsulated cells. Data showed that microencapsulation had no effect on bioluminescence signal and allowed for real-time cell tracking under conditions of normoxic growth and anoxia-induced death. In this work, we have developed a bioluminescent, controlled-growth non-β cell pancreatic substitute that, at a 3 mL graft volume, comes the closest to therapeutic insulin output compared to previous enteroendocrine constructs. The next step is to test whether a secretion of 16-24 mU of human insulin/day is therapeutically meaningful in a preclinical diabetes model.

4.2 Introduction

Cell-based therapies are under development to replace current treatment options for diabetes, as they offer significant promise in providing improved regulation of daily blood glucose levels by continuously, rather than discretely, restoring homeostasis. In particular, engineering and transplanting autologous non-β cell sources could address donor cell scarcity and avoid autoimmune destruction [184]. Although non-β cell candidates like engineered intestinal endocrine cell lines have restored normoglycemia in preclinical diabetes models, tumor formation has prevented its clinical applicability [15, 16]. Encapsulated configurations can control cell growth, but have stymied therapeutic efficacy [17, 20]. A probable hindrance to success is suboptimal construct design, but the critical factors that influence graft outcome *in vivo* are difficult to delineate. There is a need to improve controlled-growth non-β cell systems and expand *in vivo* graft fate understanding.

This need may be partially addressed by altering the encapsulation configuration. In fabricating an encapsulation device, the choice of biomaterial, cell loading capacity, and preservation of cell function are critical factors [198]. Bara et al. seeded human insulin-

secreting L cells in a macrocapsule device for transplantation [18-20], but blood glucose levels were unaffected; detecting human insulin in the blood was, however, promising. Unniappan et al. found that alginate microencapsulated insulin-producing intestinal K cells were also unable to control blood sugars until a drug-inducible element was incorporated into the insulin transgene [17]. Limitations imposed by the choice of encapsulation configuration may have been partially responsible for their failure as standalone diabetes treatments.

Limitations to the macrocapsule device fabricated by Bara et al. were its inability to load high cell densities and its significant detriment to apparent insulin secretion rates per cell relative to secretion from unencapsulated cells grown on tissue culture plastic, perhaps due to delayed diffusion via mm length scales between cells and the *in vivo* environment [21]. One of the major disadvantages *in vivo* was construct weakness and breakage observed from explanted constructs, which was the likely cause for immune attack [41].

Instead of using a macrodevice, Unniappan et al. developed engineered K cell grafts by applying a microcapsule configuration [17]. Such a configuration should better prevent capsule breakage, permit nutrient diffusion over micron length scales, and allow for high cell density loading. However, Unniappan et al. were still unable to achieve therapeutic efficacy in diabetic mice in the absence of a drug-inducible element and periodic drug administration. A potential limitation to the study may have been the choice of 1.5% sodium alginate and a calcium chloride cross-linking solution which was found by Duvivier-Kali et al. to result in significantly more capsule overgrowth and breakage *in vivo* compared to 3.3% (wt/vol) alginate microcapsules cross-linked in barium chloride solution

[149]. Although the major reason for therapeutic failure was likely insufficient insulin secretion per engineered K cell, neither fibrosis nor microcapsule breakage were reported, which may have at least partially contributed to *in vivo* graft failure.

Previous configurations that have been applied to insulin-secreting enteroendocrine cells should be improved by optimizing diffusion, cell loading density for sufficient insulin output, and biomaterial composition for reduced breakage and host response. Although optimizing these factors are believed to be important, the data do not exist from previous studies which ascertain the precise causes for engineered enteroendocrine graft failure *in vivo*. For this reason, the development process is slower than it should be and methods must be developed which allow researchers to isolate the key factors that contribute to graft failure.

In most cases, graft efficacy is assessed by endpoint measurements from the animal model, which offers limited information into what is happening to the graft itself. The efficacy of insulin-secreting cell grafts is typically evaluated by measuring blood glucose, plasma C-peptide, and glycosylated hemoglobin levels [165]. However, these measurements do not allow for direct monitoring of the graft or the identification of probable causes of failure.

Magnetic resonance imaging (MRI) has been identified as a suitable tracking method for *in vivo* graft monitoring [176, 177], with its own advantages and limitations [178]. Some studies have investigated the application of ^{19}F nuclear magnetic resonance (NMR) spectroscopy to measure the oxygen concentration at the graft site in mice post-transplantation of microencapsulated β cells [179, 180]. This method, however, only allowed for indirect graft monitoring. Alternatively, ^{1}H NMR has been applied for direct

monitoring of encapsulated β cells, but the macrocapsule construct design that allowed for such monitoring was not optimal for cell function [181]. The ideal monitoring method should allow for minimally-invasive *in vivo* real-time tracking of the transplant while preserving construct design for optimal graft function.

Bioluminescence imaging (BLI) is a powerful tool to directly monitor cell fate in animals due to its low cost, high sensitivity, ease of operation, near background-free imaging conditions, and reduction of inter-animal variability [165, 166]. The first proof-of-concept BLI study with free islets offered encouraging results, as it demonstrated that islets transduced *in vitro* with a luciferase lentivirus could be quantitatively monitored long-term after transplantation in the kidney capsule of diabetic mice [167]. Subsequent studies investigated the use of BLI in early detection of islet graft rejection [168], islet survival immediately post-transplantation [169], and guided timing for corrective interventions [170].

As the field progressed into using tissue engineered microencapsulation strategies, BLI incorporation did not follow. Some studies have applied BLI to macrocapsule or fixed systems that retained the cells at a particular anatomic locale [171-174], but these strategies lack certain advantages of freely floating microcapsules [184] and may not be optimal for cell function. Quantitative effects of microencapsulation on BLI signal and real-time cell survival tracking capabilities remain unknown.

In this work, we altered previous encapsulation configurations and applied a BLI method to develop an optimized, controlled-growth non-β cell pancreatic substitute with real-time monitoring capabilities. In addition, we used the early passage GLUTag-EINS cells previously engineered in our lab, based on the GLUTag-INS cell line [18], with

significantly enhanced recombinant insulin secretion. We demonstrated that our microcapsule configuration permitted insulin secretion and BLI signal detection, and that *in vitro* quantitative BLI could be used for real-time survival tracking of encapsulated cells under conditions of growth and anoxia-induced death. The implications of developing such a pancreatic substitute for preclinical efficacy will be discussed.

4.3 Materials and Methods

4.3.1 Luciferase Reporter Gene Incorporation

GLUTag-EINS (EINS) cells were seeded at a density of $1x10^5$ cells/cm^2 in a 24-well plate. Cells were transduced with firefly luciferase lentivirus (F-Luc Lentivirus; Capital Biosciences, Rockville, MD) at a Multiplicity of Infection (MOI) of 30 following the company's protocol, expanded, passaged, and conventionally frozen as a new cell line: GLUTag-EINS-Fluc (Fluc). The lentiviral vector contained the luciferase reporter gene driven by the constitutive cytomegalovirus (CMV) promoter.

4.3.2 Cell Microencapsulation and Culture

EINS and Fluc cells were microencapsulated in LVM alginate (LVM; Novamatrix, Drammen, Norway) cross-linked in 30 mM $BaCl_2$ solution using an electrostatic droplet generator (Nisco Engineering, Zurich, Switzerland), as previously described [180]. The diameter of the resulting microcapsules was 730 ± 94 μm (average ± standard deviation). Microencapsulated EINS and Fluc cells were cultured in non-treated T-75 flasks in Dulbecco's modified Eagle's medium (DMEM) with 25 mM glucose, without L-glutamine

(Corning cellgro, Manassas, VA), and supplemented with 10% fetal bovine serum and 1% penicillin/streptomycin. Cultures were kept on a rocker plate in a humidified incubator at 37ºC/5% CO_2.

4.3.3 *In Vitro* BLI Characterization

4.3.3.1 BLI and Metabolic Activity Correlations

To determine the effect of microencapsulation on BLI and metabolic activity correlations, cultures of Fluc monolayers and microcapsules were initiated at varying cell numbers ranging from 0.3-2x10^6 cells; bioluminescence and metabolic activity were measured one day later. In all studies, metabolic activity was measured using alamarBlue™ (Life Technologies, Grand Island, NY) as previously described [192] with an incubation period of one hour. Two independent experiments were performed at four different cell numbers each, resulting in eight data points for each correlation.

4.3.3.2 Growth and Death Characterization

To characterize BLI tracking of cell growth in microcapsules, microencapsulated Fluc cells were cultured for a period of 17 days. Metabolic activity, total DNA, light microscopy images, and BLI were obtained on days 1, 3, 7, 11, 14, and 17. Data were compared to day 1 for statistical analysis.

To evaluate real-time BLI response to microencapsulated cell death, a fraction of the microcapsule population (corresponding to approximately 6 x 10^6 cells) was transferred on day 14 to tubes containing 2 mL unsupplemented DMEM (Sigma, St. Louis, MO) with 5

mM glucose; tubes were hermetically sealed with no gas headspace. Anoxic conditions arose due to oxygen consumption by cells. Prior to measurement, microcapsules from tubes were cultured under normoxic conditions for one hour to allow recovery of any living cells. Metabolic activity and bioluminescence were measured every 12 hours in the first 36 hours post-sealing to capture the initial dynamic phase of cell death and an additional sample was taken at 84 hours to ascertain any additional cell death at later time points.

For DNA measurements, 0.1 mL capsules were solubilized in ethylenediaminetetraacetic acid disodium salt dihydrate solution (ED2SS; 0.2 M; pH 9) for three minutes, then DNA purification (Mammalian cell lysis kit; Life Technologies) and Quant-iT PicoGreen dsDNA assay (Life Technologies) were performed according to the manufacturer's protocols.

4.3.4 Pancreatic Substitute Fabrication

Insulin secretion rate (ISR) tests were performed on EINS and Fluc cells passaged 3-7 times post-lentiviral transduction. Monolayers were seeded in 12-well plates and subjected to basal conditions (DMEM with 5mM glucose) for two hours followed by a two hour step-up period under stimulating conditions (basal medium with 2% meat hydrolysate (MH); Sigma). Insulin measurements were made using an insulin radioimmunoassay (RIA; Millipore, Billerica, MA).

One and fourteen days post-encapsulation, ISR tests were performed on 0.1 mL volumes of microcapsules in 100 μm strainers placed in 12-well plates. Viable cell counts were only possible one day post-encapsulation, before cell aggregation within microcapsules prevented reliable hemacytometer cell counting. For this reason, metabolic

activity measurement via alamarBlue™ was used to track viable microencapsulated cells over time. After an ISR test, microcapsules were either solubilized for trypan blue (Sigma) viable cell counting or incubated in alamarBlue™ for one hour.

4.3.5 Bioluminescence Imaging

Bioluminescence imaging was performed using the IVIS Lumina (Perkin Elmer, Grayson, GA). Once the sequence was acquired, photon emission was quantified from a selected region of interest (ROI). *In vitro* monolayers and microencapsulated cells were imaged in 12-well plates by adding D-luciferin (RPI Corp, Mount Prospect, IL) at a final concentration of 180 mg/mL immediately before imaging. The ROI and settings were kept constant for all experiments.

4.3.6 Statistical Analysis

All data were analyzed using Minitab software (Minitab, Inc., State College, PA) and reported as mean ± standard error; each mean was the average of data from three or more independent experiments. Significance was determined using a one-way analysis of variance (ANOVA) with the general linear model, with significance defined as $p \leq 0.05$.

4.4 Results and Discussion

4.4.1 Bioluminescence Incorporation

Fluc monolayers expressed a stable bioluminescence signal of 80 photons $cell^{-1}$ s^{-1} (Figure 4.1A). Basal and stimulated ISR from Fluc cells were comparable to EINS cells,

and remained significantly higher than the non-transduced GLUTag-INS cells (Figure 4.1B). Insulin secretory function was, therefore, preserved after luciferase lentivirus transduction.

4.4.2 BLI Characterization

4.4.2.1 BLI and Metabolic Activity Correlations

Microencapsulation of Fluc cells within Ba^{2+} cross-linked alginate resulted in no attenuation of bioluminescence signal. Additionally, microencapsulation did not change the close correlation between metabolic activity and bioluminescence over varying cell-seeding densities (Figure 4.2A). A similar positive correlation was also observed in temporal studies where cells proliferated within microcapsules for 14 days (Figure 4.2B); the higher variability of the data noted in this case was likely due to differences in cell aggregation and remodeling within microcapsules over time. Figure 4.3 is a pictorial representation of the positive correlation between cell proliferation and bioluminescence signal within the microcapsules.

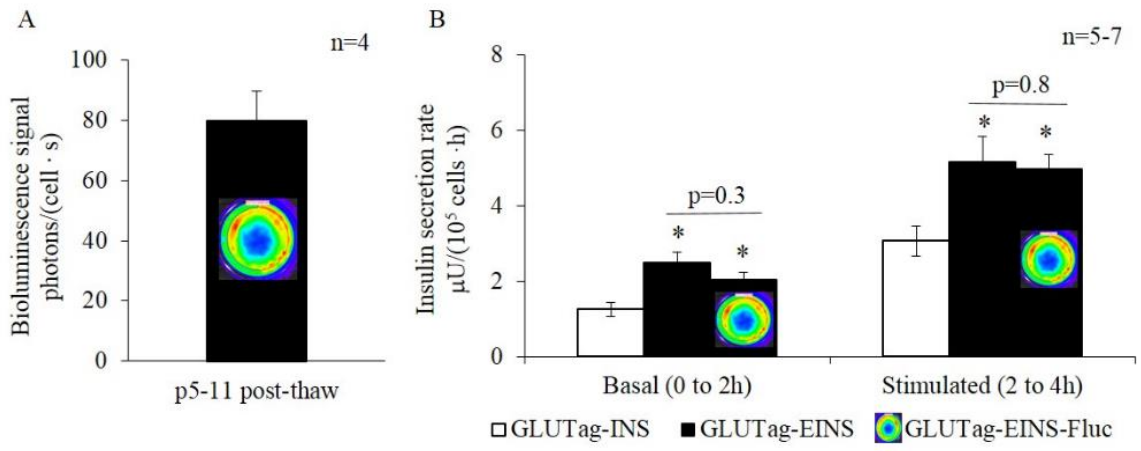

Figure 4.1: Bioluminescence incorporation into EINS cells via luciferase lentivirus transduction. A) Stable bioluminescence signal from Fluc monolayers over several passages post-transduction. B) Bioluminescence incorporation had no apparent effect on ISR. Asterisks indicate statistical difference from non-transduced GLUTag-INS cells under each condition.

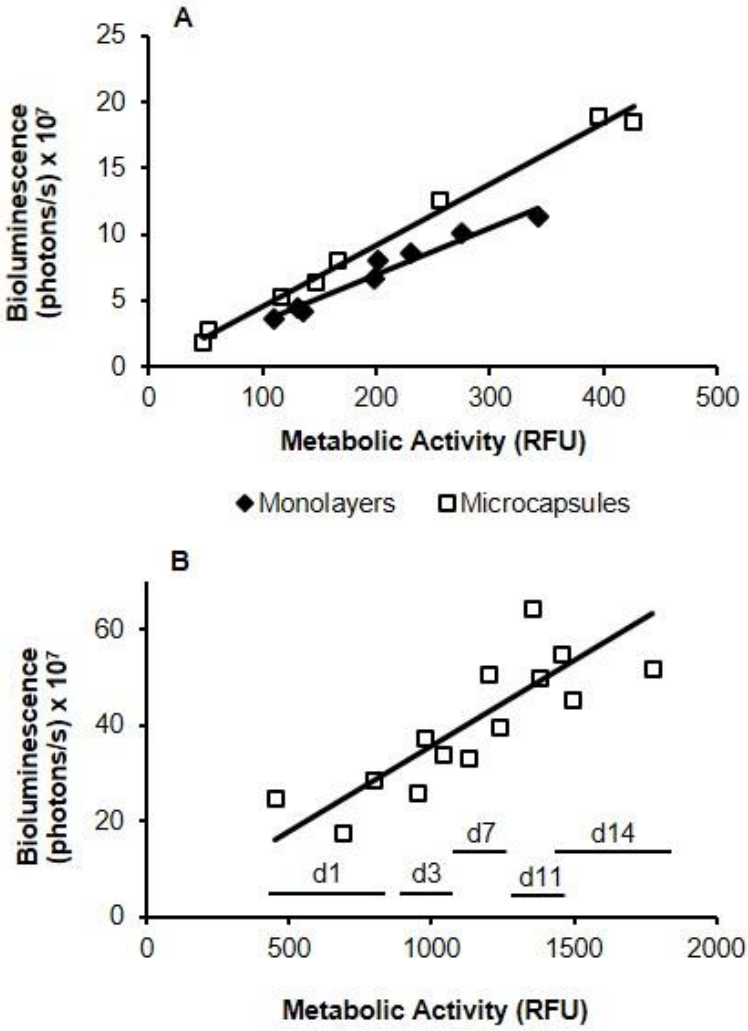

Figure 4.2: The strong positive correlation between bioluminescence and metabolic activity of Fluc cells remained the same after microencapsulation and during proliferation in culture. A) Cell monolayer and microencapsulated cell correlations one day after seeding at varying cell densities. B) Microencapsulated cell correlation with cells allowed to proliferate over 14 days *in vitro*. The number of days after encapsulation are indicated underneath the corresponding set of data points and labeled as d1, d3, d7, d11, and d14.

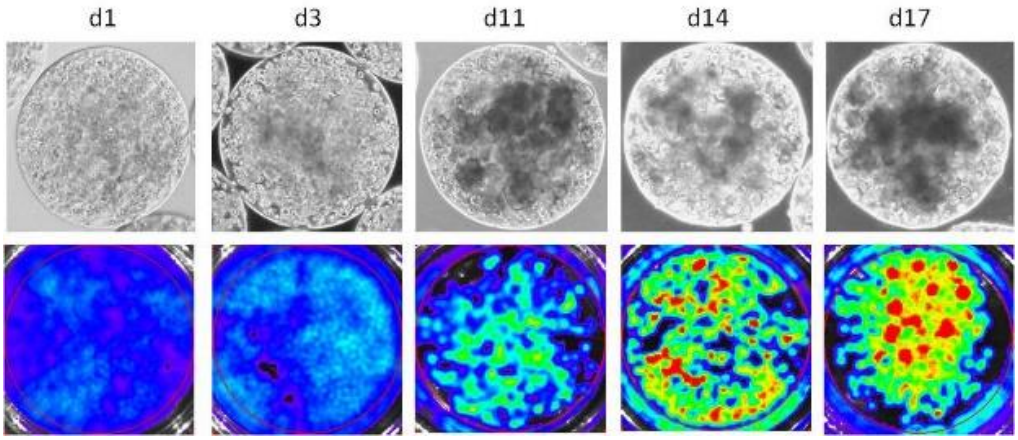

Figure 4.3: Representative bright field microscopy images of a single microcapsule over 17 days in culture (top row) and BLI images of a 0.1 mL microcapsule volume in a single well of a 12-well plate over 17 days (bottom row). Days post-encapsulation are indicated by d1, d3, d11, d14, and d17.

4.4.2.2 Growth and Death Characterization

To fully characterize the monitoring capabilities of bioluminescence from cells growing within microcapsules, Fluc cells were encapsulated and tracked for 17 days *in vitro*. Bioluminescence signals exhibited similar levels of increase to metabolic activity and total DNA until day 7 to 12 post-encapsulation; this increase was followed by a plateau for the remainder of the study (Figure 4.4). This plateau was likely due to an eventual equilibrium between cell growth and death, which is reached at a viable cell density that depends on the capsule characteristics and surrounding oxygen concentration [199, 200]. Total DNA appeared to take longer to plateau relative to bioluminescence and metabolic activity (Figure 4.4B), likely resultant from accumulation of both viable and non-viable cellular DNA within the microcapsules over time. On the other hand, BLI captured growth dynamics of only viable cells, closely tracking cell metabolic activity.

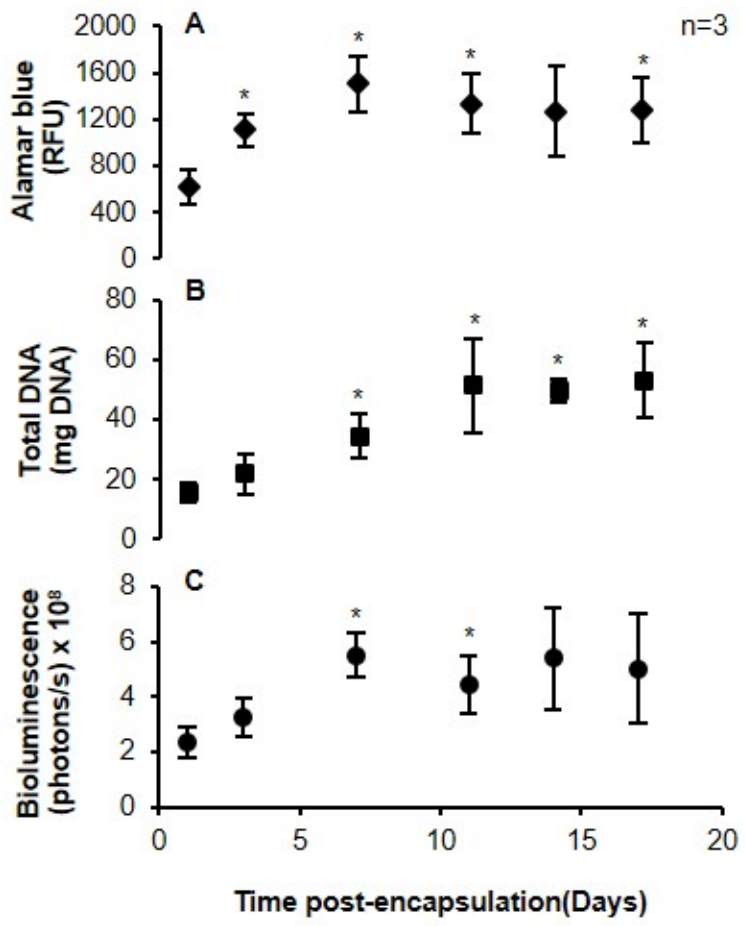

Figure 4.4: Bioluminescence tracked metabolic activity trends of microencapsulated Fluc during cell growth in culture. A) Metabolic activity measured by alamarBlue™, B) total DNA, and C) bioluminescence signal were followed over time in culture for 17 days. For each time point and measurement, a 0.1 mL volume of microcapsules was sampled from each culture. *$p<0.05$: Statistically higher than day 1.

To determine the response time of bioluminescence signal to cell viability loss, death of microencapsulated cells was prompted by anoxia. Cell death due to reduced dissolved oxygen is physiologically relevant, as severe hypoxia occurs in the peritoneal cavity especially after transplantation of encapsulated cells [179, 180]. After stopping culture oxygenation, a significant decline in bioluminescence signal occurred over twelve

hours followed by a more gradual decrease until the end of the experiment at 84 hours. Again, bioluminescence signal closely tracked the metabolic activity with no apparent time lag between the two measurements over the entire study period (Figure 4.5).

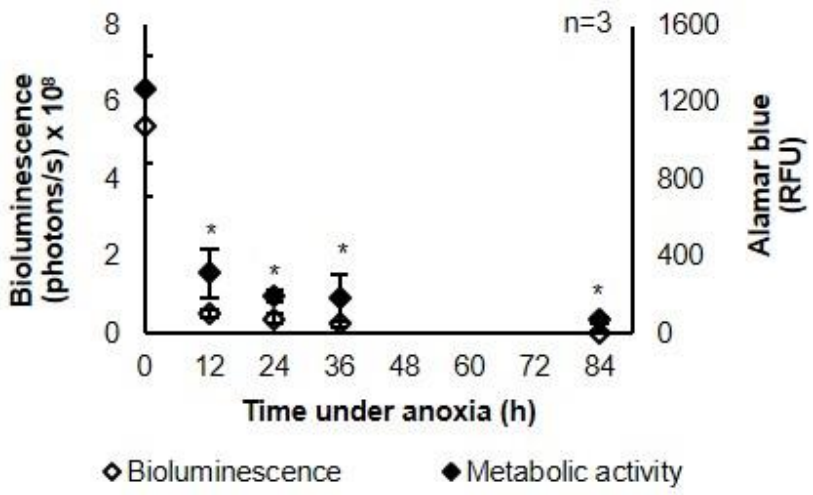

Figure 4.5: Bioluminescence tracked the decline in metabolic activity of microencapsulated Fluc in real-time over 84 hours during cell death induced by anoxia. *p<0.05: Statistically lower than at 0 h.

4.4.3 Pancreatic Substitute Fabrication

Microencapsulation had no apparent effect on insulin secretion per cell and no statistical difference existed between EINS and Fluc secretion one day post-encapsulation (Figure 4.6B). However, 14 days post-encapsulation, less secretion per Fluc microcapsule volume was observed (Figure 4.6C) while the stimulation index remained the same (Figure 4.6D). Interestingly, Fluc exhibited 52% less metabolic activity, as assessed by alamarBlue™, than EINS on day 14 possibly due to slower Fluc cell growth within

microcapsules leading to lower insulin output per microcapsule. These data instigated the fabrication of a mixed microcapsule system consisting of mostly EINS to maximize insulin output and enough Fluc to retain BLI monitoring capabilities.

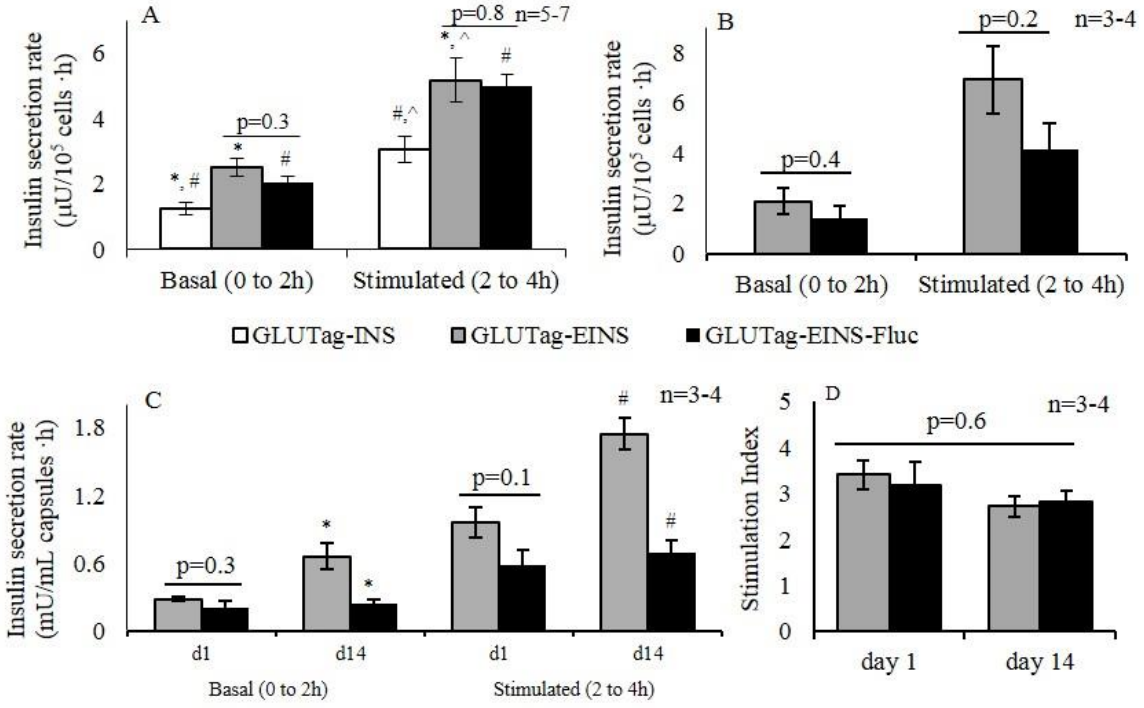

Figure 4.6: *In vitro* pancreatic substitute fabrication and characterization. A) Basal and stimulated ISR from GLUTag-INS, GLUTag-EINS, and GLUTag-EINS-Fluc cell monolayers. B) ISR normalized to viable cell number from microencapsulated EINS and Fluc cells one day post-encapsulation. C) ISR per mL volume of microencapsulated EINS and Fluc cells 1 and 14 days post-encapsulation (d1 & d14). D) Stimulation indices (stimulated/basal ISR) of microencapsulated EINS and Fluc cells 1 and 14 days post-encapsulation. Shared symbols above bars indicate significant differences (*, #, ^ $p<0.05$). In Figure A, statistical comparisons were made between basal and stimulated data for each group and between groups for each condition. In Figures B-C, statistical comparisons were made only between groups under each condition. All data in Figure D were compared.

Estimates of transplant volumes that would be required to normalize glycemia were based on reported insulin secretion from microencapsulated βTC-tet cells that restored normoglycemia in STZ-induced diabetic mice upon i.p. injection [180]. EINS data from Figure 4.6 indicated that 7.5 mL microcapsules would need to be transplanted to match βTC-tet graft secretion. Due to mouse model space restrictions however, 3 mL (corresponding to $9x10^7$ EINS cells or 42% of βTC-tet graft secretion) will be the maximum volume attempted for transplant (Table 4.1). Based on these approximations, lowered blood glucose levels in diabetic mice without complete normoglycemic restoration are expected.

Table 4.1: Estimated therapeutic potential of GLUTag-EINS grafts based on secretion output from successful βTC-tet grafts [180].

Cell type	Implant Volume	Encapsulation Density	Total # Cells Implanted	Insulin Secreted from Graft
βTC-tet	0.2 mL	2 x 10^7 cells/mL	4 x 10^6 cells	1.38 μmol/day
GLUTag-EINS	3 mL	3 x 10^7 cells/mL	9 x 10^7 cells	0.58 μmol/day
			% βTC-tet:	**42%**

Altering the previous macrocapsule configuration (agarose disc construct containing GLUTag-INS cells) to 3.3% high mannuronic acid alginate microcapsules cross-linked in barium chloride solution containing the enhanced GLUTag-EINS cells resulted in a superior controlled-growth graft that secreted roughly 100-fold more insulin per day than the macrocapsule graft formerly developed [19]. The microcapsule

configuration allowed for 3.5-fold higher cell loading densities ($3.0x10^7$ cells/mL alginate versus $8.6x10^6$ cells/mL agarose) and 30-fold more total cell numbers in one, 3 mL graft volume ($9.0x10^7$ cells) compared to the 350 μL macrocapsule construct that supported only $3.0x10^6$ viable cells.

Contrary to the macrocapsule device which significantly hindered the apparent insulin secretion rate per cell, alginate microencapsulation had no such effect. The 3.3% barium alginate microcapsule configuration was also applied to prevent host cell overgrowth and capsule breakage which have been observed in previous studies of calcium alginate microcapsules [149]. The goal is to minimize host cell adhesion to the semi-permeable alginate membrane and therefore minimize the blockage of nutrient and insulin diffusion to and from the transplanted cells. Additionally, minimizing capsule breakage will in effect minimize the host response. In order to determine whether the configuration is advantageous in this way, it will be evaluated in therapeutic efficacy studies.

A BLI system was established in the same pancreatic substitute for temporal monitoring of microencapsulated cells. Although these microencapsulated cell transplants are a common configuration, BLI has not previously been applied to such a system. *In vitro* studies elucidated that luciferase lentivirus transduction resulted in stable bioluminescence signal without seriously compromising insulin secretion. In addition, microencapsulation had no effect on BLI signal and bioluminescence closely tracked temporal changes due to cell growth and anoxia-induced death within microcapsules. With real-time monitoring BLI capability such as this *in vitro*, it can be reasonably expected that the graft will show similar capabilities *in vivo* and help to identify key factors that contribute to graft failure.

In this work, we have developed a bioluminescent, controlled-growth non-β cell pancreatic substitute that comes the closest to therapeutic insulin secretion output when compared to successful β cell diabetes therapies and is the first with real-time monitoring capabilities. The next step is to test the therapeutic efficacy of transplanting this developed construct, based on engineered L cells, in a preclinical diabetes mouse model.

CHAPTER 5: IN VIVO THERAPEUTIC EFFICACY AND SURVIVAL EVALUATION OF AN ENHANCED, BIOLUMINESCENT PANCREATIC SUBSTITUTE*

5.1 Abstract

Cell-based insulin therapies can potentially improve glycemic regulation in insulin dependent diabetes patients. Enteroendocrine cells engineered to secrete recombinant insulin have exhibited glycemic efficacy, but are primarily studied as uncontrollable growth systems in immune incompetent mice. In addition, reports suggest that suboptimal insulin secretion and the absence of real-time tracking methodologies remain barriers to expanded application. Genetic and tissue engineering strategies were previously applied to optimize recombinant insulin secretion from intestinal L cells on both a per-cell and per-graft basis; the luciferase reporter gene was also incorporated for bioluminescence (BLI) monitoring. To provide a growth-controlled and immune protective environment without affecting secretory capacity or BLI signal, cells were microencapsulated in barium alginate. *In vivo* BLI was characterized in normal mice at subtherapeutic cell numbers and approximately 9 x 10^7 microencapsulated cells were injected intraperitoneally in immune-competent streptozotocin-induced diabetic mice for therapeutic efficacy evaluation. Transient normoglycemia was achieved in treated mice two days after transplantation, and endogenous insulin was sufficient to sustain body weights of treated mice receiving minimal supplementation. Glycemic efficacy of a bioartificial pancreas based on insulin

*Modification of a paper published in **Transplantation** (in press)

secreting enteroendocrine cells is insufficient as a standalone therapy, despite enhancement of graft insulin secretion capacity. Supplemental strategies to alleviate secretion limitations should be pursued.

5.2 Introduction

In 2011, the CDC reported that 25.8 million people in the United States alone are affected with Diabetes, and 6.7 million of them are dependent on insulin [1]. To prevent long-term complications in patients with insulin dependent diabetes (IDD), blood glucose levels must be tightly regulated with multiple daily insulin injections or continuous subcutaneous insulin infusion (CSII) by pump [2]. Even with diligent monitoring and insulin administration, many patients fail to achieve recommended control of their blood sugars. There is a clear need for a diabetes treatment that improves glycemic regulation without further burdening patients, to reduce morbidity and improve quality of life.

A cell-based approach, islet transplantation, has had some clinical success in addressing this need. However, widespread use is still hindered by islet scarcity and immune rejection producing limited durability [3]. These hurdles have motivated researchers to explore the possibility of using autologous non-β cells as a replacement therapy, by engineering the diabetic patient's own healthy non-β cells to become meal or glucose-responsive insulin secretors. Three enteroendocrine cell types, gastric G cells [12], intestinal L cells, and intestinal K cells [13], inherently possess a secretory mechanism like β cells. These cells also express the necessary prohormone convertases for proinsulin to insulin processing, making them promising β cell surrogate candidates.

Initial proof-of-concept studies showed that mice transgenic for human insulin-secreting K cells were resistant to streptozotocin (STZ)-induced diabetes [12]. Similarly, insulin-secreting G cells significantly reduced mouse blood glucose levels [14]. The engineering of enteroendocrine cells, such as K cells isolated from the heterogeneous immortalized STC-1 cell line [15, 16] and stably transfected with an insulin transgene, have permitted preclinical evaluation without resorting to transgenics. Insulin-secreting K cell clones were selected and tested for efficacy after cell transplantation into diabetic mice. Both studies reported restoration of normoglycemia, but mice became hypoglycemic as unrestricted cell proliferation increased insulin production beyond therapeutic levels. Additionally, immune-incompetent mice were used as the preclinical model to avoid transplant rejection.

Encapsulating cells to control cell growth and provide immune protection, and transplanting in immune-competent diabetic mice addressed both issues. Unniappan et al. found that microencapsulated insulin-producing K cells were unable to control blood sugars until a drug-inducible element was incorporated into the insulin transgene [17]. Alternatively, Bara et al. seeded human insulin-secreting L cells in a macrocapsule device for transplantation [18-20]. Human insulin was detected in mouse plasma, but blood glucose levels were unaffected. Insufficient insulin secretion and limitations imposed by macrocapsules were two likely barriers that prevented these controlled-growth enteroendocrine cell systems from serving as standalone diabetes treatments. In addition, the inability to delineate the critical factors that influenced graft survival and function over clinically relevant time scales should be addressed to accelerate therapy development.

Bioluminescence imaging (BLI) is a powerful tool to directly monitor cell fate in animals, but it remains unknown whether free microcapsules, a routine transplant configuration for insulin therapy [152, 179, 201-205], can indeed be successfully monitored *in vivo* using BLI. A potential barrier to achieving real-time BLI indications of graft survival using this configuration is increased imaging distances that could result from dynamic *in vivo* microcapsule dispersion. It is therefore important to determine whether such an approach is worth pursuing.

In the first part of this study, we evaluated the extent to which free injectable alginate microcapsules containing insulin-secreting, bioluminescent intestinal L cells could be monitored *in vivo* for survival via BLI. We have demonstrated that *in vivo* graft survival can be identified by BLI measurements consistently above background in mice following transplantation by intraperitoneal (i.p.) injection. In the second part of this study, we report the therapeutic effects of enhanced insulin-secreting and bioluminescent L cells, based on recombinant GLUTag cells [18], that were microencapsulated in barium alginate and transplanted i.p. in STZ-diabetic mice. We discuss the implications of this study in the context of a standalone enteroendocrine cell therapy and the potential benefit of a dual cell therapy for complete normoglycemic restoration.

5.3 Materials and Methods

5.3.1 Cell Lines and Culture Conditions

GLUTag-INS [18], GLUTag-EINS (EINS), and GLUTag-EINS-Fluc (Fluc) cells were cultured as in [191] using Dulbecco's modified Eagle's medium (DMEM) with 25 mM glucose, without L-glutamine (Corning cellgro, Manassas, VA), and supplemented

with 10% fetal bovine serum and 1% penicillin/streptomycin. Cultures were propagated in a humidified incubator at 37°C/5% CO_2. The EINS cell line had been generated by transduction of GLUTag-INS with the wild-type human insulin lentivirus (WT-INS; Emory University; Dr. John Shires) and the Fluc cell line had been generated by transduction of EINS with the firefly luciferase lentivirus (Capital Biosciences, Rockville, MD).

5.3.2 *In Vivo* BLI Characterization

All procedures were approved by the Georgia Institute of Technology's Animal Care and Use Committee. Seven week old male BALB/c mice were obtained from The Jackson Laboratory (Bar Harbor, ME). On day 0, Fluc cells were encapsulated at $3x10^7$ cells/mL alginate, and a 1 mL capsule volume was transplanted i.p. through an 18 gauge needle in each of six mice under isoflurane anesthesia, while an approximate 1 mL volume was cultured in parallel *in vitro* for direct comparison. Cell-free microcapsules were transplanted in one mouse as a negative control. To monitor possible hypoglycemia, glucose concentrations were measured in blood samples collected from the tip of the tail using a TRUEtrack glucose monitor (Nipro Diagnostics, Fort Lauderdale, FL). Bioluminescence images were acquired from *in vivo* and *in vitro* groups on days 3, 7, 11, 14, and 17 post-transplantation.

Three mice were euthanized on each of days 11 and 17. These two days were carefully chosen in order to gain mid- and end-point *in vivo* graft insight without unnecessarily sacrificing mice for every imaging day. Incisions were made through the skin and muscle of the abdomen and capsules were retrieved with a pipette following

peritoneal washes. Explanted capsules were cultured under normoxic conditions for two hours, then metabolic activity and bioluminescence signal were measured. Other explant assessments included light microscopy imaging, live/dead analysis, histology, and insulin secretion. Live/dead analysis was performed as in [180] and by following the manufacturer's protocol (LIVE/DEAD® Viability/Cytotoxicity Kit; Life Technologies). Hematoxylin/eosin (H&E) histology images of microcapsules were obtained as previously described [179] with resin embedding.

5.3.2.1 Statistical Analysis

All data were analyzed using Minitab software (Minitab, Inc., State College, PA) and reported as mean ± standard deviation; each mean was the average of three or more independent experiments. Significance was determined using a one-way analysis of variance (ANOVA) with the general linear model, with significance defined as $p \leq 0.05$.

5.3.3 Therapeutic Efficacy Evaluation

All procedures were approved by the Georgia Institute of Technology's Animal Care and Use Committee. Six week old male BALB/c mice were obtained from The Jackson Laboratory (Bar Harbor, ME). Six days before transplantation, diabetes was induced by i.p. injection of 180 mg/kg streptozotocin (STZ; Sigma) solubilized in sodium citrate solution (22.5 g/L; pH 4.5). Lantus® insulin was injected subcutaneously based on a predetermined criteria.

All microcapsules were fabricated one day before transplantation. On day 0, aliquots of microencapsulated EINS (2 mL) and Fluc (1 mL) cells were mixed in five

centrifuge tubes (3 mL each). Four tubes were prepared with 3 mL acellular microcapsules in each. Microcapsules were then washed eight times in 50 mL unsupplemented high glucose DMEM and loaded into 3 mL syringes. Five diabetic mice received the EINS/Fluc microcapsules (experimental group; n=5) and four received the acellular microcapsules (control group; n=4). Microcapsules were injected i.p. through an 18 gauge needle in mice under isoflurane anesthesia. Approximately 1 mL of the EINS/Fluc microcapsule mixture was cultured *in vitro* as a control, run parallel to *in vivo* groups.

Random, daily glucose concentrations were measured in blood samples collected from the tip of the mouse tail using a TRUEtrack glucose monitor (Nipro Diagnostics, Fort Lauderdale, FL); body weight was also measured daily. Mice were fed ad libitum until day 16 when mice were fasted overnight (16-18 hours) to examine effects of eating. See Schematic 5.1 for a visual representation of the efficacy evaluation study.

5.3.3.1 Exogenous Insulin Administration Criteria

Exogenous insulin (1-2 U Lantus® insulin every two days as long as mice were diabetic (higher than 350 mg/dl)) was administered to maintain body weight and avoid extreme hyperglycemia (higher than 450 mg/dl). To avoid hypoglycemia (lower than 50 mg/dl) and adjust for insulin produced by the grafts, transplanted animals only received 1 U Lantus® for persistently extreme hyperglycemia.

5.3.3.2 Explant Analyses

Mice were euthanized on day 17 and serum was collected by cardiac puncture, incubated in CAPIJECT® blood collection tubes with no additives at room temperature for

20 minutes, and centrifuged for 10 minutes at 4^{o} C and 1,600 xg for supernatant collection and insulin measurement. Grafts were retrieved by making incisions through the skin and muscle of the abdomen and collecting microcapsules with a pipette following peritoneal washes. Explant assessments included ISR and intracellular insulin measurement, BLI, metabolic activity measurement, live/dead analysis, light microscopy imaging, and hematoxylin/eosin (H&E) histological analysis. Live/dead analysis was performed by following the manufacturer's protocol (LIVE/DEAD® Viability/Cytotoxicity Kit; Life Technologies). Histology was performed as in [179] with resin embedding.

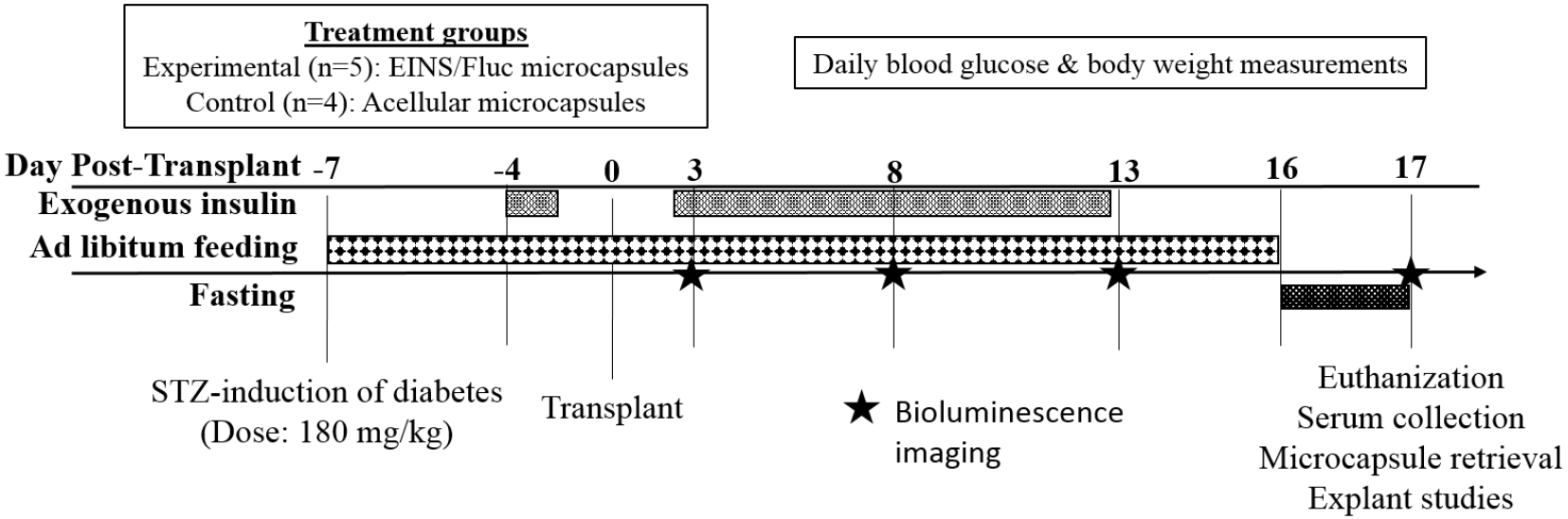

Schematic 5.1: Therapeutic efficacy study timeline.

5.3.3.3 Statistical Analysis

All data were analyzed using Minitab software (Minitab, Inc., State College, PA) and reported as mean ± standard error; each mean was the average of data from three or more independent experiments or mice. Significance was determined using a one-way analysis of variance (ANOVA) with the general linear model, with significance defined as $p \leq 0.05$.

5.3.4 Bioluminescence Imaging

Bioluminescence imaging was performed using the IVIS Lumina (Perkin Elmer, Grayson, GA). Once the sequence was acquired, photon emission was quantified from a selected region of interest (ROI). Microencapsulated cells (0.1 mL capsule volume) were imaged in 12-well plates by adding D-luciferin (RPI Corp, Mount Prospect, IL) at a final concentration of 180 mg/mL immediately before imaging. The ROI and settings were kept constant for all experiments. For *in vivo* imaging, mice were placed under isoflurane anesthesia (1.2%) and injected i.p. with D-luciferin at 200 mg/kg five minutes before an image acquisition of less than 20 seconds. The ROI was auto-adjusted to include the entire signal and thus account for microcapsule dispersion that could temporally change the ROI location. Bioluminescence data from each animal are reported in photons/s.

5.3.5 Insulin Secretion Rate Test

ISR tests were performed on 0.1 mL volumes of microcapsules in 100 μm strainers placed in 12-well plates. Microencapsulated cells were subjected to basal conditions (DMEM with 5mM glucose) for two hours followed by a two hour step-up period under stimulating conditions (basal medium with 2% meat hydrolysate (MH); Sigma). Media samples were taken at 0 and 2 hours (t0, t2-) after adding basal medium and 0 and 2 hours (t2+, t4) after changing to stimulation medium. Secretion data from microcapsules were normalized to metabolic activity measured by alamarBlue^{TM} (Life Technologies, Grand Island, NY) as in [192] using a one hour incubation period.

5.4 Results

5.4.1 *In Vivo* BLI Characterization

In vivo BLI characterization studies were conducted at sub-therapeutic levels in normal mice to establish the applicability of BLI to monitoring encapsulated cells in a generalizable, simplified animal model without confounding factors related to a diabetic state. Sub-therapeutic cell numbers were estimated based on insulin secreted from capsules, which was 10-15% of the amount of insulin needed to affect BALB/c glucose homeostasis [180].

Representative bioluminescence images from two of the six mice injected i.p. with a 1 mL volume of microencapsulated Fluc cells over the 17 day experiment are shown in Figure 5.1. Image acquisition began three days post-transplantation; high signal intensities (on the order of 10^9 photons/s) were obtained for the entire study duration. A representative image of one negative control mouse transplanted with cell-free microcapsules is included

in Figure 5.1 to illustrate the negligible BLI background levels (on the order of 10^5 photons/s). A distinct, sustained difference of four orders of magnitude between experimental and control groups gave clear indication of graft survival. BLI also allowed for spatial monitoring of microcapsules and indicated random dispersion throughout the peritoneal cavity.

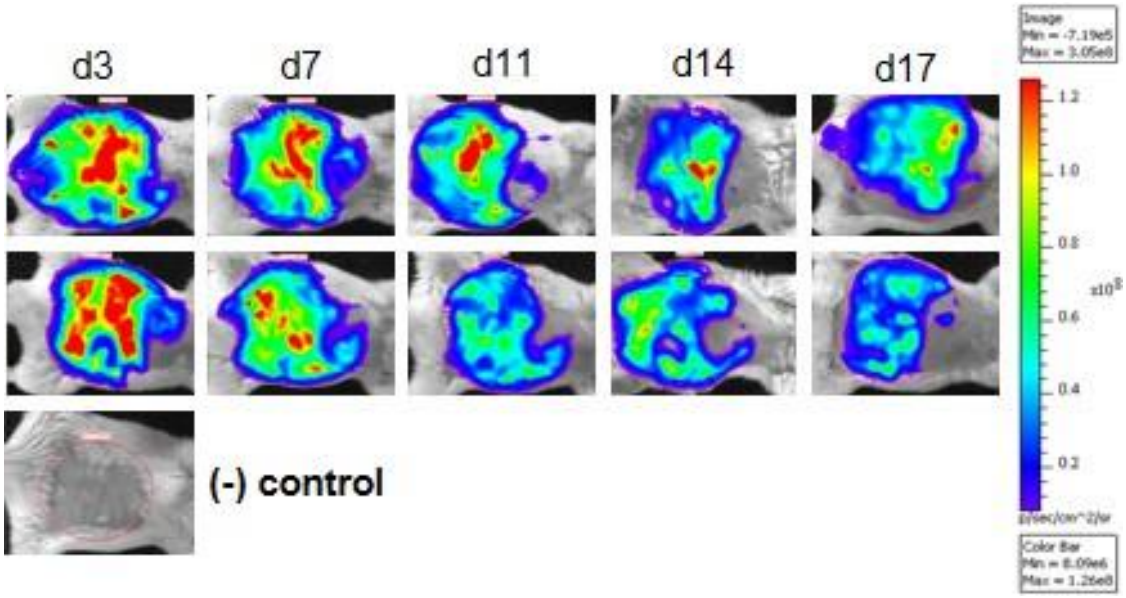

Figure 5.1: BLI allowed for survival and spatial monitoring of microencapsulated Fluc cells for 17 days after i.p. injection in six BALB/c mice. Representative *in vivo* IVIS images are shown from two of the six mice receiving a 1 mL volume of bioluminescent microencapsulated cells (different mice are separated by rows). The number of days after microencapsulation/transplantation are indicated by columns and labeled as d3, d7, d11, d14, and d17. One representative image of the negative control is shown in the third row as a mouse injected with cell-free microcapsules to indicate background signal.

Alongside *in vivo* studies, microencapsulated Fluc cells were cultured and characterized *in vitro*. Bioluminescence data were compared between the following

microcapsule groups: *in vitro*, *in vivo*, and microcapsules explanted on days 11 and 17 (Figure 5.2A). Comparable trends were observed between the *in vitro* and *in vivo* groups except on day 14, when *in vivo* BLI appeared lower than *in vitro*. This difference, however, was not significant on day 17 ($p = 0.3$), perhaps due to *in vitro* data variability. Interestingly, BLI from the explant group was consistently comparable to that from the *in vitro* group, suggesting that microencapsulated cells proliferated similarly *in vivo* as they did *in vitro*.

In agreement with the BLI data, comparable trends were observed between the *in vitro* and explant groups for metabolic activity on day 11 (1331 ± 254 and 1192 ± 184 Relative Fluorescence Units (RFU), respectively, $p = 0.49$) and day 17 (1277 ± 278 and 1190 ± 133 RFU, respectively, $p = 0.65$). Explant insulin secretory function on day 17 was not significantly impaired relative to *in vitro* microcapsules under both basal and stimulated conditions (explant: 192 ± 16 and 566 ± 202 μU (mL capsule)$^{-1}$ h^{-1}; *in vitro:* 300 ± 60 and 888 ± 226 μU (mL capsule)$^{-1}$ h^{-1}; $p = 0.10$ and $p = 0.21$ for basal and stimulated conditions, respectively). To investigate host cellular attachment to the graft, light microscopy imaging, live/dead confocal imaging, and histology were performed on retrieved microcapsules. Light microscopy revealed no host cell attachment to the periphery of the microcapsules (Figure 5.2B), which was further corroborated by H&E histology images (Figure 5.2C). There were no observable differences between the *in vitro* and explant live/dead confocal images which clearly indicated cell growth from day 11 to 17 for both groups (Figure 5.2D).

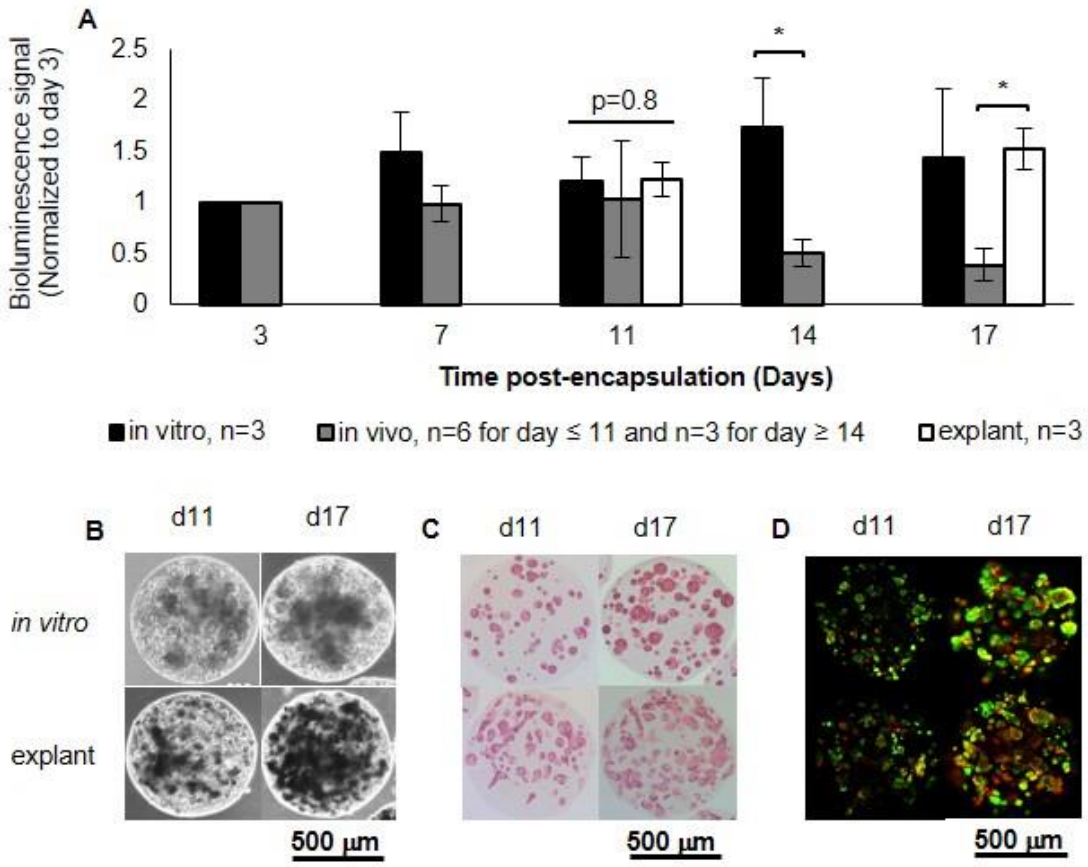

Figure 5.2: BLI trend comparisons between *in vivo*, parallel *in vitro* controls, and explanted microcapsules improved *in vivo* graft fate understanding. A) For comparison, i*n vivo* data were normalized to day 3 *in vivo* BLI signals; *in vitro* and explant data were normalized to *in vitro* day 3 bioluminescence signals. *p<0.05: Statistical difference between indicated groups. *In vitro* and explant images of a single microcapsule at 10x magnification were compared on days 11 and 17 using B) light microscopy, C) H&E histology, and D) 2D images from live/dead confocal microscopy.

5.4.2 Therapeutic Efficacy Evaluation

A mixed microcapsule population was fabricated as a result of previous *in vitro* data indicating that microencapsulated Fluc cells secreted less insulin over time compared to EINS. The Fluc to EINS ratio was determined based on the first part of this study, *in vivo* BLI characterization, revealing that 1 mL of microencapsulated Fluc cells allowed for

abundant BLI signal and cell survival monitoring *in vivo*. Since the total transplant volume was fixed at 3 mL, a 1:2 ratio of Fluc:EINS microcapsules was chosen to allow for BLI signal and sufficient insulin output.

Diabetic mice were injected i.p. at the 1:2 ratio of Fluc:EINS microcapsules and strikingly, experimental mice became normoglycemic two days later, whereas control mice remained hyperglycemic (Figure 5.3A); neither group received exogenous insulin before day 2 (Figure 5.3B). Correction was short-lived however and mice reverted back to hyperglycemia by day 4. Control mice exhibited significantly higher blood glucose levels than the experimental mice on one other day of the study (day 8). Overnight fasting revealed higher blood glucose levels in controls compared to experimental mice on day 17; exogenous insulin was withdrawn 3-4 days before fasting.

Figure 5.3B indicates the average daily exogenous insulin administration; overall, control mice received 7.8-fold more insulin ($p<0.001$). No differences were detected in body weight trends between the two groups on any day of the study (Figure 5.3C). Figure 5.3D-E depict dynamic BLI signals, indicating proliferation from day 3 to 8 and likely some cell death from day 8 to 17.

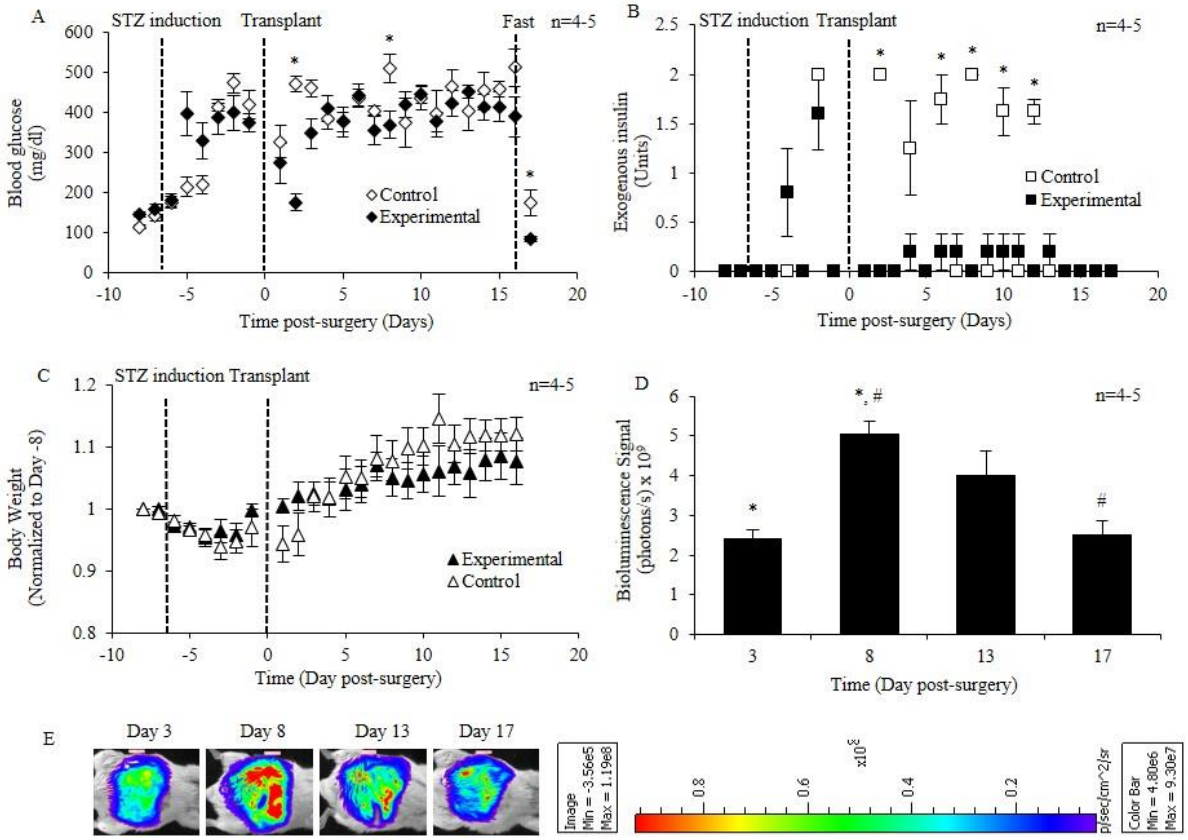

Figure 5.3: *In vivo* therapeutic efficacy evaluation. A) Average blood glucose measurements per day between control mice receiving acellular microcapsules and experimental mice receiving EINS:Fluc microcapsules at a 1:2 ratio. B) Average exogenous Lantus® insulin administered per day and C) average body weight per day normalized to day -8, for control and experimental groups. D*) In vivo* BLI signals obtained from experimental mice every 4-5 days and E) representative bioluminescence images of experimental mice over time post-transplantation (d3, d8, d13, d17). In Figures A-C, * indicates a significant difference between the control and experimental groups on that day ($p<0.05$). In Figure D, shared symbols above bars indicate significant differences (*, # $p<0.05$).

5.4.3 Explant Analyses

On day 17 mice were euthanized, 0.5-1 mL blood was collected via cardiac puncture, and approximately 90% of the microcapsules were retrieved for explant analyses under the assumption that microcapsules remained at a 1:2, Fluc:EINS ratio. No difference in BLI was found between explanted ($2.6\pm0.3 \times 10^8$ photons/s) and *in vitro* control groups ($2.2\pm0.9 \times 10^8$ photons/s); live/dead images also indicated similar viability between groups (Figure 5.4A). From light microscopy images, the periphery of microcapsules appeared to be clear of any fibrosis (Figure 5.4B), which was corroborated by H&E histology (Figure 5.4C). Live/dead and light microscopy images also appeared to indicate higher cell densities within microcapsules that had spent 17 days *in vivo* compared to those *in vitro*.

Interestingly, explanted cells were 2.7 times less metabolically active with a 3-fold lower insulin secretion capacity compared to *in vitro* controls (Figure 5.5A-B). Therefore, when normalized to metabolic activity, there was no longer any difference in ISR between groups (Figure 5.5C). Similarly, explant intracellular insulin content was 2-fold lower than *in vitro* controls (Figure 5.5D), but metabolic activity normalization showed no difference (Figure 5.5E). Serum human insulin concentrations were high in experimental mice, ranging from 12-62 μU/mL, and close to zero in controls (Figure 5.5F).

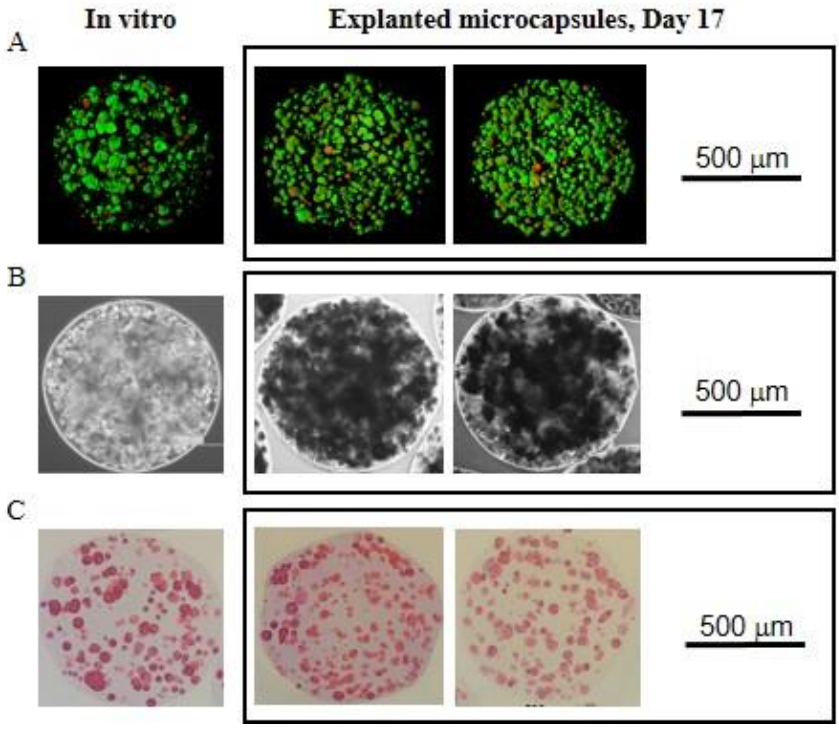

Figure 5.4: Qualitative assessment of explanted pancreatic substitutes from treated mice. Representative images of explanted microencapsulated EINS/Fluc cells compared to *in vitro* control group on day 17 using A) 3D Confocal live/dead, B) light microscopy, and C) H&E histological analyses.

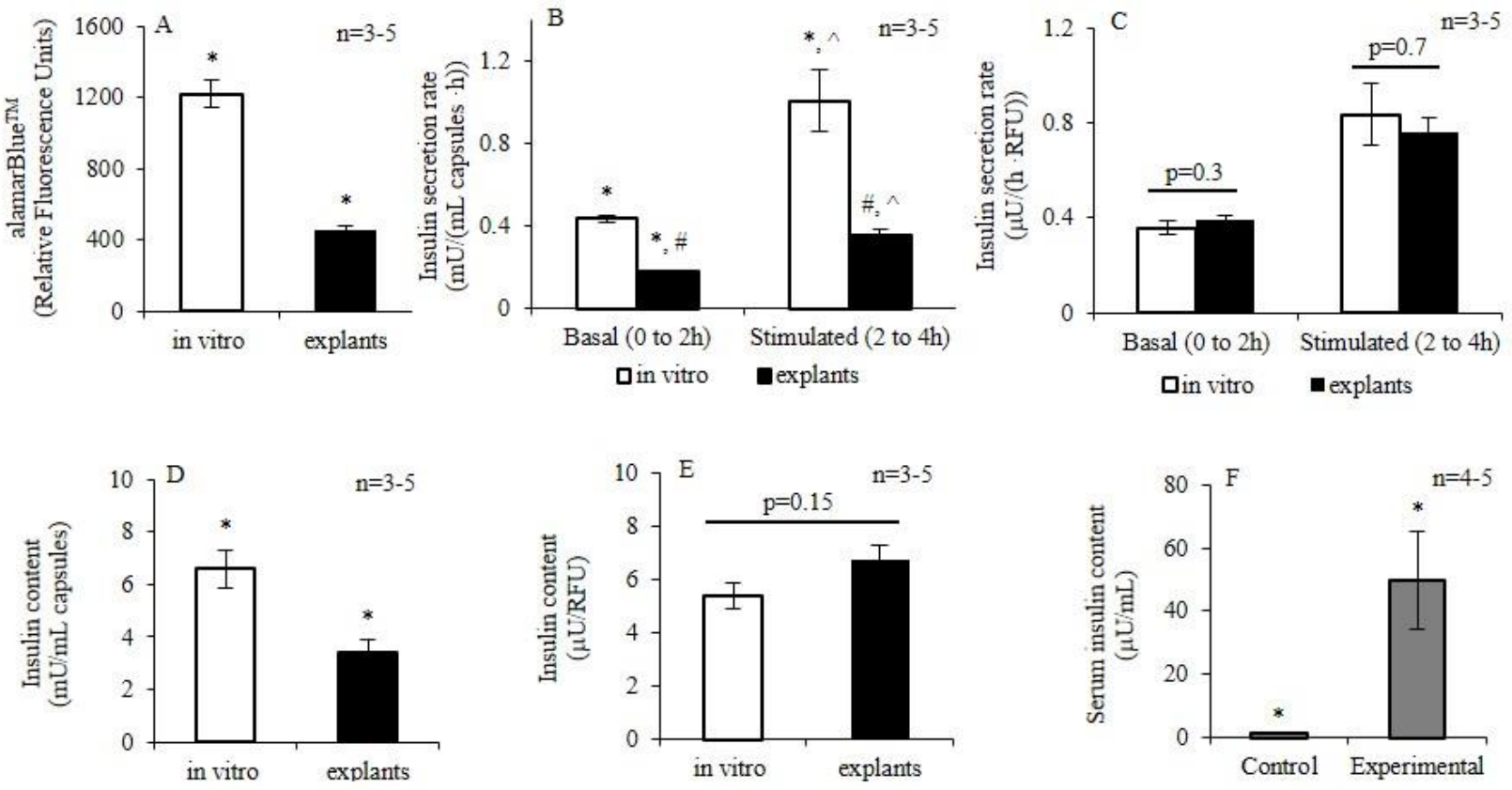

Figure 5.5: Quantitative explant analyses on day 17. A) Metabolic activity, measured by alamarBlue™ in relative fluorescence units (RFU), per mL explanted microcapsules compared to *in vitro* controls, B) ISR per mL explanted microcapsules versus *in vitro* controls, and C) ISR per mL microcapsules normalized to metabolic activity. D) Intracellular insulin content per mL explanted versus *in vitro* microcapsules and E) intracellular normalized to metabolic activity. F) Human insulin concentrations in serum collected from control and experimental mice. Shared symbols above bars indicate significant differences (*, #, ^ $p<0.05$).

5.5 Discussion

5.5.1 *In Vivo* BLI Characterization

A BLI system was established for temporal monitoring of microencapsulated cells cultured *in vitro* and injected i.p. *in vivo*. Although these microencapsulated, i.p. delivered cell transplants are a common configuration, BLI has not previously been applied to such a system. BLI measurements produced signals that were consistently four orders of magnitude higher than background, clearly demonstrating graft survival in mice for 17 days. In addition, comparing explanted and parallel *in vitro* cultures of microencapsulated cells revealed the potential of using this BLI method to identify probable causes for graft success or failure in preclinical animal models, as will be discussed.

In islet studies, BLI capability is incorporated by isolating islets from luciferase-expressing transgenic animals [168, 170] or by virally transducing islets from wild-type animals with the luciferase gene [167, 169]. Viral luciferase incorporation in primary cells such as islets would require genetic manipulation of the graft in every transplant procedure, making routine BLI application costly and time-consuming. On the other hand, incorporating the BLI methodology by luciferase incorporation to cell line transplants is inexpensive and easy especially if, as in the present study, cells retain their bioluminescence and functional characteristics during expansion and freezing/thawing.

In studies of islets within TheraCyte® macrocapsule devices, BLI was used to investigate the long-term fate of allogeneic islets for 50 days [174], or skin fibroblasts for up to one year [172], after transplantation in mice or rhesus monkeys, respectively. Outside of diabetes therapy, only two other BLI studies have been applied to encapsulated cell systems for *in vivo* monitoring, including L929 cells suspended in Matrigel prior to

subcutaneous injection [171] and CHO cells in SeaPlaque agarose before i.p. transplantation in mice [173]. The encapsulation methods mentioned, however, were fixed systems that retained the cells at the graft site, which are generally less advantageous in sustaining therapeutic cell numbers compared to the microcapsules employed in this study [184]. Additionally, these studies attributed an increase or attenuation in BLI signal to cell growth or death without confirming this correlation *in vitro* and in explant studies, as was done in the present study.

Propagating *in vitro* cultures in parallel to *in vivo* experiments, when feasible, can provide enhanced insight into graft behavior *in vivo*, as it did in the present study. On day 17, *in vitro*, *in vivo*, and explant groups were evaluated and the only difference among them was an apparently lower *in vivo* BLI signal compared to the explant group. Extensive cell death *in vivo* was ruled out as the cause of this difference because bioluminescence indicated similar viable cell numbers between explant and *in vitro* groups, which was corroborated by comparable metabolic activity and cell secretory function. Furthermore, histology, live/dead, and microscopy images demonstrated virtually no host cellular adhesion to microcapsule surfaces, hence BLI attenuation due to fibrotic overgrowth of capsules was also ruled out as a cause. Loss of transplant metabolic activity in the peritoneal environment due to hypoxia [180] is possible but unlikely due to the long timescale from transplantation to BLI signal loss. The more likely cause of reduced *in vivo* bioluminescence was the movement of microcapsules away from the surface of the mouse abdomen. This became more apparent during microcapsule retrieval: some microcapsules were found beneath organs or near deeper tissues. This finding should serve as a caveat to

applying BLI in this particular configuration, and underline the importance of *in vitro* and explant evaluation.

5.5.2 Therapeutic Efficacy Evaluation

Enhancement and microencapsulation of the previously engineered GLUTag-EINS cells produced a superior graft that secreted roughly 100-fold more insulin per day than the macrocapsule graft formerly developed [19]. Even with dramatic secretion augmentation, grafts were only able to restore normoglycemia two days after transplantation in diabetic mice, after which grafts were likely unable to completely correct hyperglycemia [206]. Treated mice were, however, able to maintain body weight and avoid extreme hyperglycemia with significantly less exogenous insulin than controls. Fasting blood glucose levels and serum human insulin concentrations on day 17 revealed a still-functioning graft *in vivo* and BLI was able to define temporal survival of the grafts.

Reduced food consumption during post-surgical recovery likely contributed to the normoglycemia of treated mice on day 2; insulin secretion from grafts being temporarily sufficient to control blood glucose levels. A less likely possibility is that the graft was initially effective, but secretory function eventually declined to a non-therapeutic level, resulting in recurrence of hyperglycemia. BLI data, however, contradicted this rationale by indicating an approximate 2-fold increase in viable cells from day 3 to 7. It therefore seemed unlikely that cells, during such a proliferative time, would experience significant secretion impairment.

Fasting blood glucose data collected from experimental and control mice were similar to those reported in the literature for normal and STZ-diabetic mice, respectively

[207]. Overnight fasting elucidated that ad libitum feeding contributed significantly to hyperglycemia; a difference between groups is therefore more likely with controlled food consumption. From these findings, it was reasonably inferred that the grafts were insufficient in secreting the insulin levels required to overcome extreme hyperglycemia in freely eating diabetic mice.

The average human insulin serum concentration in treated mice was 9-fold higher than that reported from diabetic mice treated with macrocapsule GLUTag-INS constructs, and similar to mouse insulin serum concentrations in healthy mice [20]. Blood insulin concentration profiles were generated to determine whether serum insulin measurements were likely to be accurate (Figure 5.6). Profiles were produced based on ISR data from explanted grafts (969 μU/h), insulin clearance rates [208], and assuming all insulin secreted from the grafts appeared in the blood. Clearance rates of 13 and 63 mL/h were estimated by proportionally scaling down, based on body weight, from the physiological range of insulin clearance in a 70 kg man (700-3350 mL/min) [208] to a 22 g mouse. Since scaling down to rats is approached in this way [209], using the same method for mouse clearance rate estimations were assumed to be acceptable. The steady state blood insulin concentration range fell between 15 and 75 μU/mL; the average measured serum insulin concentration from mice on day 17 (50 μU/mL) was indeed within this range.

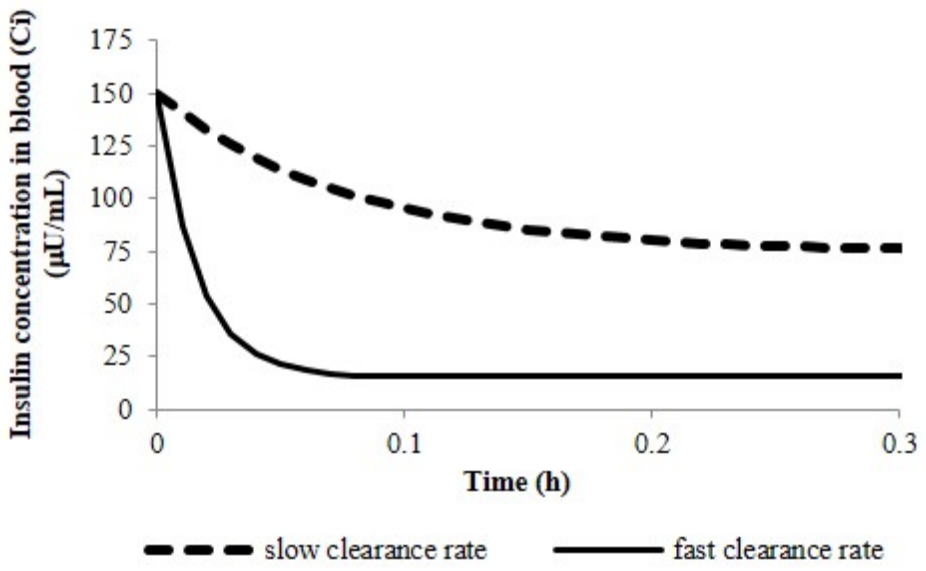

Figure 5.6: Blood insulin concentration profiles based on insulin secretion data from explanted grafts, estimated insulin clearance rates in mice, and the assumption that all insulin secreted from grafts appeared in the blood stream. The following equation was generated to obtain profiles for both fast (c=63 mL/h) and slow (c=13 mL/h) clearance rates: $\boldsymbol{Ci} = \frac{\boldsymbol{isr}}{\boldsymbol{c}} + (\boldsymbol{Ci}(\boldsymbol{0}) - \frac{\boldsymbol{isr}}{\boldsymbol{c}}) \cdot \boldsymbol{e}^{-\boldsymbol{c}\cdot\boldsymbol{t}}$, where Ci=blood insulin concentration, isr=explanted graft insulin secretion rate (969 μU/h), c=clearance rate (mL/h), and t=time (h). An arbitrary initial blood insulin concentration of 150 μU/mL was chosen and the total blood volume of a mouse was estimated to be 1 mL.

The effects of mouse insulin antibodies are unknown, but human insulin RIAs have been shown to produce falsely high measurements due to human insulin autoantibody interference [210]. It is also documented that human insulin may be immunogenic in BALB/c mice [211], but in the present study, control mice receiving significant amounts of exogenous human insulin had negligible insulin serum concentrations measured by RIA. However, since the response in transplant groups may not be equivalent to controls, interference cannot be completely ruled out. Nevertheless, serum human insulin was within the expected concentration range and high insulin quantities in treated mice were evident from their comparable body weight and blood glucose trends with controls while receiving

almost 8-fold less insulin supplementation. Importantly, even though using human insulin-secreting grafts is the prevalent method in the field, diabetic rodent models have shown resistance to exogenous porcine and human insulin, requiring 20-40 times more porcine insulin than the prescribed human dose [212]. This challenge, in conjunction with overeating, may explain why normoglycemia was not achieved here, despite very high serum human insulin levels.

Explant tests provided graft insight regarding long-term secretory function and viability. Interestingly, it appears that *in vivo* conditions caused an impairment in both metabolism and secretory function without instigating significant cell death. Schneider et al. reported similar findings after transplanting microencapsulated islets in immune competent diabetic mice [213]. After 10 weeks, viability was estimated at >85%, but insulin secretion capacity was more significantly reduced. Skiles et al. saw a similar effect *in vitro* after culturing encapsulated MIN6 aggregates under hypoxia for weeks [214, 215]. Although these findings relate to β cells, L cells also rely on glucose metabolism for stimulated secretion [216] which is disrupted under hypoxic conditions [217]. In this study, transplanting a large number of microencapsulated cells in the peritoneal cavity likely led to a significant reduction in available oxygen [180] and a consequent reduction in cell metabolic activity and secretion capacity. Furthermore, during BLI characterization studies, three times less microencapsulated cells were transplanted and no secretory or metabolic impairments were observed. It is therefore unlikely that simply transplanting higher cell numbers will be a therapeutic option.

Two factors of pancreatic construct fabrication in previous work contributed to its greatly improved secretion: 1) Additional insulin gene introduction via lentivirus allowing

for 1.7-2 times more insulin secretion and 2) microencapsulation for retaining monolayer secretion and allowing for larger transplanted cell numbers. Findings from this study imply that significant progress in the field is needed to fabricate a preclinically relevant enteroendocrine cell-based pancreatic construct. We estimate that the cells in this study need to secrete six times their current insulin output to limit the number of oxygen-consuming cells and allow for a realistic 1 mL transplant volume.

An alternative method is to complement the graft from this study with a hepatic cell therapy. Hepatic cells genetically engineered for glucose-responsive insulin secretion [118] can serve as the basal release portion of the biphasic insulin response and enteroendocrine cells can supply the quick-phase burst via their meal-responsive secretory granule system [191]. This dual cell system may relieve the secretion burden from enteroendocrine cells while improving glycemic regulation of current hepatic cell-based insulin therapies.

CHAPTER 6: CONCLUSIONS AND FUTURE DIRECTIONS

6.1 Conclusions

A cell-based approach to insulin therapy for IDD patients is promising toward achieving the tight regulation required to maintain blood glucose concentrations within the normal physiologic range and eliminate the long-term secondary complications that significantly burden both the patient and the health care system. Clinical applicability, however, is still a long way off due to substantial challenges that preclude therapeutic efficacy and safety. As discussed earlier, the cell-based research avenues encompass a wide range including islet transplantation, engineered β cell lines, stem cell differentiation into β-like cells, *in vivo* gene therapy, and genetic engineering of isolated autologous non-β cells. The focus of the work in this thesis was on the latter approach because autologous non-β cells have the potential to address both donor cell availability and immune rejection issues, and in particular, enteroendocrine cells were chosen as they are endogenously similar to β cells. The major limitations of most non-β cells are their lack of glucose responsiveness and low levels of recombinant insulin secretion after conventional viral or non-viral insulin transgene incorporation. Additionally, as in all the cell-based approaches, little is understood regarding *in vivo* graft integration and the causes for failure; this further slows the development of clinically acceptable therapies.

The objective of the work presented in this thesis was to substantially improve a previously engineered pancreatic substitute developed in our lab, in an effort to bring it the closest in the field to a therapeutically effective non-β cell insulin therapy. To accomplish

this, the thesis was split into three specific aims which progressed from the genetic and molecular level for insulin secretion improvement on a per-cell basis, to the tissue level for secretion enhancement on a per-graft basis, and lastly to the preclinical level for therapeutic assessment in a diabetic mouse model.

Results from the first aim, described in CHAPTER 3, provided important information regarding the ability of enteroendocrine L cells to secrete high levels of recombinant insulin. Additional incorporation of the wild-type human insulin gene via lentivirus transduction of the GLUTag-INS cells caused only a transient increase in insulin mRNA levels and secretion. Disproportionate effects of insulin mRNA on secretion led us to conclude that the transgene copy number is not the main step that limits insulin secretion.

Looking at various steps within the RSP identified proinsulin processing as a likely limitation to high insulin production and treating cells with TSA corroborated this point. TSA was not only used as a tool to identify limiting steps in the RSP, but it was also investigated as a novel method for secretion enhancement based on its effects on insulin mRNA as well as downstream steps. Long-term effects of a one-time, 24 h TSA treatment on microencapsulated cells showed that secretion enhancement was sustained for as long as seven days, indicating the potential of HDACi as a treatment regimen for transplant recipients. It is an especially attractive approach because some oral HDACi drugs are already FDA-approved for cancer and epilepsy patients [218]. In an effort to identify key HDACs that influence RSP efficiency, cells were treated with tubacin, which had no effect. This was a first step in isolating the main mechanism for secretion enhancement by eliminating HDAC6 as playing an important role, at least in itself.

Overall, the combined enhancement method resulted in recombinant insulin secretion rates of 655-888 fmol/(10^6 cells·h), significantly surpassing reported secretion from previously engineered intestinal endocrine cells by over 6-fold. We therefore concluded that achieving therapeutic insulin production from L cells may be plausible by both increasing transgene incorporation and RSP efficiency.

In the second aim, described in CHAPTER 4, a TEPS was developed and characterized for bioluminescence capabilities, controlled cell growth, and insulin secretory function over time. Studies for this aim were based on early passaged GLUTag-EINS cells developed in specific aim 1, to test the effect of per-cell enhanced secretion. Findings revealed that stable bioluminescence was attainable and microencapsulation had no effect on signal or cell survival tracking abilities under conditions of normoxic growth and anoxia-induced death. It was therefore reasonably expected that successful real-time survival tracking of microencapsulated cells could be accomplished *in vivo* as well.

Microencapsulation had no effect on cell insulin secretion rates and it was estimated that a 3 mL volume of microencapsulated GLUTag-EINS would secrete approximately 0.6 μmoles of insulin per day, or 42% of the reported secretion from therapeutically successful βTC-tet grafts [180]. It is important to keep in mind, however, that significantly more human than rodent insulin is required to reduce blood glucose levels in rodents [212]. This introduced an additional challenge to achieving therapeutic efficacy in diabetic mice. Compared to the GLUTag-INS-containing macrocapsule formerly developed in the lab, a 3 mL volume of 3.3% (wt/vol) alginate microcapsules characterized by high mannuronic acid and cross-linked with barium ions containing GLUTag-EINS cells resulted in an approximate 100-fold increase in total insulin secretion output. It was therefore concluded

that the microcapsule configuration considerably improved the chances of observing a therapeutic effect of the GLUTag-EINS-containing TEPS in preclinical diabetes models.

Finally, the third aim was covered in CHAPTER 5 and consisted of two major parts: sub-therapeutic *in vivo* BLI characterization of microencapsulated Fluc cells and *in vivo* therapeutic efficacy evaluation of the bioluminescent TEPS developed in the second aim. It was concluded from the first part of the study that microencapsulated cell survival is clearly indicated by BLI signals consistently above background levels. A caveat to this method, however, is that signal change or attenuation can be an artifact of microcapsule dispersion and increasing penetration distances. Nevertheless, inclusion of *in vitro* and explant analyses will help to clarify the observed changes *in vivo*. The major advantage of this BLI approach is that it is generalizable to any encapsulated cell technology and can provide insight into the causes of graft failure in an effort to accelerate the development of clinically acceptable cell therapies.

In the second part of the study, it was encouraging to find that normoglycemia was achieved two days after i.p. injection of the alginate microcapsule constructs, even if only for a transient period. Although mice reverted back to the diabetic state, they required 7.8-fold less exogenous insulin than controls, body weight was maintained, and extreme hyperglycemia was prevented for the duration of the study. This is the first time that an enteroendocrine cell-containing, controlled-growth system has shown therapeutic effects such as these in diabetic rodents.

Findings from the studies in this thesis imply that significant progress in the field is needed to fabricate a preclinically relevant enteroendocrine cell-based pancreatic construct. It is estimated that the cells in this study need to secrete six times their current

insulin output to limit the number of oxygen-consuming cells and allow for a realistic 1 mL transplant volume. If this cannot be attained, it is unlikely that insulin-secreting enteroendocrine cells can serve as a standalone therapy and supplemental strategies such as HDACi treatment or the incorporation of engineered hepatocytes must be developed to achieve therapeutic efficacy.

6.2 Future Directions

6.2.1 Targeting Limiting Steps in the RSP for Enhanced Secretion

After identifying proinsulin processing as a possible limiting step in the RSP of GLUTag-INS and GLUTag-EINS cells, a full mechanistic study should be performed to isolate the cause for proinsulin buildup. The challenge to this approach will be the lack in understanding of the L cell RSP mechanism. Based on what is known, however, there are various possible reasons for proinsulin buildup such as insufficient production or activity of prohormone convertases, proinsulin aggregation in the golgi apparatus, or improper vesicle packaging.

From previous work, it appeared that L cells produced similar quantities of prohormone convertases PC1/3 and PC2 [18, 87]. PC1/3 is known to cleave proglucagon to produce GLP-1 and PC2 cleaves proglucagon to produce glucagon. Since L cells are programmed to secrete GLP-1 rather than glucagon, perhaps PC1/3 has higher enzymatic activity than PC2 or PC2 is inhibited in some manner, to allow cleavage only at the appropriate proglucagon site. It was demonstrated by Damholt et al. that glucagon was not produced in L cells even though proglucagon, PC2, and the PC2 chaperone 7b2 were

present [219]. This may suggest that an additional component is required to activate the chaperone and/or the enzyme for cleavage.

Another consideration is whether mouse prohormone convertases PC1/3 and PC2 can cleave human proinsulin as efficiently as they can cleave mouse proinsulin. Although PC1/3 and PC2 are well conserved between humans and rodents [220], the cleavage sites of human insulin versus mouse insulin are not completely homologous. Such a study does not currently exist in the literature, but perhaps it would be insightful to compare the cleaving efficiencies of mouse PC1/3 and PC2 on human versus mouse proinsulin, and thus evaluate the validity of the model used in this thesis for testing human insulin production in mouse L cells.

Before investigating these specific mechanisms, however, the most enlightening experiment would be to tag proinsulin with a fluorescent reporter gene for transfection into GLUTag-INS and track its progression through the RSP using a high-speed super resolution microscope (20 nm resolution). A similar study by Dompierre et al. has been performed using a previously described imaging system [221] to track BDNF in the secretory granules and vesicles of neuronal cells [190]. This way, the steady state distribution of proinsulin may be visualized and buildup in one particular location of the RSP could be identified. This would help to narrow the scope of the following studies which would place emphasis only on the major bottleneck locations. For example, if most of the proinsulin was found within vesicles, investigating PC1/3 and PC2 efficiencies would be insightful. However, if proinsulin buildup occurs in the golgi apparatus, a different set of experiments must be designed, perhaps to investigate problems with proinsulin aggregation.

Although enhancement of human insulin mRNA levels did not strongly contribute to secretion augmentation, it was a good supplement to increased RSP efficiency. Therefore, placing some emphasis on increasing the transcription of the insulin transgene would be beneficial. Perhaps coming up with better gene delivery strategies for stable transgene incorporation will be valuable. If this is to be pursued, the mechanism of gene silencing should be studied to identify the cause: lentivirus or CMV promoter? The lentivirus method was originally chosen based on short-term studies that showed better secretion after transduction with lentivirus as opposed to AAV. However, AAV transduction similarly increased secretion and should be studied long-term to determine whether silencing also occurs when using this approach. Studying the strength and stability of various promoters to drive insulin transgene expression would also help in optimizing the gene delivery strategy. Designing a study similar to the one performed by Hock et al. would be effective in finding the best promoter/enhancer for optimal expression of the gene of interest [222]. The study methodically screened several different promoters/enhancers to identify vectors that would provide optimal expression of the gene of interest.

Therapeutic insulin secretion from cell lines needs to be achieved to truly prove the efficacy of this approach in preclinical animal models. However, once this is accomplished, the next hurdle will be to identify a gene delivery strategy for efficient insulin transgene transfer into primary enteroendocrine cells either *in vivo* or *ex vivo*. In 2010, Nikoulina et al. came up with a modified crypt cell isolation and culture procedure which yielded a primary mouse colonic crypt model enriched for enteroendocrine L cells [223]. This could be the best place to start in testing gene delivery strategies on primary cultures in preparation for an *ex vivo* clinical approach. Unfortunately, human L cell isolation for *ex*

vivo culture has been challenging and requires further study and optimization. A recent study this year, by Dame et al., reported successful methods for the isolation and *in vitro* maintenance of human colonic crypts [224]. This may therefore be a promising place to start in the pursuit of an *ex vivo* approach.

In vivo gene delivery to L cells for stable recombinant insulin expression would be difficult due to the rapid turnover of the intestinal epithelium. Furthermore, a targeted approach must be used so as not to engineer other cell types for insulin secretion, potentially resulting in insulin overproduction, which could be fatal. The major benefit of an *ex vivo* over an *in vivo* approach, is that the cells can be genetically engineered within a closely controlled environment which would improve safety. The development of a TEPS based on *ex vivo* insulin transgene delivery to autologous L cells could further enhance safety by allowing for construct retrieval and real-time monitoring.

6.2.2 HDACi Treatment for Sustained Graft Secretion Enhancement

Studies from specific aim 1 have identified HDACi treatment as a potential method for enhancing graft secretion that could eventually be used in transplant recipients, especially since some HDAC inhibitors have already been FDA-approved for cancer and epilepsy patients [218]. The long-term *in vitro* study of microencapsulated cells was a good starting point which led to the discovery that a one-time 24 h TSA treatment had lasting secretion enhancement effects even after seven days. The next step is to design and perform an *in vitro* optimization experiment in which various conditions such as TSA dose, treatment time, and encapsulation configuration are evaluated. Additional *in vitro* studies could be run in parallel to these studies which test the effects of specific HDACi treatment,

such as the evaluation of tubacin in this work, to better identify the mechanism for insulin secretion augmentation. Isolating and using one HDACi for treatment rather than TSA, which inhibits ten different HDACs, will be a more targeted approach and likely reduce the possibility of side effects if brought to the clinic.

Near the end of such *in vitro* optimization and characterization studies, experiments can move to preclinical diabetic animal models for *in vivo* evaluation and optimization. The major benefit of using HDACi drugs is that they can be orally administered. If this approach is indeed successful, IDD patients could undergo one surgical procedure in which a TEPS is transplanted and recipients may be able to take an HDACi pill regularly thereafter to achieve normoglycemia. This could dramatically improve IDD patient quality of life and reduce health care costs associated with secondary complications.

6.2.3 Therapeutic Efficacy in Pair-Fed STZ-Diabetic Mice

Based on the *in vivo* therapeutic efficacy study, it was highly likely that STZ-induced diabetic mice were eating significantly more than normal, non-diabetic mice. The literature also suggests this, reporting that STZ-induced diabetic mice experienced hyperphagia [206]. This could have been a major factor contributing to the graft's inability to sustain normoglycemia since significantly more insulin would be required to offset the extreme hyperglycemic state. In order to determine the therapeutic efficacy of a diabetic mouse eating normal portions, a carefully designed, pair-feeding study should be pursued. Pair-feeding is an experimental method that limits food intake in the same way between all animal groups. This could be accomplished by using a food intake monitor and controller module that continuously records food intake every 15 min on a computer which is

analyzed by the appropriate software (FDM-300s, Melquest, Toyama, Japan) [225]. This approach would eliminate blood glucose data variability between animals and isolate the real therapeutic value of the L cell graft. This approach is also clinically valid because graft transplantation in conjunction with a guideline for daily caloric intake could be a feasible option for treating IDD patients.

6.2.4 A Dual Cell-Based Insulin Therapy

The TEPS developed in this thesis, based on recombinant insulin-secreting enteroendocrine L cells, was insufficient as a standalone therapy in ad libitum fed STZ-diabetic mice. An alternative method is to complement the graft from this study with a hepatic cell therapy. Perhaps hepatic cells genetically engineered for glucose-responsive insulin secretion [118] can serve as the basal release portion of the biphasic insulin response and enteroendocrine cells can supply the quick-phase burst via their meal-responsive secretory granule system [191]. This dual cell system may relieve the secretion burden from enteroendocrine cells while improving glycemic regulation of current hepatic cell-based insulin therapies. Durvasula et al. computationally developed combinatorial insulin secretion profiles of these two cell types based on separate, experimentally measured secretion profiles and found that tuning of the first and second phases through varying cell ratios could better match β cell secretion kinetics than either one alone [191].

Preclinical efficacy studies must first be conducted to evaluate the potential of such a dual therapy approach. More specifically, studies should involve the *in vivo* viral delivery of a liver-specific, glucose responsive insulin transgene that has already been demonstrated

to be efficacious in STZ-diabetic rodents *in vivo* [226], followed by i.p. injection of the L cell-containing TEPS described in this thesis.

As a result of the work in this thesis, exciting new research avenues have emerged, promising to accelerate both the understanding of important enteroendocrine cell mechanisms and the development of a non-β cell-based insulin therapy with real clinical success.

APPENDIX A: CELL DENSITY EFFECTS ON RECOMBINANT INSULIN SECRETION

A.1 Introduction

Evaluating the effects of cell density on secretion function is important in developing an appropriate pancreatic substitute. Since genetically engineered non-β cells secrete significantly less than islets, considerably more engineered cells must be transplanted for therapeutic efficacy. For this reason, it is important to determine whether increasing cell density inhibits recombinant L cell function and their ability to secrete insulin. To accomplish this, both GLUTag-INS and EINS were investigated for their response to increasing cell densities both in 2D and 3D. The monolayer data in this appendix were collected by undergraduate researcher, José Antonio Vásquez Porto-Viso.

A.2 Results and Discussion

As GLUTag-INS and EINS became more confluent in the 12-well plates, basal insulin secretion appeared to be affected sooner than stimulated insulin secretion, which only declined at very high cell densities between 1 and 1.5×10^6 cells/cm^2 (Figure A.1). Interestingly, stored levels of insulin declined sooner than stimulated insulin secretion. These findings may suggest that basal insulin secretion was more sensitive to increasing cell density and that stimulated insulin secretion was only affected after stored insulin levels were reduced.

A similar experiment was also performed on microencapsulated EINS cells to determine whether cell proliferation could limit insulin secretion from the pancreatic substitute. Figure A.2 indicates that insulin secreted per graft volume increased disproportionately to increasing cell density within microcapsules such that the per-cell insulin secretion rate within microcapsules appeared to decline as cells proliferated. As EINS cells reached a density of approximately $1x10^8$ cells/mL alginate, secretion appeared to plateau. Therefore, increasing cell numbers will not solve the issue of insufficient insulin secretion. This further supports research toward enhancing recombinant insulin secretion on a per-cell basis rather than simply transplanting higher cell numbers.

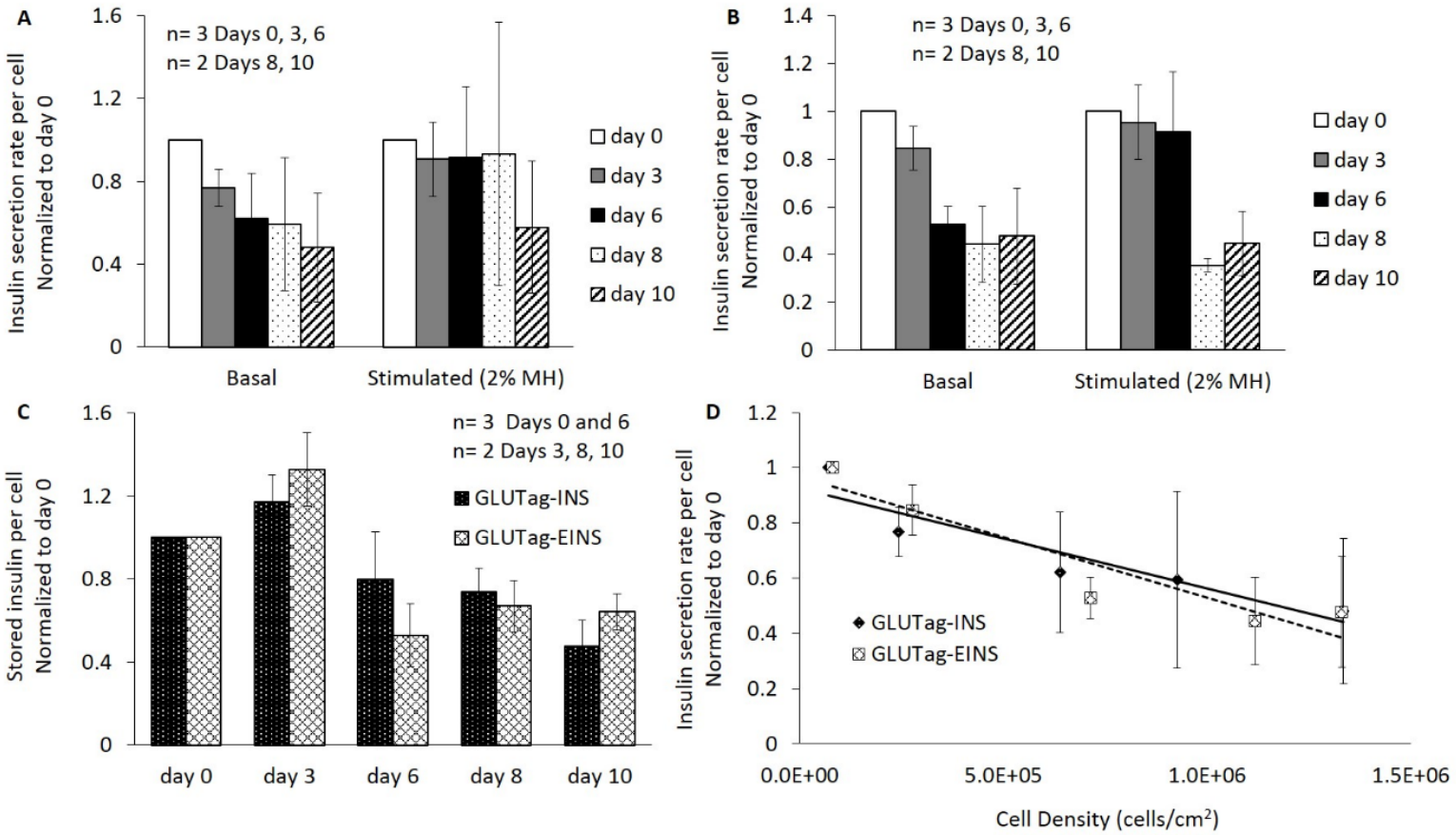

Figure A.1: Effects of cell density on insulin secretion function and storage capacity. GLUTag-INS and GLUTag-EINS cells were seeded as monolayers in 12-well plates at an initial cell density of $8x10^4$ cells/cm^2 and expanded for 10 days. On days 0, 3, 6, 8, and 10, ISR tests were performed, intracellular insulin collected, and viable cell numbers were quantified using trypan blue. ISR normalized to day 0 are indicated for A) GLUTag-INS and B) GLUTag-EINS cells. C) Intracellular insulin normalized to day 0 for both GLUTag-INS and GLUTag-EINS. D) Basal ISR normalized to day 0 versus cell density. Each point represents the mean ± SEM of 2-3 independent experiments.

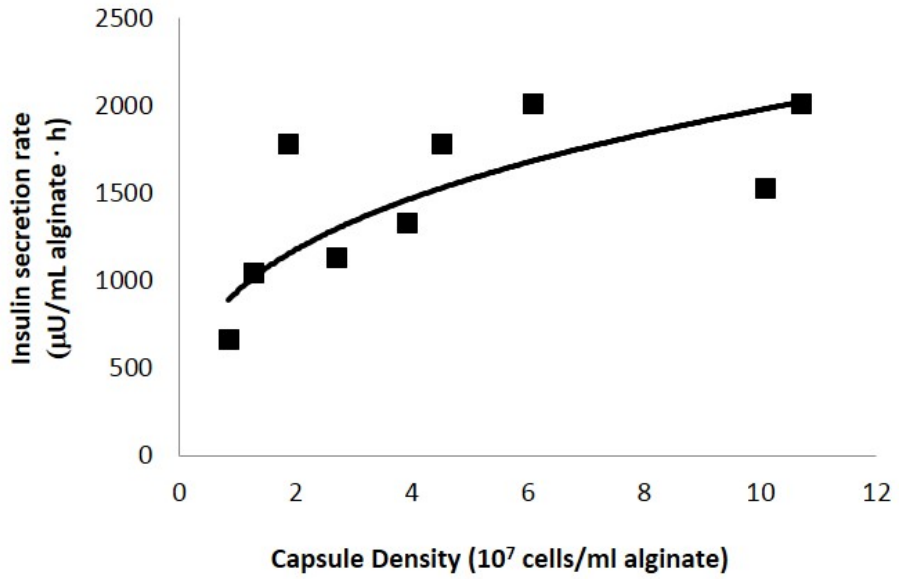

Figure A.2: Effect of EINS cell density within microcapsules on insulin secretion rate per graft volume. EINS cells were initially microencapsulated at a density of approximately $1x10^7$ cells/mL alginate. On days 1, 7, and 14 after encapsulation, stimulated insulin secretion samples were collected and cell density within microcapsules was approximated based on metabolic activity measurements using alamarBlue™ and total DNA using the picoGreen dsDNA kit. Three independent experiments were performed to collect these data.

APPENDIX B: WILD-TYPE INSULIN LENTIVIRUS TRANSDUCTION STUDIES

B.1 MOI Optimization Study

Additional insulin transgene incorporation into the GLUTag-INS cells via lentiviral transduction was identified by Kiranmai Durvasula as a promising strategy in our lab for insulin secretion enhancement. However, only a multiplicity of infection (MOI) of up to 30 had been investigated. The purpose of this study was 1) to compare new lentivirus preparations (ART) to original preparations by Dr. Durvasula (KD) and 2) to find an optimal MOI which enhanced insulin secretion without requiring a large virus volume. Figure B.1 shows the results of transducing GLUTag-INS with the new ART preparations at MOIs of 30 and 60. Data indicate that the new lentivirus preparations were comparable to the previous one and that increasing the MOI to 60 had no additional enhancing effects. Therefore, an MOI of 30 was chosen to conserve virus.

B.2 Lentivirus Transduction of Parental Enteroendocrine Cell Lines

Insulin transgene incorporation via lentivirus transduction (LV1) into parental enteroendocrine cell lines, GLUTag and STC-1, was investigated (Figure B.2). Although insulin secretion rates and storage were significantly lower compared to GLUTag-INS and EINS cells, the stimulation indices were much higher and interestingly, transduced STC-1 cells (STC-1-LV1) responded better (SI=5.6) to meat hydrolysate than transduced GLUTag cells (GLUTag-LV1) (SI=3). It therefore appeared that using lentivirus

transduction for initial insulin transgene incorporation in parental enteroendocrine cells was suboptimal for achieving high insulin secretion, but was better in maintaining nutrient responsiveness.

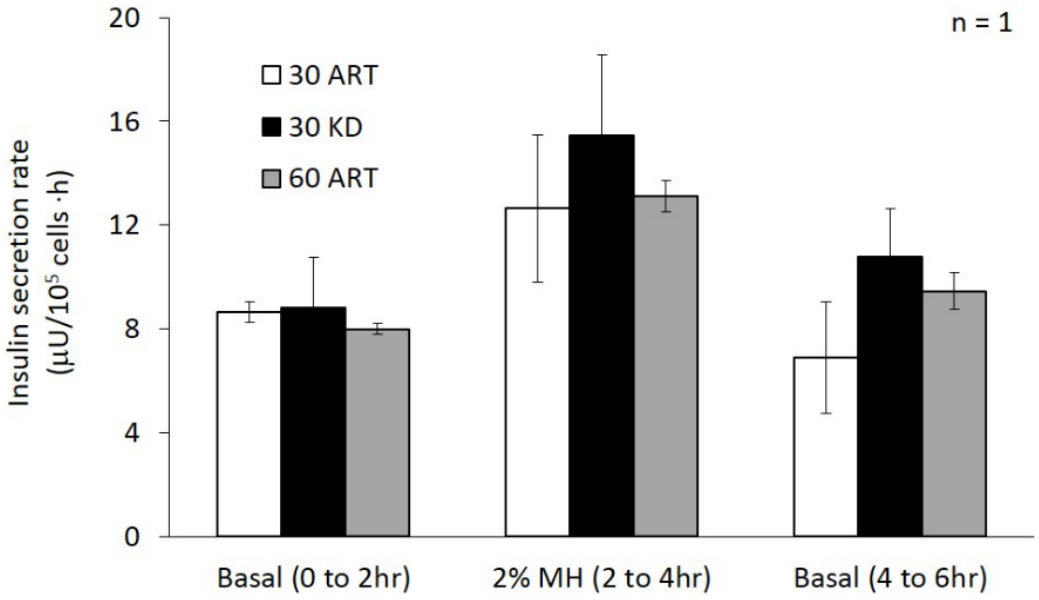

Figure B.1: Determining the optimal multiplicity of infection (MOI) for the lentiviral transduction of GLUTag-INS with wild-type human insulin (LV-WT-INS). GLUTag-INS cells were seeded in a 12-well plate at a density of $1.3x10^5$ cells/cm^2, allowed to grow for 2 days, transduced with lentivirus and polybrene (at a final concentration of 8μg/mL) for 24 hours, and changed to fresh medium under normal culture conditions. ISR tests were performed 7 days post-transduction and viable cell numbers were determined using trypan blue cell counting. Initials ART and KD indicate the researcher who produced and purified that particular lentivirus preparation. KD lentivirus preparations were used as controls since these were originally used by Kiranmai Durvasula to show that lentivirus transduction resulted in promising enhancement of insulin secretion from GLUTag-INS. MOIs of 30 and 60 were tested to identify which resulted in better insulin secretion enhancement. The error bars represent duplicate wells from one experiment.

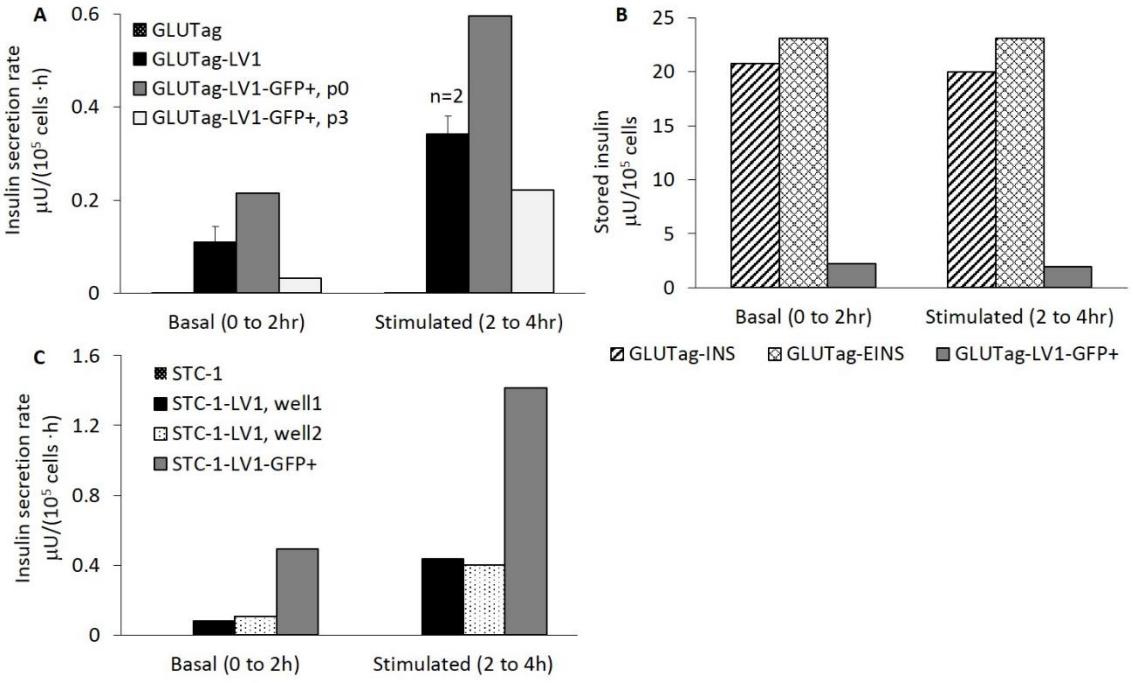

Figure B.2: Lentivirus transduction of the parental GLUTag L cell line and the heterogeneous STC-1 cell line with the wild-type human insulin transgene. Lentivirus transduction was performed in the same way as previously described at an MOI of 30, after which FACS was performed to generate a pure population of transduced cells. GLUTag cells were transduced with lentivirus (LV1) on day 0, ISR tests and FACS were performed on day 7 (GLUTag-LV1). ISR tests were then performed 3 days after FACS (GLUTag-LV1-GFP+, p0) and again after 3 passages (GLUTag-LV1-GFP+, p3). The same experiment was performed on STC-1 cells except ISR tests were not performed over passaging of the sorted GFP+ cells. A) Insulin secretion rates from GLUTag cells transduced with LV1 (LV-WT-INS). B) Stored insulin levels from GLUTag-LV1-GFP+ cells compared to GLUTag-INS and EINS cells. C) Insulin secretion rates from STC-1 cells transduced with LV1 (LV-WT-INS). Well 1 and well 2 were parallel wells.

B.3 Investigating Effects of the IRES-GFP Sequence in the Lentiviral Vector

A recent study by Mansha et al. has suggested that IRES-GFP expression vectors may interfere with the translation of smaller sized genes placed upstream of the IRES-GFP sequence [227]. To investigate whether the IRES-GFP was inhibiting insulin secretion after lentivirus transduction of GLUTag-INS, we removed only the IRES-GFP sequence from

the lentiviral vector (Schematic B.1), produced a new lentivirus which we called LV-INS, and tested ISR from GLUTag-INS cells transduced with either the new LV-INS or the original IRES-GFP-containing lentivirus, which will be referred to as LV-INS-GFP (Figure B.3).

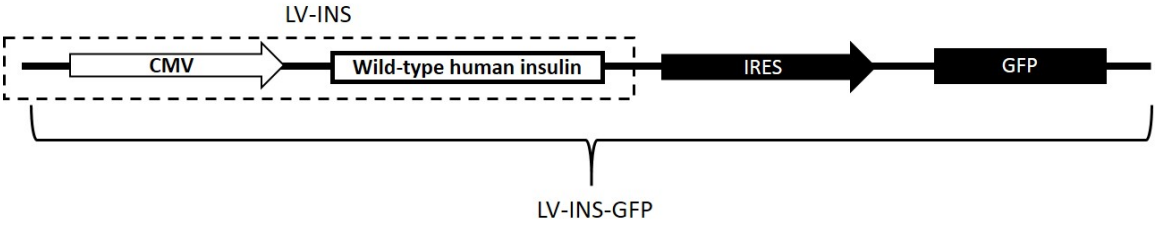

Schematic B.1: The IRES-GFP sequence was removed from the lentiviral vector to determine its effect on insulin secretion. LV-INS-GFP will refer to the original lentiviral vector containing the IRES-GFP sequence and LV-INS will refer to the vector with no IRES-GFP.

Results from ISR tests indicated that there was no difference in insulin secretion rates from GLUTag-INS transduced with the new LV-INS compared to those transduced with the original LV-INS-GFP vector (Figure B.3). We therefore continued to use the original lentiviral vector in transduction studies since the IRES-GFP sequence appeared to have no inhibitory effect on secretion.

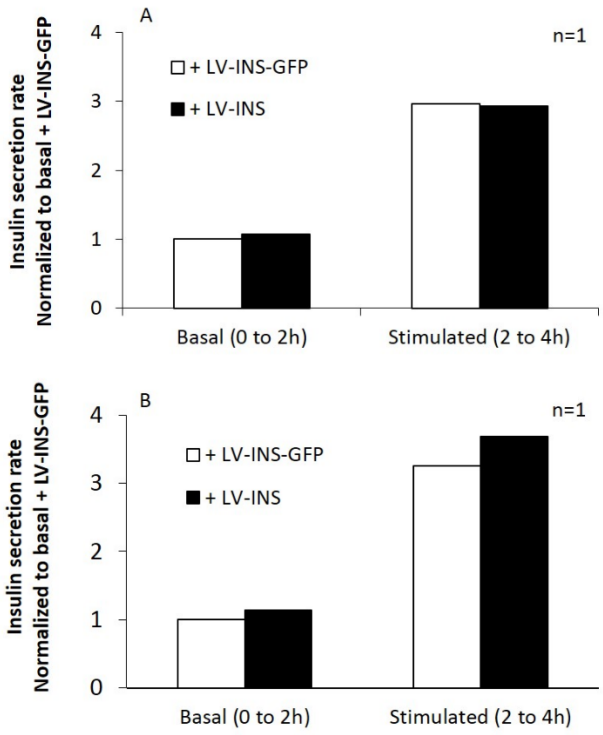

Figure B.3: GLUTag-INS transduced with either LV-INS-GFP or LV-INS. A) Insulin secretion rates three days post-transduction, p0 and B) Thirteen days post-transduction, p3. Data were normalized to the basal secretion rate of GLUTag-INS cells transduced with the original LV-INS-GFP lentiviral vector.

APPENDIX C: ADDITIONAL HISTONE DEACETYLASE INHIBITOR STUDIES ON RECOMBINANT L CELLS

C.1 Other Studied Effects of Trichostatin A

Out of curiosity, a brief preliminary study was performed to evaluate the effect of TSA on glucose-responsiveness from EINS monolayers. The rationale for this was based on the previous findings reported in CHAPTER 3 which appeared to show a stronger effect of TSA on increasing basal insulin secretion levels than stimulated secretion levels. The question then became *does TSA increase the sensitivity of these engineered L cells to glucose?* In subjecting TSA-treated EINS cells to a 16 mM step-up in glucose concentration from 5 mM glucose, the secreted response was comparable to that from TSA-treated EINS subjected to a step-up in 2% MH (Figure C.1). Non-treated cells, however, appeared to have less of a stimulated response to 16 mM glucose compared to 2% MH. Since only one experiment was performed, more studies should be carried out to clarify this result.

In addition to showing glucose-responsiveness, Figure C.1 also depicts the results from an attempted long-term TSA study of EINS monolayers. Since it was challenging to passage TSA-treated EINS cells, 3D microcapsule studies were pursued as reported in CHAPTER 3. However, this study was interesting because it showed that after one passage, TSA-treated EINS cells were secreting just 1.8 to 2-fold more than the non-treated controls. This agrees with secretion results from one day post-encapsulation of TSA-treated EINS cells. These results could suggest that TSA effects decline after cell trypsinization, and an

approach should be investigated to allow for TSA treatment of microencapsulated cells after, rather than before, trypsinization.

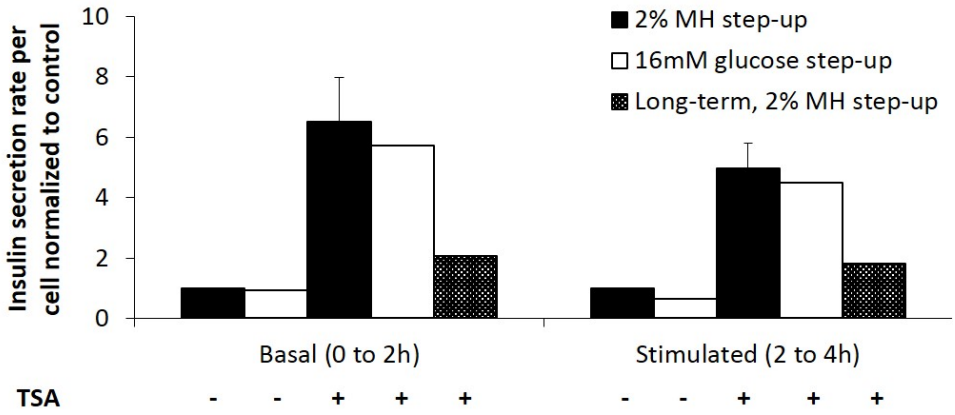

Figure C.1: TSA effects on glucose-responsiveness and long-term TSA effects in EINS monolayers. After TSA treatment, EINS were subjected to either a 2% MH step-up or a 16 mM glucose step-up for ISR testing. 2% MH step-up refers to cells that were subjected to basal medium (5 mM glucose) for 2 hours and then switched to stimulating medium (5 mM glucose + 2% MH) for 2 hours. 16 mM glucose step-up refers to cells that were also subjected to 5 mM glucose basal medium, but were switched to 16 mM glucose stimulating medium. ISR data were normalized to non-treated, 2% MH step-up, EINS cells under each condition for easy comparison. Bars labeled long-term refer to TSA-treated EINS cells that were passaged once and grown to confluency for ISR testing.

C.2 Another HDACi: Tubastatin A Hydrochloride

The HDACi tubacin was chosen to inhibit the specific function of HDAC6 that deacetylates α-tubulin and regulates vesicular trafficking. However, no effect was reported on GLUTag-INS or EINS insulin secretion after tubacin treatment. To investigate the role of HDAC6 more generally, a preliminary study was carried out involving the treatment of GLUTag-INS and EINS cells with tubastatin A hydrochloride, a specific inhibitor of

HDAC6. The basal and stimulated insulin secretion results from this study are shown in Figure C.2 and indicate that HDAC6 may play a very minor role in insulin secretion. More experiments would need to be performed for statistical comparisons, but the observed effects from this study were too small to be of significance in producing therapeutic insulin-secreting L cells.

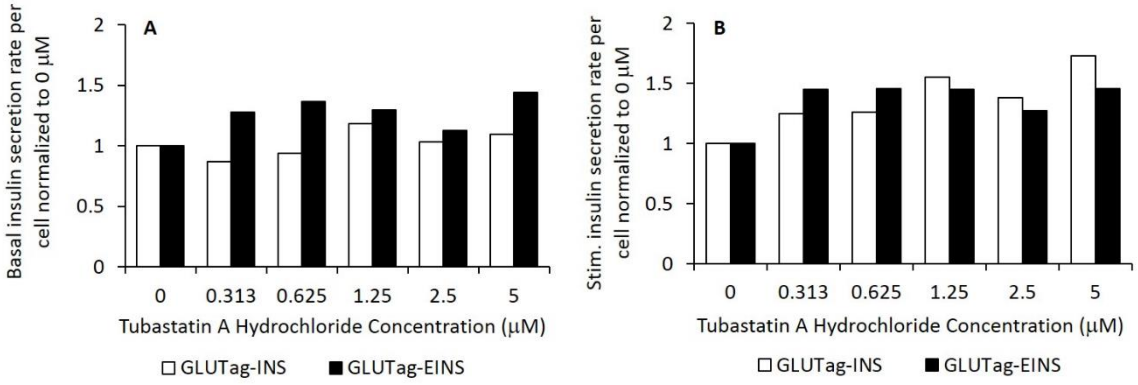

Figure C.2: A) Basal and B) stimulated insulin secretion rates from GLUTag-INS and EINS cells after a 24 h treatment with varying concentrations of Tubastatin A Hydrochloride. Secretion data were all normalized to 0 μM Tubastatin A and experiments were carried out in the same way as all previous HDACi treatment studies.

C.3 Adhesive Matrices and Enhanced Secretion

Cytoskeleton remodeling plays a major role in glucose-mediated β cell secretion and impacts the secretory granule system. In particular, it has been found that focal adhesion kinases (FAKs) affect glucose-induced cytoskeleton remodeling, insulin granule docking, and fusion to the plasma membrane [228]. A similar phenomenon is likely in L cells which also possess a secretory granule system, but release GLP-1 rather than insulin.

It may therefore be critical that the engineered L cells form focal adhesions in order to function properly. However, when cells are trypsinized and microencapsulated, they are essentially cells in suspension with a reduced number of focal adhesion sites as opposed to cells that are able to adhere to a surface as they do in monolayer cultures. This was perhaps why the enhanced secretion effect of TSA was lowered after trypsinization and microencapsulation. Maybe if more potential sites for focal adhesion were available within microcapsules, more insulin could be released from EINS cells. As a first, preliminary study, we evaluated the effect of adhesive alginate matrix microencapsulation on insulin storage and secretion from TSA-treated EINS cells (Figure C.3).

Comparisons were made between Group 4 (TSA-treated EINS cells microencapsulated in RGD-modified LVM alginate, prepared by Dr. Hajira Ahmad, and cross-linked in calcium) and Group 1 (non-treated EINS cells microencapsulated in LVM alginate and cross-linked in barium). Comparisons were made to Group 1 because this was the configuration used throughout all the studies of this thesis. The black dotted lines in Figure C.3 indicate the secreted and stored insulin levels reported from day 1 in the long-term TSA studies (CHAPTER 3, Figure 3.7) as a way of comparing the TSA-treated results in adhesive versus non-adhesive matrices. Interestingly, there appeared to be more stored and secreted insulin from TSA-treated EINS within an adhesive versus non-adhesive environment. It therefore may be interesting to pursue studies of various adhesive matrices and their effects on insulin storage and secretion from engineered L cells.

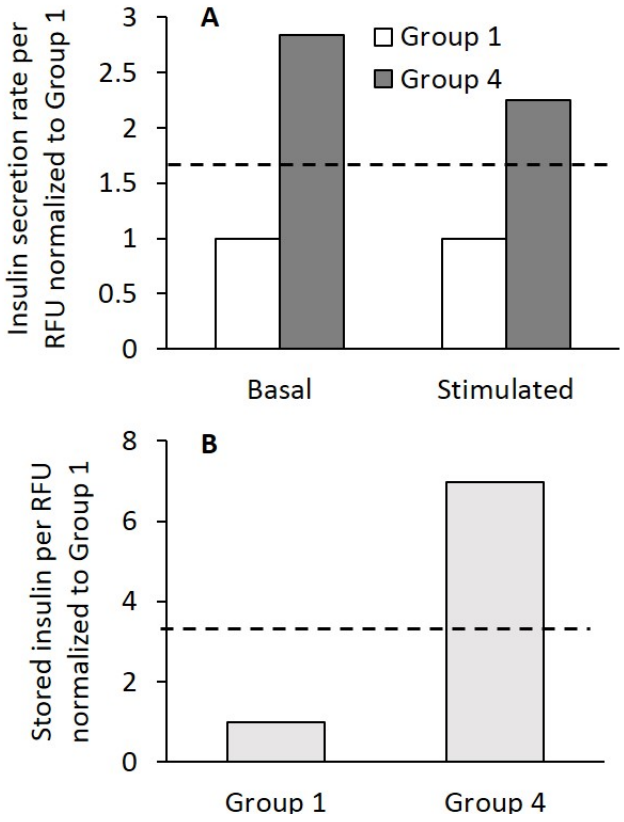

Figure C.3: A) Insulin secretion rates and B) stored insulin levels of cells one day after microencapsulation in an adhesive matrix compared to the alginate used in the previous studies. Group 1 consisted of non-treated EINS cells microencapsulated in LVM alginate cross-linked with barium at a density of $3x10^7$ cells/mL alginate. Group 4 consisted of TSA-treated EINS cells microencapsulated in LVM alginate modified to contain adhesive peptide RGD, and cross-linked with calcium at a density of $8x10^6$ cells/mL alginate. The black dotted lines in this figure indicate the secreted or stored insulin levels one day after EINS microencapsulation that were reported from CHAPTER 3 in the long-term TSA studies.

APPENDIX D: HISTONE DEACETYLASE INHIBITOR STUDIES ON BETA AND L CELL LINES

D.1 Abstract

Histone deacetylase (HDAC) inhibitors were recently identified as having significant clinical potential in reversing β-cell functional inhibition caused by inflammation, a shared precursor to Type 1 and Type 2 diabetes. However, HDAC inhibitors are highly complex and little is known of their direct effect on cell secretion pathways that are important for proper blood glucose regulation. The aims of the present study were to investigate the effect of HDAC inhibition on β-cell function and GLP-1 secretion from L-cells. The β-cell line βTC-tet or the L-cell line GLUTag were exposed to trichostatin A for 24 hours. Effects on insulin or GLP-1 mRNA, storage, processing efficiency, and secretion were measured and determined by real-time PCR and ELISA. Viable cell numbers were counted using trypan blue. HDAC inhibition significantly increased secretion per viable cell in a dose-dependent manner for both cell types. Effects on mRNA levels were variable among cell types, but enhanced storage and secretion were relatively comparable. HDAC inhibition enhances β- and L-cell secretion pathways in a way that could significantly improve blood glucose regulation in diabetes patients.

D.2 Introduction

The prevalence of diabetes is doubling every 10 years, with 347 million people affected worldwide. The World Health Organization projects that diabetes will be the 7th leading cause of death in 2030. Since current treatments place considerable burden on the healthcare system, the need exists for a novel, clinically feasible treatment that cures or prevents diabetes. Recently, exciting new studies have identified histone deacetylase (HDAC) inhibitors (HDACi) as having significant clinical potential in reversing β-cell functional inhibition caused by inflammation, a shared precursor to Type 1 and Type 2 diabetes. Since some small molecule HDACi drugs have been FDA-approved for epilepsy and cancer therapies, repurposing their use for diabetes treatment is a tangible option.

Several small molecule HDACi drugs are currently under clinical investigation to reactivate repressed gene expression in patients with cancer and neurodegenerative disorders such as Parkinson's or Alzheimer's disease. It is now recognized that acetylation also plays an important role in diabetes etiology. For example, it regulates the master transcription factor in the inflammation nuclear factor, (NF)-kB, which is critical to inducing β-cell death when activated [229, 230]. Two groups have demonstrated *in vitro* that HDACi treatment indeed helps to prevent cytokine-induced β-cell death [231, 232]. An *in vivo* study reported that twice weekly i.p. injections of HDACi in mice that spontaneously developed diabetes reduced blood glucose and T-cell mediated β-cell destruction [233]. In addition to this effect, HDACi drugs have shown evidence of alleviating insulin resistance and glucose uptake in skeletal muscle and liver cells [234, 235]. HDACi effects on other cells whose functions are critical to β-cell function, such as glucagon-like peptide-1 (GLP-1)-secreting intestinal L-cells, have not been investigated.

Although HDACs are known to play a key role in chromatin remodeling by acting on histone proteins, recent findings have shown that HDACs also act on 875 other classes of proteins [197]. These small molecule inhibitors are therefore inherently non-specific, complex, and can have many effects other than anti-inflammation in diabetes patients. As β-cell function is critical for proper blood glucose regulation, investigating the direct HDACi effects on β-cell function is among the most vital of studies toward developing a clinically acceptable treatment. Some studies have observed Trichostatin A (TSA), suberoylanilide hydroxamic acid (SAHA), or sodium butyrate (NaB) effects on β-cell line or islet function, but only as an aside to their primary investigation in determining anti-inflammatory effects [231, 232] or developing a pre-culture method for improved islet transplantation [189]. The reported effects have therefore been contradictory. Luef et al. studied the direct effects of valproic acid (VPA) on human islets to investigate the cause for increased postprandial insulin levels in epilepsy patients treated with VPA [188]. The group reported a dose-dependent increase in secreted insulin from islets incubated with VPA, but this effect was attributed to the behavior of VPA as a fatty acid derivative rather than as an HDACi. In support of using HDACi as a novel diabetes treatment, Christensen et al. state that further investigation into HDACi effects on the secretion pathway of β-cells is necessary [236].

The overall objective of this work was to fill in the gap in the literature regarding HDACi effects on the function of cells that are important in the prevention or treatment of diabetes. In this work, we report the effects of HDACi treatment on the secretion pathways of murine β- and L-cell lines. The impact of this work towards developing HDACi prevention and treatment options for diabetes patients are discussed.

D.3 Materials and methods

Cells Murine insulinoma βTC-tet cells were cultured in Dulbecco's modified Eagle's medium (DMEM; Sigma, St. Louis MO) with 25 mM glucose and supplemented with 10% fetal bovine serum (FBS), 1% penicillin/streptomycin (P/S), and L-glutamine to a final concentration of 6 mM. GLUTag cells were cultured as in [191] using DMEM with 25 mM glucose, without L-glutamine (Corning cellgro, Manassas, VA, Cat. #15-017), and supplemented with 10% FBS and 1% P/S. Cell cultures were propagated in a humidified incubator at 37ºC/5% CO_2.

Relative mRNA quantitation Cells were harvested for RNA isolation using the E.Z.N.A Total RNA Kit I (OMEGA bio-tek, Norcross, GA) followed by cDNA synthesis using the High Capacity cDNA Reverse Transcription Kit (Applied Biosystems, Grand Island, NY). cDNA was synthesized from 1μg of RNA and the manufacturer's protocols were followed closely. Real-time, relative quantitation of mRNA was accomplished using the SYBR Select Master Mix (Applied Biosystems) and the StepOnePlus Real-Time PCR System (Life Technologies) for measurement and comparative C_T method analysis. Mouse insulin (INS-1) and GLP-1 primers were designed using National Center for Biotechnology Information's (NCBI's) Primer-BLAST design software and mouse beta-actin (ACTB) primers were used as endogenous controls. Primer sequences were as follows: forward mouse insulin-1 5'-CTT GTT GGT GCA CTT CCT AC-3', reverse mouse insulin-1 5'-TGC AGT AGT TCT CCA GCT GG-3', forward GLP-1 5'-ACA GCA AAT ACC TGG ACT CCC GCC GT-3', reverse GLP-1 5'-CCT CGG CCT TTC ACC AGC CAA GCA A-3', forward mouse ACTB 5'-GCA CAG CTT CTT TGC AGC TC-3', reverse mouse

ACTB 5'-CTT TGC ACA TGC CGG AGC C-3'. All primers were purchased from Eurofins MWG Operon, Huntsville, AL and used at 300 nM concentrations.

Dose-response curves Dose-response curves were constructed to determine the effect of varying TSA (Sigma) concentrations on secretion and viable cell numbers. TSA was carefully chosen for these studies due to its similarity in structure to the FDA-approved HDACi drug, Vorinostat [237]. Serial dilutions of TSA were made in dimethyl sulfoxide (DMSO; Sigma) starting at 2.5 μM (six concentrations were tested: 0, 0.156, 0.313, 0.625, 1.25, and 2.5 μM). After a 24 hour incubation at these varying TSA concentrations, wells were washed twice in Dulbecco's Phosphate-Buffered Solution (DPBS; Corning cellgro) containing calcium and magnesium to remove any dead cells and changed to stimulating medium (βTC-tet: 16.7 mM glucose for 30 minutes, GLUTag: 5 mM glucose + 2% MH for 2 hours). Medium samples were collected after the incubation periods and cells were subsequently trypsinized for trypan blue (Sigma) viable cell counting using a hemocytometer for data normalization.

Effects on secretion pathways To study the secretion pathway, cells were seeded in 12-well plates (βTC-tet: $1.8x10^5$ cells/cm^2, GLUTag: $2.1x10^5$ cells/cm^2) two days before TSA treatment. Initial cell densities were chosen to achieve a similar level of confluency, approximately 85%, among groups on the day of treatment. On day 0, culture medium was changed to fresh in each well and TSA was added at an intermediate concentration of 0.625 μM. Non-treated control groups were used for direct comparisons. On day 1, insulin or GLP-1 secretion rate tests were performed and cells in parallel wells were harvested for

intracellular insulin or GLP-1 and total RNA collection. To collect intracellular proteins, TSA and non-treated cell pellets were lysed using the Mammalian Cell Lysis Kit (Sigma). Proinsulin and insulin concentrations were measured from βTC-tet samples by Mouse Insulin and Rat/Mouse Proinsulin ELISA kits (Mercodia Inc., Winston Salem, NC) and GLP-1 concentrations were measured from GLUTag samples by GLP-1 (Active) ELISA (Mercodia Inc.).

Effects of tubacin (Sigma) were investigated to determine the specific role of HDAC6 in the effects observed from TSA treatment, which acts on HDACs1-10. This choice of HDACi is based on reports that inhibition of HDAC6, a cytoplasmic HDAC, increases vesicular transport and secretion of hormones in neuroendocrine cells by increasing acetylated α-tubulin levels [190]. Tubacin treatment was identical to TSA treatment, except a final concentration of 4 μM was used. This concentration was estimated based on cytoblot analyses of TSA and tubacin effects on acetylated tubulin levels in A549 cells. An approximate tubacin treatment of 4 μM caused a similar increase in acetylated α-tubulin levels as TSA at around 0.625 μM [193]. Tests such as this one, with other specific HDACi, may provide more insight into the main mechanisms for the observed effects of TSA treatment.

Insulin secretion rate test ISR tests performed on βTC-tet cells involved subjecting cells to basal conditions (DMEM with 0 mM glucose) for one hour followed by a thirty minute step-up period under stimulating conditions (DMEM with 16.7 mM glucose). Secretion tests on GLUTag cells involved subjecting cells to basal conditions (DMEM with 5mM glucose) for two hours followed by a two hour step-up period under stimulating conditions

(basal + 2% meat hydrolysate (MH); Sigma). Media samples were taken before and after each incubation period for rate determinations.

Statistical analyses All data were analyzed using Minitab software (Minitab, Inc., State College, PA) and reported as mean ± SEM; each mean was the average of data from three or more independent experiments. Significance was determined using a one-way analysis of variance (ANOVA) with the general linear model, with significance defined as $p \leq 0.05$.

D.4 Results

Dose-response curves After 24 hours of treating βTC-tet and GLUTag cells with varying TSA concentrations, a similar dose-dependent response was observed between stimulated insulin and GLP-1 secretion per viable cell; effects on viable cell numbers also followed comparable trends between groups (Figure D.1). At a TSA concentration of 0.313 μM or higher, both groups secreted significantly more than non-treated controls and appeared to plateau near a TSA concentration of 1.25 μM. The inverse was true for TSA effects on viable cell numbers which were significantly lower than non-treated controls at and above 0.313 μM TSA, plateauing near 1.25 μM TSA. The viability, or fraction of viable cells from the total cell number, after TSA treatment only declined slightly and plateaued around 80% for all groups, suggesting that secretion tests were performed on a population consisting of mostly viable cells.

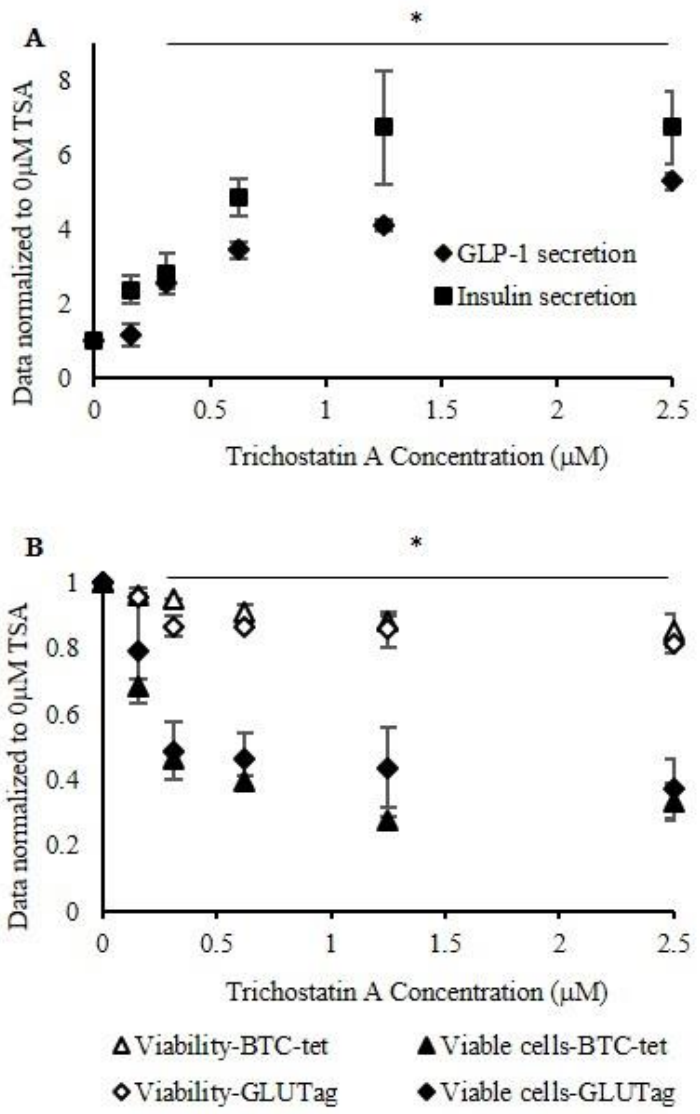

Figure D.1: TSA dose-response curves for βTC-tet and GLUTag L-cells. Effects of 24 hour TSA treatment on A) secretion and B) viable cell numbers. Accumulated GLP-1 released from GLUTag cells was measured after a 2 hour incubation in medium containing 5 mM glucose and 2% MH. Accumulated insulin released from βTC-tet cells was measured after a 30 minute incubation in medium containing 16.7 mM glucose. Accumulated secretion data were normalized to viable cell numbers prior to normalization of all data to 0 μM TSA controls. Asterisks indicate statistical difference from 0 μM TSA (*$p<0.05$).

Effects on secretion pathways To avoid excessive toxicity, an intermediate concentration of 0.625 μM TSA was chosen to specifically assess HDACi effects on insulin and GLP-1 mRNA, storage, and secretion rates. It was surprising to find that TSA-treated β- and L-

cells had lower levels of insulin (78% of control) and GLP-1 (36% of control) mRNA, respectively, relative to their non-treated controls (Figure D.2).

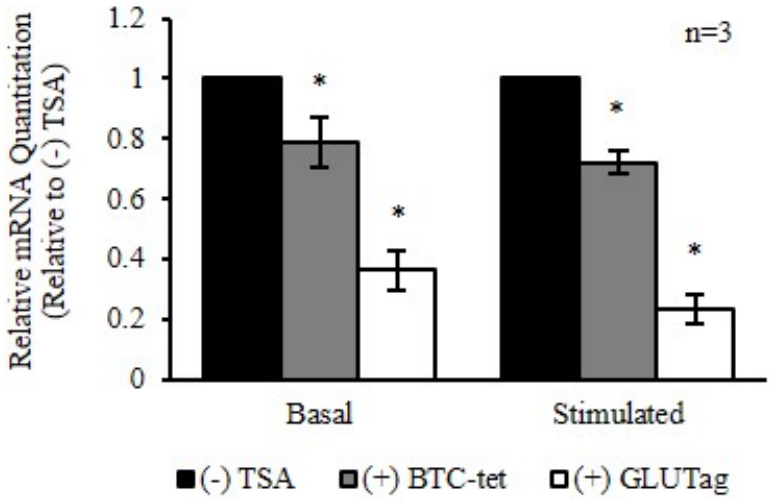

Figure D.2: Relative quantitation of INS-1 mouse insulin mRNA in TSA-treated βTC-tet cells and GLP-1 mRNA in TSA-treated GLUTag cells relative to their non-treated controls under basal and stimulated conditions. A one hour incubation in the following medium for each cell type was performed prior to total RNA collection. Asterisks indicate statistical difference from non-treated control groups (*$p<0.05$).

TSA treatment of βTC-tet cells caused a 2.5-fold increase in stored insulin and a 2-fold increase in glucose-stimulated insulin secretion but had no significant effect on constitutive insulin secretion under basal conditions (Figure D.3; βTC-tet). TSA treatment of GLUTag cells also increased stored and MH-stimulated GLP-1 secretion by 2 and 1.9-fold, respectively, but had an even greater effect on basal GLP-1 secretion (5 mM glucose) which increased by almost 9-fold (Figure D.3; GLUTag). The effect on stimulated

secretion, however, was only significant with 90% confidence (p=0.09). No significant effects were observed in either cell type after 24 hour, 4μM tubacin treatments.

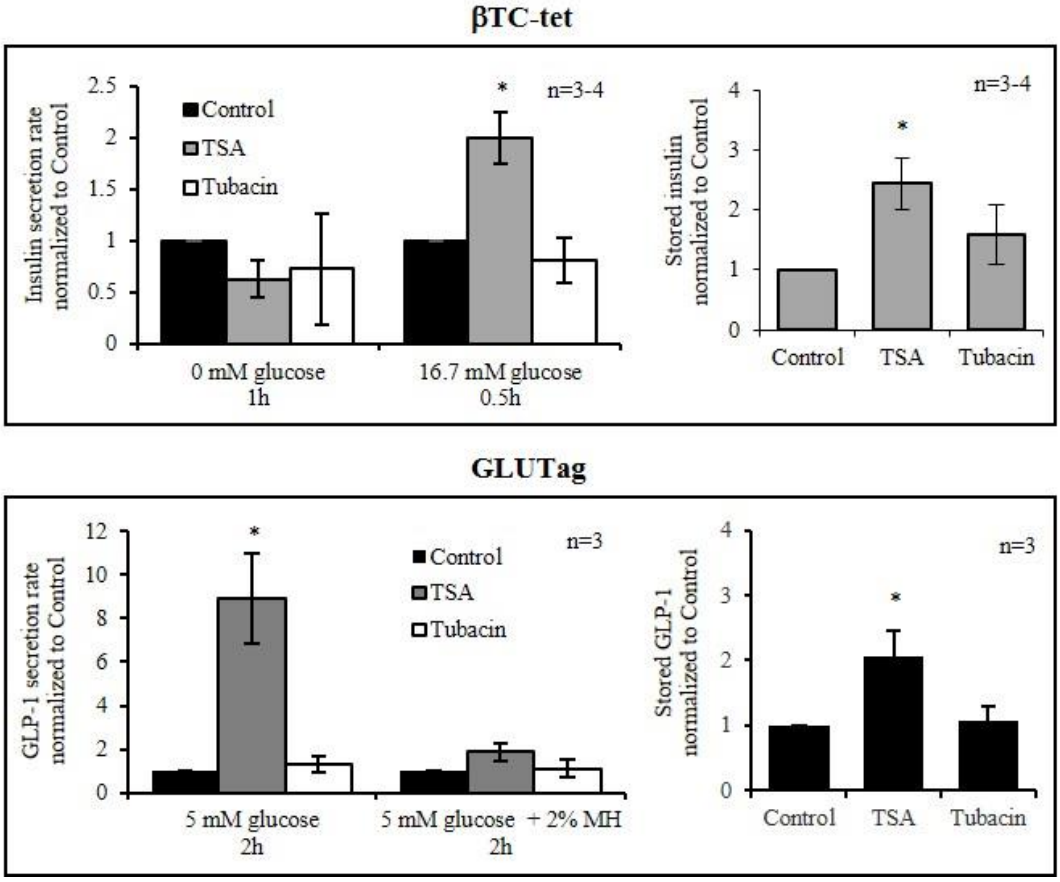

Figure D.3: TSA (0.625 mM) and tubacin (4 mM) effects on stored and secreted mouse insulin from βTC-tet cells and GLP-1 from GLUTag cells. All data were normalized to viable cell number prior to normalization to non-treated controls. Asterisks indicate statistical difference from control group under each condition (*p<0.05).

A small, but significant, 10% increase in secreted proinsulin to insulin conversion was found in TSA-treated βTC-tet cells under 16.7 mM glucose conditions (Figure D.4A), but no difference was detected in stored insulin processing efficiency relative to non-

treated controls (Figure D.4). Processing efficiencies of proglucagon to GLP-1 in parental GLUTag cells were not determined because commercially available proglucagon ELISA kits (RayBiotech, Inc., Norcross, GA) are expected to measure other small peptides such as glicentin and glicentin-related polypeptide (GRPP) that are synthesized from proglucagon in L-cells. Accuracy of processing efficiency would therefore be difficult to obtain.

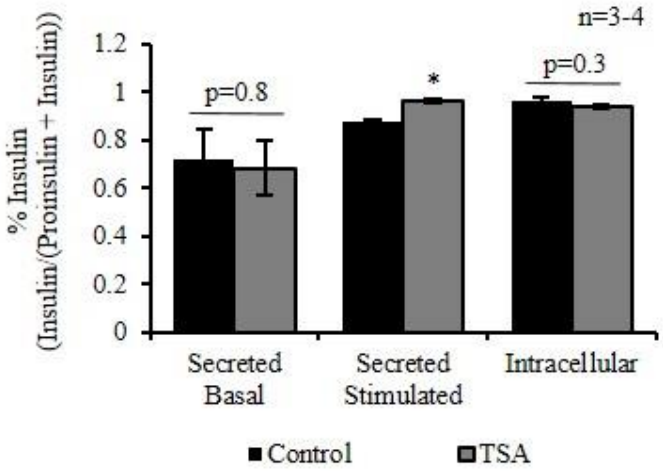

Figure D.4: Effects of TSA on the efficiency of proinsulin to insulin processing of basal/stimulated secretion and intracellular storage in βTC-tet cells. Asterisk indicates a statistical difference from the control group (*$p<0.05$).

D.5 Discussion

With the recent presence of HDAC in the diabetes literature [236], and the newfound potential for HDACi therapy to protect cytokine-mediated β-cell death [231, 232], there is little information regarding the impact of HDACi on other important factors that play major roles in diabetes. In this work, we have demonstrated the potential benefits

of HDACi for the direct and indirect functional enhancement of β-cells through increasing insulin storage and secretion capacity as well as GLP-1 storage and secretion from L-cells.

Enhancing effects of TSA on βTC-tet cells in this study are in accordance with reports of a dose-dependent increase in insulin secretion from human islets treated with VPA [188] and increased insulin secretion after the use of a culture technique on rat islets involving 0.1 μM TSA treatment for 24 hours [189]. The specific effects of TSA on rat islets in the latter study, however, were not assessed and results from the former study were attributed to the structural similarity of VPA to free fatty acid secretagogues. In contrast to these studies, Larsen et al. observed a reduction in insulin release from rat INS-1 β-cells treated with 0.2 μM TSA for two days. The timescale for the experiment was properly designed, as it was meant to test effects of TSA on cytokine-mediated apoptosis, but it was inappropriately long for assessing the direct effects of TSA on β-cell function. Additionally, β-cell secretion was not normalized to viable cell numbers for appropriate comparisons of the functional effects of TSA-treated and non-treated populations on a per-cell basis. For these reasons, conclusions of direct TSA effects on β-cells could not be made with certainty.

The observed 21% reduction in insulin mRNA levels in TSA-treated βTC-tet cells and the 64% reduction in GLP-1 mRNA levels in TSA-treated GLUTag cells are not yet understood and investigation in future studies is needed, as they are beyond the scope of this study. There are various possible explanations such as cellular mRNA degradation due to TSA-induced apoptosis [238], direct effects of TSA on mRNA stability [239], or repressed gene transcription which is a common effect of HDACi [240]. The first reason is unlikely since global mRNA degradation due to early-stage apoptosis should cause the

endogenous control, actin-beta mRNA, to degrade as well, but there was no evidence of this from the PCR results (mean (SD) C_T values for βTC-tet: ACTB- 25.4 (3.9), ACTB+ 25.7 (3.9); p=0.9; n=3 and GLUTag: ACTB- 19.1 (0.5), ACTB+ 19.5 (1.1); p=0.4; n=5). Apoptosis therefore was not measured, especially since cell death and apoptotic effects of HDACi have already been well studied [231, 232].

The purpose of using the βTC-tet cell line as opposed to islets in this study was to simply investigate the direct effects of HDACi on β-cell function. HDACi effects on islets are highly complex and change in insulin secretion and expression may be an indirect effect of TSA stress on neighboring cells. A limitation to studying the β-cell line, however, is that it is less clinically relevant and studies in islets will still need to be performed.

Oral HDACi administration could impact various cells within the body. In diabetes patients, proper GLP-1 secretion from intestinal L-cells is critical to glucose-stimulated β-cell function. Interestingly enough, GLP-1 increases *in vitro* global acetylation of histone H3 in β-cells [241] and may therefore be acting on mechanisms similar to the ones which HDACi act on. As expected, based on secretion pathway similarities between β- and L-cells, TSA had similar enhancing effects on GLUTag cells. However, a stronger effect on glucose-induced GLP-1 secretion was observed than on MH-induced secretion. Although the stimulation index was lost when inducing with peptides like MH, perhaps a shift to glucose-controlled secretion occurred after TSA treatment. Significantly higher secretion of GLP-1 in response to glucose in type 2 diabetes patients would be extremely beneficial in the local stimulation of β-cell insulin secretion for improved glucose regulation. This method would be a better alternative to the oral GLP-1 analog therapies that have suboptimal pharmacokinetics and blood glucose regulation compared to natural body

functions. To clarify the impact of HDACi on L-cell glucose-responsiveness, further investigation is necessary. In addition, animal studies should be performed to assess the clinical consequences of losing the GLP-1 burst response to peptides and gaining glucose-responsiveness.

Evidence from this study further supports the potential role of HDACi therapy in preventing or treating diabetes mellitus by expanding knowledge in the field about the additional benefits of HDACi on β- and L-cell function. To determine clinical feasibility, preclinical effects of FDA-approved HDACi like Vorinostat, with structural similarities to TSA, should be studied in non-obese diabetic (NOD) mice to evaluate diabetes prevention and in low-dose, STZ-induced high order animals to assess diabetes treatment.

APPENDIX E: ADDITIONAL BIOLUMINESCENCE STUDIES

E.1 AAV Transduction for Luciferase Gene Incorporation

Prior to using the lentivirus for luciferase reporter gene incorporation, AAV transduction of GLUTag-INS was investigated. AAV transduction was performed in the same way as with lentivirus, but the MOI used for this study was much higher (MOI 2000). Even with such a high MOI, luciferase delivery via AAV resulted in an average of only $1.6x10^6$ photons/s (Figure E.1) compared to over $2.4x10^7$ photons/s emitted from a similar number of lentivirally-transduced EINS cells at an MOI of 30. In addition, after only one passage, AAV-transduced GLUTag-INS no longer expressed bioluminescence. For these reasons, lentivirus transduction was pursued for stable luciferase reporter gene incorporation.

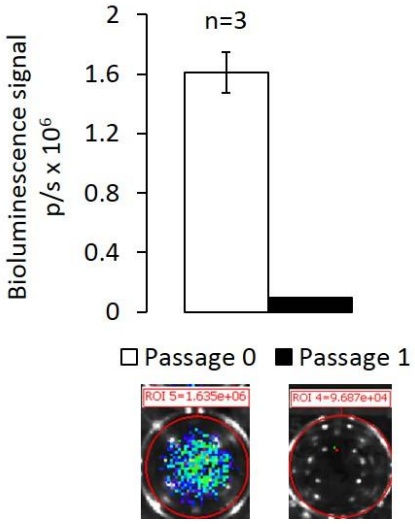

Figure E.1: Transduction of GLUTag-INS cells with an AAV containing the luciferase reporter gene. Passage 0 = 3 days post-transduction, Passage 1 = 5 days post-transduction. Initial cell seeding density was 7.9×10^4 cells/cm^2.

E.2 Optimal Time for Bioluminescence Imaging

A brief preliminary study was performed to determine the optimal bioluminescence imaging time after i.p. injection of luciferin in mice (Figure E.2). As strong bioluminescence signal was observed after only 5 minutes post-luciferin injection, it was chosen as the imaging time for all studies. A short imaging time was favorable in order to keep mice under anesthesia for only a limited time and reduce stress to the mice.

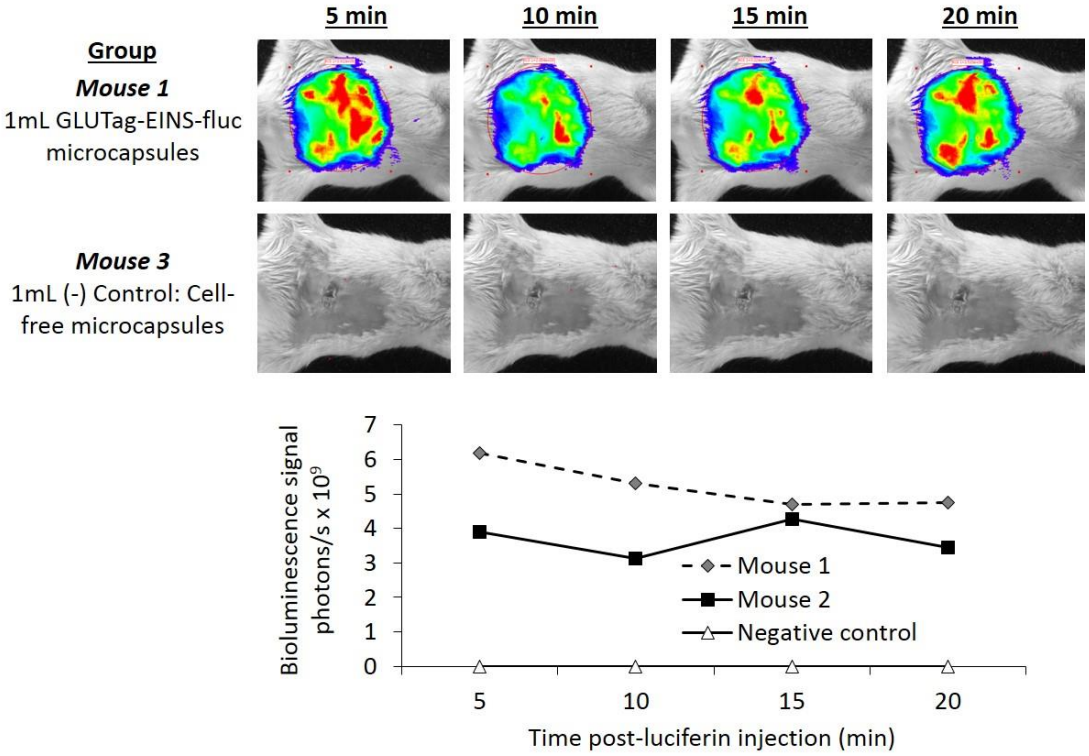

Figure E.2: BLI over the course of 20 minutes in three mice after luciferin injection. Two of the mice (Mouse 1 and 2) were i.p. injected with 1 mL of microencapsulated Fluc cells and one mouse (Negative control) was injected i.p. with 1 mL of cell-free microcapsules. Representative images of the same mouse imaged at 5, 10, 15, and 20 minutes after luciferin injection are shown at the top of this figure to indicate the strength of BLI. Quantitative bioluminescence over time for each mouse is indicated in the graph at the bottom of the figure.

APPENDIX F: OPTIMIZATION OF THERAPEUTIC EFFICACY STUDY

F.1 Results from the First Therapeutic Efficacy Study

The first therapeutic efficacy study allowed for proper optimization of the protocol. It was clear from the data represented in Figure F.1 that mice became extremely hyperglycemic after an STZ injection of 230 mg/kg. On day 0, all but two of the mice were giving readings of "HI" on the glucometer. However, mice receiving the microencapsulated βTC-tet cells were able to restore normoglycemia while the EINS or Fluc-receiving mice continued to read "HI" on the glucometer. Since mice were in this state for three consecutive days after transplantation, they were sacrificed according to the IACUC protocol. Promising pieces of data were that mice receiving EINS or Fluc cells were able to recover in body weight and high levels of human insulin were detected in the blood (Figure F.1).

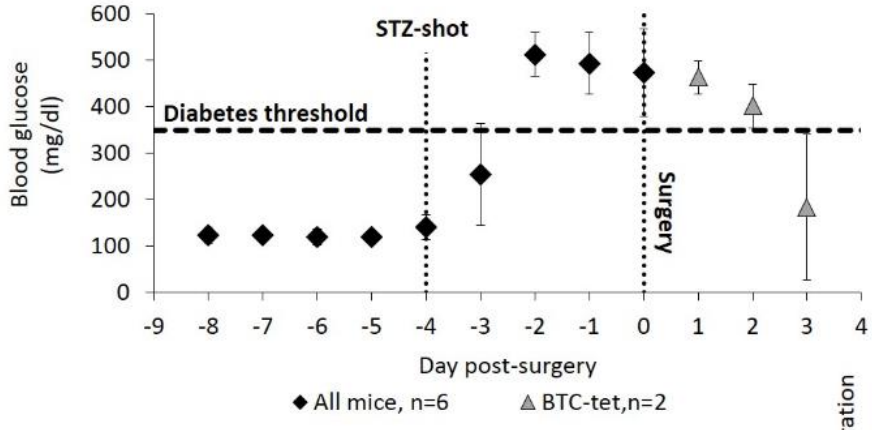

Mouse	Implanted cells	BG on day 0
1	GLUTag-EINS	540
2	βTC-tets	HI
3*died on d2	GLUTag-EINS	407
4	GLUTag-EINS-fluc	HI
5	βTC-tets	HI
6	GLUTag-EINS-fluc	HI

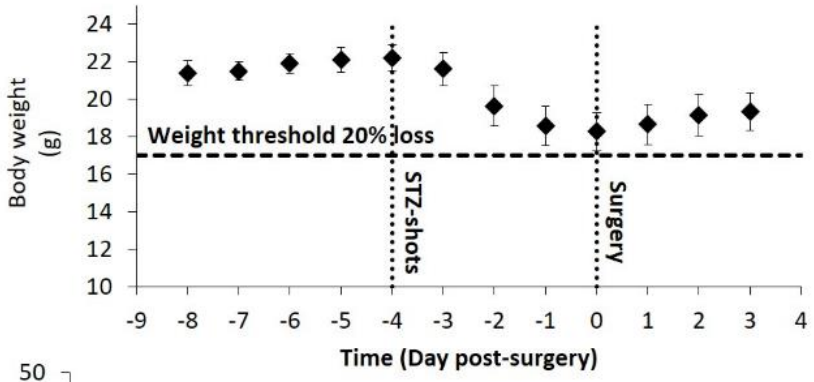

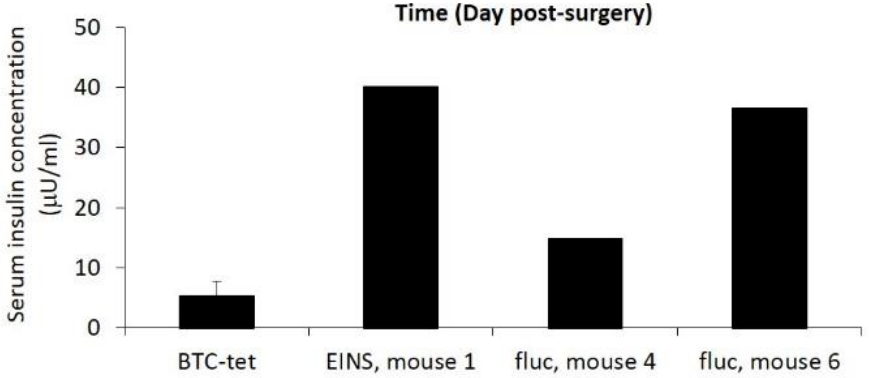

Figure F.1: Results from the first therapeutic efficacy experiment. Mice were injected i.p. with STZ (230 mg/kg) four days before the surgery to induce diabetes. Three groups were evaluated: 2 mice received 3 mL microencapsulated EINS cells, 2 mice received 3 mL microencapsulated Fluc cells, and 2 mice received 0.4 mL microencapsulated βTC-tet cells to serve as positive controls. Results are shown as blood glucose levels (upper and lower left), body weight (upper right), and serum human insulin concentration at the end of the study (lower right). The table indicates the mice that had blood glucose level readings of "HI" by the glucometer on day 0. These readings were not included in the blood glucose graph since they were not numerical.

F.2 Exogenous Insulin Administration

In the second therapeutic efficacy study, the following changes were made: 1) exogenous insulin was administered (long-acting human insulin-Lantus®) to avoid extreme hyperglycemia and 2) a 2:1 ratio of either GLUTag-INS:Fluc or EINS:Fluc microcapsules were transplanted due to *in vitro* studies indicating that EINS functioned better over time in microcapsules compared to Fluc (CHAPTER 4, Figure 4.6). Although exogenous insulin administration reduced extreme hyperglycemia, the issue of hypoglycemia arose since dosing of human insulin was difficult in the mice (Figure F.2). It appeared that administering 2 U of Lantus® insulin in the span of 24 hours was too high for Mouse 2 which became extremely hypoglycemic on day 4 and had to be euthanized. Even less than 1.5 U caused Mouse 3 to become extremely hypoglycemic on day 10. For this reason, we decided that lowering the STZ dose, as well as the exogenous insulin dose administered, may allow for the avoidance of both extreme hyperglycemia and hypoglycemia in treated mice.

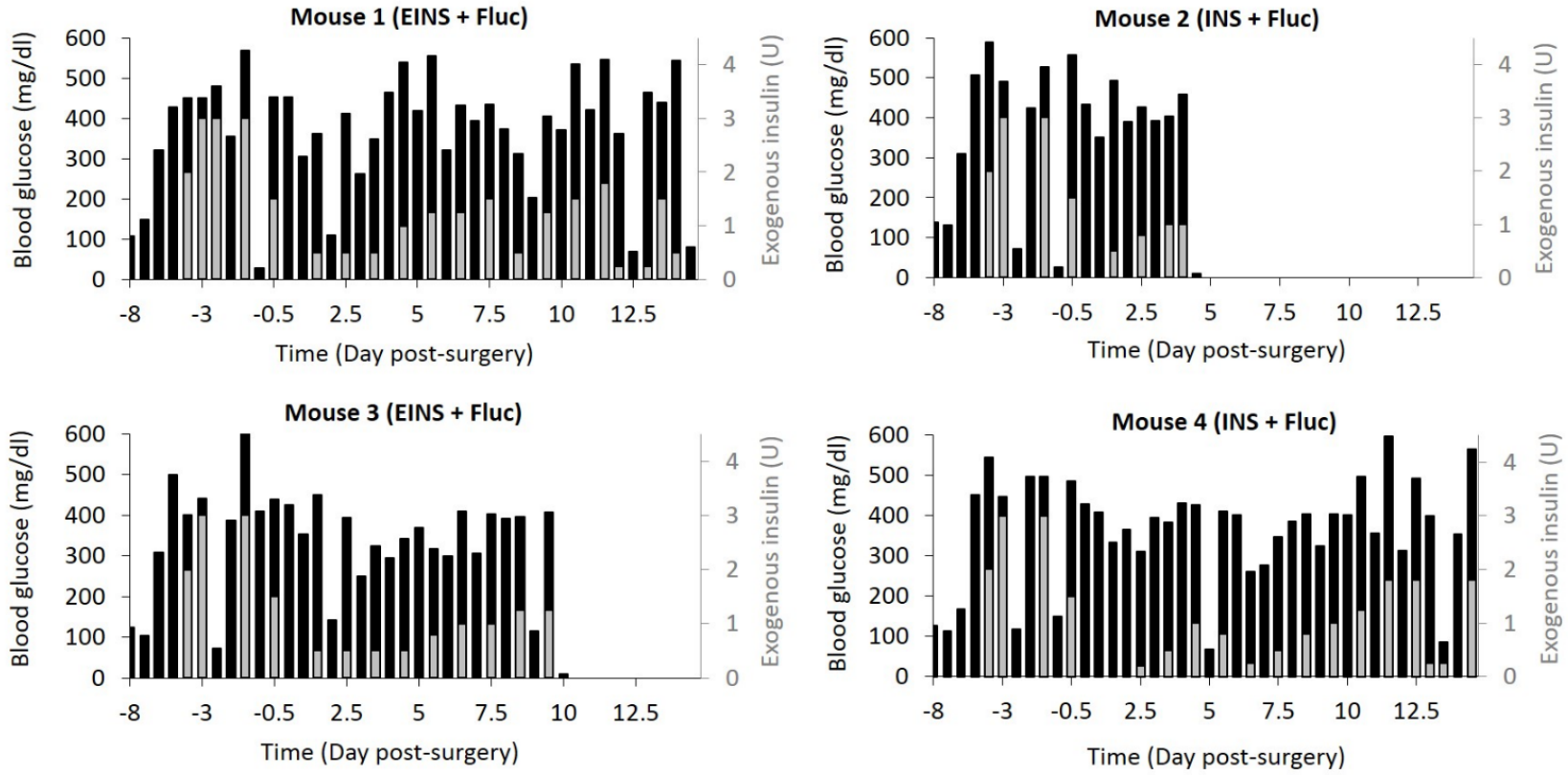

Figure F.2: Blood glucose and doses of exogenous insulin administered during the second therapeutic efficacy test. STZ was injected i.p. in four mice 7 days before surgery. On day 0, mouse 1 and 3 were transplanted with 3 mL microencapsulated EINS (2 mL) and Fluc (1 mL) cells and mouse 2 and 4 were transplanted with 3 mL microencapsulated GLUTag-INS (2 mL) and Fluc (1 mL) cells. Black bars indicate blood glucose levels (left axis) and the grey bars indicate the dose of exogenous insulin that was administered (right axis). An empty space before the end of the study period of 14 days indicates that the mouse was euthanized due to extreme hypoglycemia, resulting from exogenous insulin administration.

F.3 Optimizing the STZ Dose

A brief study consisting of three mice was performed to determine the lowest STZ dose that would still induce diabetes (>350 mg/dl blood glucose concentration). There appeared to be a dose-dependent response to STZ injection and lower doses increased the time needed to reach a diabetic state (Figure F.3). In addition, lower doses showed less of a decline in mouse body weight. The lowest dose, 150 mg/kg STZ, did not induce diabetes. The high dose, 210 mg/kg STZ, made the mouse diabetic one day after injection. On the other hand, the intermediate dose of 180 mg/kg, made the mouse diabetic three days after injection and most of the time hyperglycemic blood glucose levels were either comparable or lower than the mouse that received the highest dose. In addition, the two diabetic mice maintained reasonable hyperglycemic blood glucose levels when administered approximately 2 U of exogenous insulin every two days.

Based on this and the previous optimization studies, therapeutic efficacy studies were carried out as follows: 1) Mice were made diabetic via i.p. STZ injection at 180 mg/kg to avoid extreme hyperglycemia, 2) non-treated diabetic mice were administered 2 U of exogenous insulin if blood glucose levels were >350 mg/dl and treated diabetic mice were only administered 1 U of exogenous insulin if blood glucose levels were >450 mg/dl for two consecutive days in order to avoid extreme hypoglycemia, and 3) mice were transplanted with a total of 3 mL microencapsulated EINS and Fluc cells at a ratio of 2 to 1.

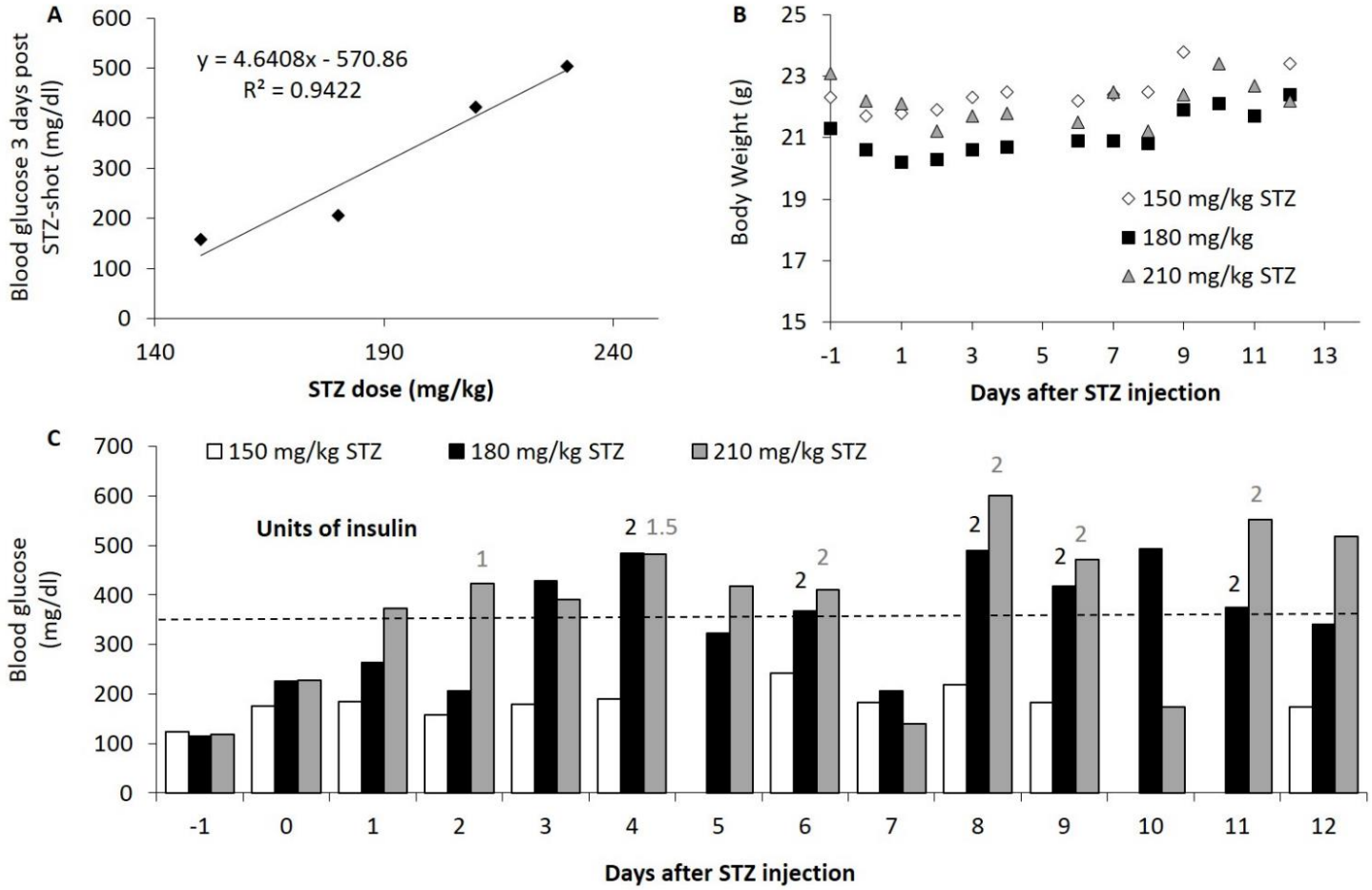

Figure F.3: Effect of STZ dose on blood glucose and body weight over 12 days. Three mice were injected i.p. with STZ at doses 150, 180, and 210 mg/kg. A) Blood glucose levels versus STZ dose three days after STZ-injection. The last data point was added (230 mg/kg) based on previous studies. B) Mouse body weight over time at various STZ doses. C) Blood glucose levels over time at various STZ doses. The numbers above bars represent the U of insulin administered to the mouse on that day.

APPENDIX G: DATA USED FOR NORMALIZATION IN LONG-TERM HDACI STUDY

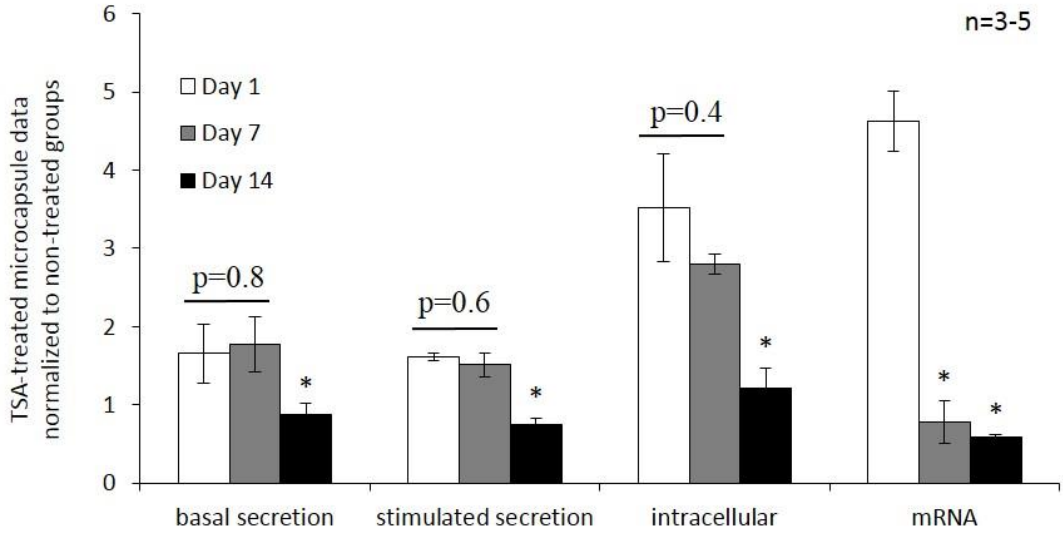

Figure G.1: Long-term TSA effects on basal and stimulated ISR normalized to alamarBlue™, intracellular insulin content normalized to alamarBlue™, and insulin mRNA from alginate microencapsulated EINS cells over 14 days. To make TSA fold-increase comparisons among secreted, intracellular, and mRNA groups, all data were normalized to non-treated microencapsulated EINS cells cultured and tested in parallel to treated groups. Asterisks indicate a statistical difference from day 1 within each respective measurement ($p<0.05$). See APPENDIX G for the table of values from non-treated groups that were used for normalization.

Table G.1: Data reported as mean (SEM) from non-treated microencapsulated EINS cells that were used to normalize the data presented in Figure G.1 (Figure 3.7 in CHAPTER 3).

	Basal secretion fmol/(mL alginate·h·RFU))	Stimulated secretion fmol/(mL alginate·h·RFU))	Intracellular fmol/(mL alginate·RFU)	mRNA
Day 1	4.2 (1.9)	5.3 (1.4)	34.0 (4.8)	1.0 (0)
Day 7	1.3 (0.4)	2.8 (0.5)	18.0 (1.2)	1.0 (0)
Day 14	3.5 (0.3)	5.9 (0.7)	16.9 (6.9)	1.0 (0)

REFERENCES

1. *Centers for Disease Control and Prevention. National diabetes fact sheet: national estimates and general information on diabetes and prediabetes in the United States, 2011. Atlanta, GA: U.S. Department of Health and Human Services, Centers for Disease Control and Prevention, 2011.*

2. *The Diabetes Control and Complications Trial Research Group. The effect of intensive treatment of diabetes on the development and progression of long-term complications in insulin-dependent diabetes mellitus.* N Engl J Med, 1993. **329**(14): p. 977-986.

3. Leitão, C.B., et al., *Current challenges in islet transplantation.* Curr Diab Rep, 2008. **8**(4): p. 324-331.

4. Hu, Q., Z. Liu, and H. Zhu, *Pig islets for islet xenotransplantation: current status and future perspectives.* Chin Med J, 2014. **127**(2): p. 370-377.

5. O'Sullivan, E.S., et al., *Islets transplanted in immunoisolation devices: a review of the progress and the challenges that remain.* Endocr Rev, 2011. **32**(6): p. 827-44.

6. Calafiore, R., et al., *Grafts of microencapsulated pancreatic islet cells for the therapy of diabetes mellitus in non-immunosuppressed animals.* Biotechnol Appl Biochem, 2004. **39**: p. 159-164.

7. Elliot, R.B., et al., *Intraperitoneal alginate-encapsulated neonatal porcine islets in a placebo-controlled study with 16 diabetic cynomolgus primates.* Transplant Proc, 2005. **37**(8): p. 3505-3508.

8. Dufrane, D., R.M. Goebbels, and P. Gianello, *Alginate encapsulation of pig islets allows correction of STZ-induced diabetes in primates up to 6 months without immunosuppression.* Transplantation, 2010. **90**(10): p. 1054-1062.

9. Dufrane, D., et al., *6-month survival of microencapsulated pig islets and alginate biocompatibility in primates: proof of concept.* Transplantation, 2006. **81**(9): p. 1345-1353.

10. Elliot, R.B., et al., *Live encapsulated porcine islets from a type 1 diabetic patient 9.5 yr after xenotransplantation.* Xenotransplantation, 2007. **14**: p. 157-161.

11. Valdes-Gonzalez, R.A., et al., *Xenotransplantation of porcine neonatal islets of Langerhans and Sertoli cells: a 4-year study.* Eur J Endocrinol, 2005. **153**(3): p. 419-427.

12. Lu, Y.C., et al., *Release of transgenic human insulin from gastric g cells: a novel approach for the amelioration of diabetes.* Endocrinology, 2005. **146**(6): p. 2610-9.

13. Schirra, J., et al., *Gastric emptying and release of incretin hormones after glucose ingestion in humans.* J Clin Invest, 1996. **97**(1): p. 92-103.

14. Cheung, A.T., et al., *Glucose-dependent insulin release from genetically engineered K cells.* Science, 2000. **290**(5498): p. 1959-1962.

15. Han, J., et al., *Engineered enteroendocrine cells secrete insulin in response to glucose and reverse hyperglycemica in diabetic mice.* Mol Ther, 2007. **15**(6): p. 1195-1202.

16. Zhang, Y., et al., *Genetically engineered K cells provide sufficient insulin to correct hyperglycemia in a nude murine model.* Acta Biochim Biophys Sin, 2008. **40**(2): p. 149-157.

17. Unniappan, S., et al., *Treatment of diabetes by transplantation of drug-inducible insulin-producing gut cells.* J Mol Med, 2009. **87**: p. 703-712.

18. Bara, H. and A. Sambanis, *Insulin-secreting L-cells for the treatment of insulin-dependent diabetes.* Biochem Biophys Res Commun, 2008. **371**(1): p. 39-43.

19. Bara, H. and A. Sambanis, *Development and characterization of a tissue engineered pancreatic substitute based on recombinant intestinal endocrine L-cells.* Biotechnol Bioeng, 2009. **103**(4): p. 828-834.

20. Bara, H., P.M. Thule, and A. Sambanis, *A cell-based approach for diabetes treatment using engineered non-beta cells.* J Diabetes Sci Technol, 2009. **3**(3): p. 555-61.

21. Robles, L., et al., *Current status of islet encapsulation.* Cell Transplant, 2013.

22. Raj, S.M., et al., *No association of multiple type 2 diabetes loci with type 1 diabetes.* Diabetologia, 2009. **52**(10): p. 2109-2116.

23. Barrett, J.C., et al., *Genome-wide association study and meta-analysis find that over 40 loci affect risk of type 1 diabetes.* Nat Genet, 2009. **41**(6): p. 703-707.

24. Willcox, A., et al., *Analysis of islet inflammation in human type 1 diabetes.* Clin Exp Immunol, 2009. **155**(2): p. 173-181.

25. Prokopenko, I., M.I. McCarthy, and C.M. Lindgren, *Type 2 diabetes: new genes, new understanding.* Trends Genet, 2008. **24**(12): p. 613-621.

26. Butler, A.E., et al., *Beta-cell deficit and increased beta-cell apoptosis in humans with type 2 diabetes.* Diabetes, 2003. **52**(1): p. 102-110.

27. Sakuraba, H., et al., *Reduced beta-cell mass and expression of oxidative stress-related DNA damage in the islet of Japanese Type II diabetic patients.* Diabetologia, 2002. **45**(1): p. 85-96.

28. Yoon, K.H., et al., *Selective beta-cell loss and alpha-cell expansion in patients with type 2 diabetes mellitus in Korea.* J Clin Endocrinol Metab, 2003. **88**(5): p. 2300-2308.

29. Kleinman, J.C., et al., *Mortality among diabetics in a national sample.* Am J Epidemiol, 1988. **128**(2): p. 389-401.

30. Rubin, R.J., W.M. Altman, and D.N. Mendelson, *Health care expenditures for people with diabetes mellitus.* J Clin Endocrinol Metab, 1994. **78**(4): p. 809A-809F.

31. Pittman, I., L. Philipson, and D. Steiner. *Insulin biosynthesis, secretion, structure, and structure-activity relationships*. 2004; Available from: http://diabetesmanager.pbworks.com/w/page/17680216/Insulin%20Biosynthesis,%20Secretion,%20Structure,%20and%20Structure-Activity%20Relationships.

32. Fu, Z., E.R. Gilbert, and D. Liu, *Regulation of Insulin Synthesis and Secretion and Pancreatic Beta-Cell Dysfunction in Diabetes.* Curr Diab Rev, 2013. **9**: p. 25-53.

33. Schmitz, O., et al., *On high-frequency insulin oscillations.* Ageing Res Rev, 2008. **7**(4): p. 310-305.

34. Vasquez-Martinez, R., et al., *Revisiting the regulated secretory pathway: From frogs to human.* Gen Comp Endocrinol, 2012. **175**(1): p. 1-9.

35. Curry, D.L., L.L. Bennett, and G.M. Grodsky, *Dynamics of insulin secretion by the perfused rat pancreas.* Endocrinology, 1968. **83**(3): p. 572-584.

36. Rorsman, P. and E. Renstrom, *Insulin granule dynamics in pancreatic beta cells.* Diabetologia, 2003. **46**(8): p. 1029-1045.

37. Taton, J., et al., *How recombinant insulin analogs improve insulin therapy of diabetes mellitus: pathophysiology, clinical practice and recommendations.* Med Sci Monit, 2001. **7**(4): p. 848-859.

38. Lenhard, M.J. and G.D. Reeves, *Continuous subcutaneous insulin infusion: a comprehensive review of insulin pump therapy.* Arch Intern Med, 2001. **161**(19): p. 2293-2300.

39. Al-Tabakha, M.M. and A.I. Arida, *Recent Challenges in Insulin Delivery Systems: A Review.* Indian J Pharm Sci, 2008. **70**(3): p. 278-286.

40. Freeman, J.S., *Insulin analog therapy: improving the match with physiologic insulin secretion.* J Am Osteopath Assoc, 2009. **109**(1): p. 26-36.

41. Bara, H. (2008). *Tissue engineering a pancreatic substitute based on recombinant intestinal endocrine cells*. (Doctoral dissertation). Retrieved from Georgia Tech Theses and Dissertations. (Accession Order No. [17726]).

42. Brunicardi, F.C. and C.R. Shackleton, *Whole-organ versus islet pancreatic transplantation.* Curr Opin Gen Surg, 1994: p. 179-185.

43. Ludwig, B., et al., *Islet Versus Pancreas Transplantation in Type 1 Diabetes: Competitive or Complementary?* Curr Diab Rep, 2010. **10**: p. 506-511.

44. Gruessner, R.W., et al., *A prospective, randomized, open-label study of steroid withdrawal in pancreas transplantation-a preliminary report with 6-month follow-up.* Transplant Proc, 2001. **33**(1-2): p. 1663-1664.

45. Naesens, M., D.R. Kuypers, and M. Sarwal, *Calcineurin inhibitor nephrotoxicity.* Clin J Am Soc Nephrol, 2009. **4**(2): p. 481-508.

46. Schlumpf, R., et al., *Is cyclosporine toxic for transplanted pancreatic islets?* Transplant Proc, 1986. **28**: p. 1169-1170.

47. Naftanel, M.A. and D.M. Harlan, *Pancreatic islet transplantation.* PLoS Med, 2004. **1**(3): p. e58.

48. Shapiro, A.M., et al., *Islet transplantation in seven patients with type 1 diabetes mellitus using a glucocorticoid-free immunosuppressive regimen.* N Engl J Med, 2000. **343**(4): p. 230-238.

49. Shapiro, A.M., et al., *International trial of the Edmonton protocol for islet transplantation.* N Engl J Med, 2006. **355**(13): p. 1318-1330.

50. Hatziavramidis, D.T., T.M. Karatzas, and G.P. Chrousos, *Pancreatic Islet Cell Transplantation: An Update.* Ann Biomed Eng, 2013. **41**(3): p. 469-476.

51. McCall, M. and A.M. Shapiro, *Update on Islet Transplantation.* Cold Spring Harb Perspect Med, 2012. **2**(7).

52. Posselt, A.M., et al., *Islet transplantation in type 1 diabetics using an immunosuppressive protocol based on the anti-LFA-1 antibody efalizumab.* Am J Transplant, 2010. **10**(8): p. 1870-1880.

53. Vaithilingam, V., G. Sundaram, and B.E. Tuch, *Islet cell transplantation.* Curr Opin Organ Transplant, 2008. **13**(6): p. 633-638.

54. MacKenzie, D.A., D.A. Hullet, and H.W. Sollinger, *Xenogeneic transplantation of porcine islets: an overview.* Transplantation, 2003. **76**(6): p. 887-891.

55. Ortiz, C., et al., *Identification of insulin variants using raman spectroscopy.* Anal Biochem, 2004. **332**(2): p. 245-252.

56. Dufrane, D. and P. Gianello, *Macro- or microencapsulation of pig islets to cure type 1 diabetes.* World J Gastroenterol, 2012. **18**(47): p. 6885-6893.

57. Patience, C., Y. Takeuchi, and R.A. Weiss, *Infection of human cells by an endogeneous retrovirus of pigs.* Nat Med, 1997. **3**(3): p. 282-286.

58. van der Laan, L.J.W., et al., *Infection by porcine endogeneous retrovirus after islet xenotransplantation in SCID mice.* Nature, 2000. **407**: p. 90-94.

59. Elliot, R.B., et al., *No evidence of infection with porcine endogenous retrovirus in recipients of encapsulated porcine islet xenografts.* Cell Transplant, 2000. **9**: p. 895-901.

60. Heneine, W., et al., *No evidence of infection with porcine endogeneous retrovirus in recipients of porcine islet-cell xenografts.* Lancet, 1998. **352**: p. 695-699.

61. Paradis, K., et al., *Search for cross species transmission of porcine endogeneous retrovirus in patients treated with living pig tissue.* Science, 199. **285**(1236-1241).

62. Efrat, S., *Cell-based therapy for insulin-dependent diabetes mellitus.* Eur J Endocrinol, 1998. **138**(2): p. 129-133.

63. de la Tour, D., et al., *Beta-cell differentiation from a human pancreatic cell line in vitro and in vivo.* Mol Endocrinol, 2001. **15**(3): p. 476-83.

64. Demeterco, C., et al., *c-Myc controls proliferation versus differentiation in human pancreatic endocrine cells.* J Clin Endocrinol Metab, 2002. **87**(7): p. 3475-85.

65. Gueli, N., et al., *In vitro growth of a cell line originated from a human insulinoma.* J Exp Clin Cancer Res, 1987. **4**: p. 281-285.

66. Levine, F., et al., *Development of a cell line from the human fetal pancreas.* Transplant Proc, 1995. **27**(6): p. 3410.

67. Narushima, M., et al., *A human beta-cell line for transplantation therapy to control type 1 diabetes.* Nat Biotechnol, 2005. **23**(10): p. 1274-82.

68. Ravassard, P., et al., *A genetically engineered human pancreatic beta cell line exhibiting glucose-inducible insulin secretion.* J Clin Invest, 2011. **121**(9): p. 3589-97.

69. Efrat, S., et al., *Beta-cell lines derived from transgenic mice expressing a hybrid insulin gene-oncogene.* Proc Natl Acad Sci U S A, 1988. **85**(23): p. 9037-9041.

70. D'Ambra, R., et al., *Regulation of insulin secretion from beta-cell lines derived from transgenic mice insulinomas resembles that of normal beta-cells.* Endocrinology, 1990. **126**(6): p. 2815-2822.

71. Fleischer, N., et al., *Functional analysis of a conditionally transformed pancreatic beta-cell line.* Diabetes, 1998. **47**(9): p. 1419-25.

72. Efrat, S., et al., *Conditional transformation of a pancreatic beta-cell line derived from transgenic mice expressing a tetracycline-regulated oncogene.* Proc Natl Acad Sci U S A, 1995. **92**(8): p. 3576-3580.

73. Mukundan, N.E., et al., *Oxygen consumption rates of free and alginate-entrapped beta TC3 mouse insulinoma cells.* Biochem Biophys Res Commun, 1995. **210**(1): p. 113-118.

74. Ahmad, H.F., et al., *Cryopreservation effects on intermediary metabolism in a pancreatic substitute: A 13C nuclear magnetic resonance study.* Tissue Eng Part A, 2012. **18**(21 and 22): p. 2323-2331.

75. Bao, S., et al., *Glucose homeostasis, insulin secretion, and islet phospholipids in mice that overexpress iPLA2beta in pancreatic beta-cells and in iPLA2beta-null mice.* Am J Physiol Endocrinol Metab, 2007. **294**(2): p. E217-229.

76. Tateishi, K., et al., *Generation of insulin-secreting islet-like clusters from human skin fibroblasts.* J Biol Chem, 2008. **283**(46): p. 31601-7.

77. Fryer, B.H., A. Rezania, and M.C. Zimmerman, *Generating b-cells in vitro: progress towards a Holy Grail.* Curr Opin Endocrinol Diabetes Obes, 2013. **20**(2): p. 112-117.

78. Boyd, A.S., et al., *A comparison of protocols used to generate insulin-producing cell clusters from mouse embryonic stem cells.* Stem Cells, 2008. **26**(5): p. 1128-1137.

79. Pokrywczynska, M., et al., *Differentiation of Stem Cells into Insulin-Producing Cells: Current Status and Challenges.* Arch Immunol Ther Exp, 2013. **61**: p. 149-158.

80. Chen, L.B., X.B. Jiang, and L. Yang, *Differentiation of rat marrow mesenchymal stem cells into pancreatic islet beta-cells.* World J Gastroenterol, 2004. **10**(20): p. 3016-3020.

81. Tang, D.Q., et al., *In vivo and in vitro characterization of insulin-producing cells obtained from murine bone marrow.* Diabetes, 2004. **53**(7): p. 1721-1732.

82. Zhang, Y., et al., *Pancreatic islet-like clusters from bone marrow mesenchymal stem cells of human first-trimester abortus can cure streptozocin-induced mouse diabetes.* Rejuvenation Res, 2010. **13**(6): p. 695-706.

83. Chandra, V., et al., *Islet-like cell aggregates generated from human adipose tissue derived stem cells ameliorate experimental diabetes in mice.* PLoS One, 2011. **6**(6).

84. Lipes, M.A., et al., *Insulin-secreting non-islet cells are resistant to autoimmune destruction.* Proc Natl Acad Sci U S A, 1996. **93**: p. 8595-8600.

85. Fodor, A., et al., *Adult rat liver cells transdifferentiated with lentiviral IPF1 vectors reverse diabetes in mice: an ex vivo gene therapy approach.* Diabetologia, 2007. **50**: p. 121-130.

86. Kozlowski, M., et al., *Adeno-associated viral delivery of a metabolically regulated insulin transgene to hepatocytes.* Mol Cell Endocrin, 2007. **273**: p. 6-15.

87. Tang, S.C. and A. Sambanis, *Differential rAAV2 transduction efficiencies and insulin secretion profiles in pure and co-culture models of human enteroendocrine L-cells and enterocytes.* J Gene Med, 2004. **6**: p. 1003-1013.

88. Muzyczka, N., *Use of adeno-associated virus as a general transduction vector for mammalian cells.* Curr Top Microbiol Immunol, 1992. **158**: p. 97-129.

89. Ellis, J. and S. Yao, *Retrovirus silencing and vector design: relevance to normal and cancer stem cells?* Curr Gene Ther, 2005. **5**(4): p. 367-373.

90. Pannell, D. and J. Ellis, *Silencing of gene expression: implications for design of retrovirus vectors.* Rev Med Virol, 2001. **11**(4): p. 205-217.

91. Jaalouk, D.E., et al., *Inhibition of histone deacetylation in 293GPG packaging cell line improves the production of self-inactivating MLV-derived retroviral vectors.* Virol J, 2006. **3**(27).

92. Chen, W.Y., et al., *Reactivation of silenced, virally transduced genes by inhibitors of histone deacetylase.* Proc Natl Acad Sci U S A, 1997. **94**(11): p. 5798-5803.

93. Katz, R.A., et al., *High-frequency epigenetic repression and silencing of retroviruses can be antagonized by histone deacetylase inhibitors and transcriptional activators, but uniform reactivation in cell clones is restricted by additional mechanisms.* J Virol, 2007. **81**(6): p. 2592-2604.

94. Okada, T., et al., *A histone deacetylase inhibitor enhances recombinant adeno-associated virus-mediated gene expression in tumor cells.* Mol Ther, 2006. **13**(4): p. 738-746.

95. Mateen, S., et al., *Silibinin synergizes with histone deacetylase and DNA methyltransferase inhibitors in upregulating E-cadherin expression together with inhibition of migration and invasion of human non-small cell lung cancer cells.* J Pharmacol Exp Ther, 2013. **435**(2): p. 206-214.

96. Shaw, J.A., et al., *Secretion of bioactive human insulin following plasmid-mediated gene transfer to non-neuroendocrine cell lines, primary cultures and rat skeletal muscle in vivo.* J Endocrinol, 2002. **172**(3): p. 653-672.

97. Hughes, S.D., et al., *Engineering of glucose-stimulated insulin secretion and biosynthesis in non-islet cells.* Proc Natl Acad Sci U S A, 1992. **89**(2): p. 688-692.

98. Hughes, S.D., et al., *Transfection of AtT-20ins cells with GLUT-2 but not GLUT-1 confers glucose-stimulated insulin secretion. Relationship to glucose metabolism.* J Biol Chem, 1993. **268**(20): p. 15205-15212.

99. Motoyoshi, S., et al., *Cellular characterization of pituitary adenoma cell line (AtT20 cell) transfected with insulin, glucose transporter type 2 (GLUT2) and glucokinase genes: insulin secretion in response to physiological concentrations of glucose.* Diabetologia, 1998. **41**(12): p. 1492-1501.

100. Ahmad, Z., et al., *Evaluation of insulin expression and secretion in genetically engineered gut K and L-cells.* BMC Biotechnol, 2012. **12**(64).

101. El-Aneed, A., *An overview of current delivery systems in cancer gene therapy.* J Control Release, 2004. **94**(1): p. 1-14.

102. Ido, Y., et al., *Prevention of vascular and neural dysfunction in diabetic rats by c-peptide.* Science, 1997. **277**(5325): p. 563-566.

103. Johansson, B.L., et al., *Beneficial effects of C-peptide on incipient nephropathy and neuropathy in patients with Type 1 diabetes mellitus.* Diabet Med, 2000. **17**(3): p. 181-189.

104. Hansen, A., et al., *C-peptide exerts beneficial effects on myocardial blood flow and function in patients with type 1 diabetes.* Diabetes, 2002. **51**(10): p. 3077-3082.

105. Ekberg, K., et al., *Amelioration of sensory nerve dysfunction by C-Peptide in patients with type 1 diabetes.* Diabetes, 2003. **52**(2): p. 536-541.

106. Lomedico, P.T., *Use of recombinant DNA technology to program eukaryotic cells to synthesize rat proinsulin: a rapid expression assay for cloned genes.* Proc Natl Acad Sci U S A, 1982. **79**(19): p. 5798-5802.

107. Laub, O. and W.J. Rutter, *Expression of the human insulin gene and cDNA in a heterologous mammalian system.* J Biol Chem, 1983. **258**(10): p. 6043-6050.

108. Selden, R.F., et al., *Regulation of insulin-gene expression. Implications for gene therapy.* N Engl J Med, 1987. **317**(17): p. 1067-1076.

109. Iwata, H., et al., *Preparation of insulin-releasing Chinese hamster ovary cell transfection of human insulin gene: its implantation into diabetic mice,* in *Polymers of Biological and Biomedical Significance*, S.W. Shalaby, et al., Editors. 1994, Oxford University Press: New York. p. 306-313.

110. Falqui, L., et al., *Reversal of diabetes in mice by implantation of human fibroblasts genetically engineered to release mature human insulin.* Hum Gen Ther, 1999. **10**(11): p. 1753-1762.

111. Abai, A.M., P.M. Hobart, and K.M. Barnhart, *Insulin delivery with plasmid DNA.* Hum Gen Ther, 1999. **10**(16): p. 2637-2649.

112. Martinenghi, S., et al., *Human insulin production and amelioration of diabetes in mice by electrotransfer-enhanced plasmid DNA gene transfer to the skeletal muscle.* Gene Ther, 2002. **9**(21): p. 1429-1437.

113. Sambanis, A., et al., *Use of regulated secretion in protein production from animal cells: an evaluation with the AtT-20 model cell line.* Biotechnol Bioeng, 1990. **35**(8): p. 771-780.

114. Moore, H.P., et al., *Expressing a human proinsulin cDNA in a mouse ACTH-secreting cell. Intracellular storage, proteolytic processing, and secretion on stimulation.* Cell, 1983. **35**: p. 531-538.

115. Stewart, C., et al., *Insulin-releasing pituitary cells as a model for somatic cell gene therapy in diabetes mellitus.* J Endocrinol, 1994. **142**(2): p. 339-343.

116. Wu, L., et al., *Engineering physiologically regulated insulin secretion in non-beta cells by expressing glucagon-like peptide 1 receptor.* Gene Ther, 2003. **10**(19): p. 1712-20.

117. Dong, H. and S.L. Woo, *Hepatic insulin production for type 1 diabetes.* Trends Endocrinol Metab, 2001. **12**: p. 441-446.

118. Thule´, P.M., J. Liu, and L.S. Phillips, *Glucose regulated production of human insulin in rat hepatocytes.* Gene Ther, 2000. **7**(3): p. 205-214.

119. Thule´, P.M. and J.M. Liu, *Regulated hepatic insulin gene therapy of STZ-diabetic rats.* Gene Ther, 2000. **7**: p. 1744-1752.

120. Jun, H.S. and J.W. Yoon, *Approaches for the Cure of Type 1 Diabetes by Cellular and Gene Therapy.* Curr Gene Ther, 2005. **5**: p. 249-262.

121. Tang, S.C. and A. Sambanis, *Preproinsulin mRNA engineering and its application to the regulation of insulin secretion from human hepatomas.* FEBS Lett, 2003. **537**(1-3): p. 193-7.

122. Lu, Y.C., et al., *Release of transgenic human insulin from gastric g cells: a novel approach for the amelioration of diabetes.* Endocrinology, 2005. **146**(6): p. 2610-2619.

123. Lee, Y.S. and H.S. Jun, *Anti-diabetic actions of glucagon-like peptide-1 on pancreatic beta-cells.* Metabolism, 2014. **63**(1): p. 9-19.

124. Duncanson, S. and A. Sambanis, *Dual factor delivery of CXCL12 and Exendin-4 for improved survival and function of encapsulated beta cells under hypoxic conditions.* Biotechnol Bioeng, 2013. **110**(8): p. 2292-2300.

125. Tang, S.C. and A. Sambanis, *Development of genetically engineered human intestinal cells for regulated insulin secretion using rAAV-mediated gene transfer.* Biochem Biophys Res Commun, 2003. **303**(2): p. 645-652.

126. Schwartz, G.P., G.T. Burke, and P.G. Katsoyannis, *A superactive insulin: [B10-aspartic acid]insulin(human).* Proc Natl Acad Sci U S A, 1987. **84**(18): p. 6408-11.

127. Brubaker, P.L., *Regulation of glucagon-like peptide-1 synthesis and secretion in the GLUTag enteroendocrine cell line.* Endocrinology, 1998. **139**: p. 4108-4114.

128. Opara, E.C., et al., *Design of a bioartificial pancreas.* J Investig Med, 2010. **58**(7): p. 831-837.

129. Lembert, N., et al., *Encapsulation of islets in rough surface, hydroxymethylated polysulfone capillaries stimulates VEGF release and promotes vascularization after transplantation.* Cell Transplant, 2005. **14**: p. 97-108.

130. Lee, K. and D. Mooney, *Hydrogels for tissue engineering.* Chemical Reviews, 2000. **101**: p. 1869-1879.

131. Peppas, N.A., et al., *Hydrogels in biology and medicine: from molecular principles to bionanotechnology.* Adv Mater, 2006. **18**: p. 1345-1360.

132. Nicodermus, G. and S. Bryant, *Cell encapsulation in Biodegradable hydrogels for tissue engineering applications.* Tissue Eng Part B Rev, 2008. **14**: p. 149-165.

133. Langlois, G., et al., *Direct effect of alginate purification on the survival of islets immobilized in alginate-based microcapsules.* Acta Biomater, 2009. **5**: p. 3433-3440.

134. Lee, B.B., et al., *Surface tension of viscous biopolymer solutions measured using the du Nouy ring method and the drop weight methods.* Polym Bull, 2012. **69**: p. 471-489.

135. Schweicher, J., C. Nyitray, and T.A. Desai, *Membranes to achieve immunoprotection of transplanted islets.* Front Biosci (Landmark Ed), 2014. **19**: p. 49-76.

136. Chick, W.L., et al., *A hybird artificial pancreas.* Trans Am Soc Artif Intern Organs, 1975. **21**: p. 8-15.

137. Sun, A.M., et al., *The use, in diabetic rats and monkeys, of artificial capillary units containing cultured islets of Langerhans (artificial endocrine pancreas).* Diabetes, 1977. **26**: p. 1136-1139.

138. Maki, T., et al., *Treatment of severe diabetes mellitus for more than one year using a vascularized hybrid artificial pancreas.* Transplantation, 1993. **55**(4): p. 713-717.

139. Galletti, P.M., et al., *Feasibility of small bore AV shunts for hybrid artificial organs in nonheparinized beagle dogs.* Trans Am Soc Artif Intern Organs, 1981. **27**: p. 185-187.

140. Pareta, R.A., A.C. Farney, and E.C. Opara, *Design of a bioartificial pancreas.* Pathobiology, 2013. **80**: p. 194-202.

141. Colton, C.K., *Implantable biohybrid artificial organs.* Cell Transplant, 1995. **4**: p. 415-436.

142. Lanza, R.P., S.J. Sullivan, and W.L. Chick, *Perspectives in diabetes. Islet transplantation with immunoisolation.* Diabetes, 1992. **41**: p. 1503-1510.

143. Kroon, E., et al., *Pancreatic endoderm derived from human embryonic stem cells generates glucose-responsive insulin-secreting cells in vivo.* Nat Biotechnol, 2008. **26**: p. 443-452.

144. Matveyenko, A.V., et al., *Inconsistent formation and nonfunction of insulin-positive cells from pancreatic endoderm derived from human embryonic stem cells in athymic nude rats.* Am J Physiol Endocrinol Metab, 2010. **299**: p. E713-720.

145. Scharp, D.W., N.S. Mason, and R.E. Sparks, *Islet immuno-isolation: the use of hybrid artificial organs to prevent islet tissue rejection.* Worl J Surg, 1984. **8**: p. 221-229.

146. de Groot, M., T.A. Schuurs, and R. van Schilfgaarde, *Causes of Limited Survival of Microencapsulated Pancreatic Islet Grafts.* J Surg Res, 2004. **121**: p. 141-150.

147. Sefton, M.V., *The good, the bad and the obvious: 1993 Clemson Award for Basic Research--Keynote Lecture.* Biomaterials, 1993. **14**(15): p. 1127-1134.

148. Kizilel, S., M. Garfinkel, and E.C. Opara, *The bioartificial pancreas: progress and challenges.* Diabet Technol Ther, 2005. **7**(6): p. 968-985.

149. Duvivier-Kali, V.F., et al., *Complete Protection of Islets Against Allorejection and Autoimmunity by a Simple Barium-Alginate Membrane.* Diabetes, 2001. **50**(8): p. 1698-1705.

150. Safley, S.A., et al., *Biocompatibility and immune acceptance of adult porcine islets transplanted intraperitoneally in diabetic NOD mice in calcium alginate poly-L-lysine microcapsules versus barium alginate microcapsules without poly-L-lysine.* J Diabetes Sci Technol, 2008. **2**(5): p. 760-767.

151. Lim, F. and A.M. Sun, *Microencapsulated islets as bioartificial endocrine pancreas.* Science, 1980. **210**(4472): p. 908-910.

152. Cui, H., et al., *Long-term metabolic control of autoimmune diabetes in spontaneously diabetic nonobese diabetic mice by nonvascularized microencapsulated adult porcine islets.* Transplantation, 2009. **88**(2): p. 160-9.

153. Duvivier-Kali, V.F., et al., *Survival of microencapsulated adult pig islets in mice in spite of an antibody response.* Am J Transplant, 2004. **4**(12): p. 1991-2000.

154. Orive, G., et al., *Challenges in cell encapsulation*, in *Applications of cell immobilisation technology*, R.W. Viktor Nedovic, Editor. 2005, Springer: The Netherlands. p. 185-196.

155. Rakieten, N., M.L. Rakieten, and M.V. Nadkarni, *Studies on the diabetogenic action of streptozotocin.* Cancer Chemother Rep, 1963. **29**: p. 91-98.

156. Lenzen, S., *The mechanisms of alloxan- and streptozotocin-induced diabetes.* Diabetologia, 2008. **51**(2): p. 216-226.

157. Sakata, N., et al., *Animal Models of Diabetes Mellitus for Islet Transplantation.* Exper Diab Res, 2012: p. 1-11.

158. Ventura-Sobrevilla, J., et al., *Effect of varying dose and administration of streptozotocin on blood sugar in male CD1 mice.* Proc West Pharmacol Soc, 2011. **54**: p. 5-9.

159. Makino, S., et al., *Breeding of a non-obese, diabetic strain of mice.* Jikken Dobutsu, 1980. **29**(1): p. 1-13.

160. Nakhooda, A.F., et al., *The spontaneously diabetic Wistar rat. Metabolic and morphologic studies.* Diabetes, 1977. **26**(2): p. 100-112.

161. Coronel, M.M. and C.L. Stabler, *Engineering a local microenvironment for pancreatic islet replacement.* Curr Opin Biotechnol, 2013. **24**(5): p. 900-908.

162. Weber, C.J., et al., *Evaluation of graft-host response for various tissue sources and animal models.* Ann N Y Acad Sci, 1999. **875**: p. 233-254.

163. Su, J., et al., *Anti-inflammatory peptide-functionalized hydrogels for insulin-secreting cell encapsulation.* Biomaterials, 2010. **31**: p. 308-314.

164. Simpson, N.E. and A. Sambanis, *Biomedical imaging of engineered tissues* in *Tissue engineering: principles and practices*, J.P. Fisher, et al., Editors. 2012, CRC Press: Boca Raton, FL.

165. Arifin, D.R. and J.W. Bulte, *Imaging of pancreatic islet cells.* Diabetes Metab Res Rev, 2011. **27**(8): p. 761-6.

166. de Almedia, P.E., J.R. van Rappard, and J.C. Wu, *In vivo bioluminescence for tracking cell fate and function.* Am J Physiol Heart Circ Physiol, 2011. **301**(3): p. H663-H671.

167. Lu, Y., et al., *Bioluminescent monitoring of islet graft survival after transplantation.* Mol Ther, 2004. **9**(3): p. 428-35.

168. Chen, X., et al., *In vivo bioluminescence imaging of transplanted islets and early detection of graft rejection.* Transplantation, 2006. **81**(10): p. 1421-1427.

169. Fowler, M., et al., *Assessment of pancreatic islet mass after islet transplantation using in vivo bioluminescence imaging.* Transplantation, 2005. **79**(7): p. 768-776.

170. Chen, X., et al., *Prolonging islet allograft survival using in vivo bioluminescence imaging to guide timing of antilymphocyte serum treatment of rejection.* Transplantation, 2008. **85**(9): p. 1246-52.

171. Cheng, D., C. Lo, and M.V. Sefton, *Effect of mouse VEGF164 on the viability of hydroxyethyl methacrylate-methyl methacrylate-microencapsulated cells in vivo: bioluminescence imaging.* J Biomed Mater Res A, 2008. **87**(2): p. 321-331.

172. Tarantal, A.F., C.C. Lee, and P. Itkin-Ansari, *Real-time bioluminescence imaging of macroencapsulated fibroblasts reveals allograft protection in rhesus monkeys (Macaca mulatta).* Transplantation, 2009. **88**(1): p. 38-41.

173. Surzyn, M., et al., *IL-10 secretion increases signal persistence of HEMA-MMA–microencapsulated luciferase-modified CHO fibroblasts in mice.* Tissue Eng Part A, 2009. **15**(1): p. 127-136.

174. Lee, S.H., et al., *Human beta-cell precursors mature into functional insulin-producing cells in an immunoisolation device: implications for diabetes cell therapies.* Transplantation, 2009. **87**(7): p. 983-91.

175. Corish, P. and C. Tyler-Smith, *Attenuation of green fluorescent protein half-life in mammalian cells.* Protein Eng, 1999. **12**(12): p. 1035-40.

176. Chen, J., et al., *In vivo tracking of superparamagnetic iron oxide nanoparticle labeled chondrocytes in large animal model.* Ann Biomed Eng, 2012. **40**(12): p. 2568-2578.

177. Ko, I.K., et al., *In vivo MR imaging of tissue-engineered human mesenchymal stem cells transplanted to mouse: a preliminary study.* Ann Biomed Eng, 2007. **35**(1): p. 101-108.

178. Aarntzen, E.H., et al., *In vivo tracking techniques for cellular regeneration, replacement, and redirection.* J Nucl Med, 2012. **53**(12): p. 1825-1828.

179. Goh, F., et al., *Dual perfluorocarbon method to noninvasively monitor dissolved oxygen concentration in tissue engineered constructs in vitro and in vivo.* Biotechnol Prog, 2011. **27**(4): p. 1115-1125.

180. Goh, F. and A. Sambanis, *In vivo noninvasive monitoring of dissolved oxygen concentration within an implanted tissue-engineered pancreatic construct.* Tissue Eng Part C Methods, 2011. **17**(9): p. 887-94.

181. Stabler, C.L., et al., *In vivo noninvasive monitoring of a tissue engineered construct using 1H NMR spectroscopy.* Cell Transplant, 2005. **14**(2-3): p. 139-149.

182. Barnett, B.P., et al., *Fluorocapsules for improved function, immunoprotection, and visualization of cellular therapeutics with MR, US, and CT imaging.* Radiology, 2011. **258**(1): p. 182-191.

183. Jamiolkowski, R.M., et al., *Islet transplantation in type I diabetes mellitus.* Yale J Biol Med, 2012. **85**(1): p. 37-43.

184. Sambanis, A., *Artificial organs: pancreas*, in *Comprehensive Biotechnology*, M. Moo-Young, Editor. 2011, Elsevier: Waltham, MA. p. 669-711.

185. Riu, E., et al., *Counteraction of type 1 diabetic alterations by engineering skeletal muscle to produce insulin: insights from transgenic mice.* Diabetes, 2002. **51**(3): p. 704-711.

186. Lei, P., et al., *Efficient production of bioactive insulin from human epidermal keratinocytes and tissue-engineered skin substitutes: implications for treatment of diabetes.* Tissue Eng, 2007. **13**(8): p. 2119-2131.

187. Tian, J., et al., *Regulated insulin delivery from human epidermal cells reverses hyperglycemia.* Mol Ther, 2008. **16**(6): p. 1146-1153.

188. Luef, G.J., et al., *Valproic acid modulates islet cell insulin secretion: a possible mechanism of weight gain in epilepsy patients.* Epilepsy Res, 2003. **55**(1-2): p. 53-58.

189. Shin, J.S., et al., *Novel Culture Technique Involving an Histone Deacetylase Inhibitor Reduces the Marginal Islet Mass to Correct Streptozotocin-Induced Diabetes.* Cell Transplant, 2011. **20**(9): p. 1321-1332.

190. Dompierre, J.P., et al., *Histone deacetylase 6 inhibition compensates for the transport deficit in huntington's disease by increasing tubulin acetylation.* J Neurosci, 2007. **27**(13): p. 3571-3583.

191. Durvasula, K., P.M. Thule, and A. Sambanis, *Combinatorial insulin secretion dynamics of recombinant hepatic and enteroendocrine cells.* Biotechnol Bioeng, 2012. **109**(4): p. 1074-82.

192. Goh, F., et al., *Limited beneficial effects of perfluorocarbon emulsions on encapsulated cells in culture: experimental and modeling studies.* J Biotechnol, 2010. **150**(2): p. 232-9.

193. Haggarty, S.J., et al., *Domain-selective small-molecule inhibitor of histone deacetylase 6 (HDAC6)-mediated tubulin deacetylation.* Proc Natl Acad Sci U S A, 2003. **100**(8): p. 4389-4394.

194. Ramshur, E.B., T.R. Rull, and B.M. Wice, *Novel insulin/GIP co-producing cell lines provide unexpected insights into Gut K-cell function in vivo.* J Cell Physiol, 2002. **192**(3): p. 339-350.

195. Rasouli, M., et al., *Engineering an L-cell line that expresses insulin under the control of the glucagon-like peptide-1 promoter for diabetes treatment.* BMC Biotechnol, 2011. **11**(99).

196. Grampp, G.E., H.F. Lodish, and G. Stephanopoulos, *Processing and secretion of insulin-related peptides in an insulinoma cell line.* Biotechnol Bioeng, 1997. **53**(3): p. 283-289.

197. Choudhary, C., et al., *Lysine acetylation targets protein complexes and co-regulates major cellular functions.* Science, 2009. **325**(5942): p. 834-840.

198. De Vos, P., A.F. Hamel, and K. Tatarkiewicz, *Considerations for successful transplantation of encapsulated pancreatic islets.* Diabetologia, 2002. **45**(2): p. 159-173.

199. Papas, K.K., et al., *Development of a bioartificial pancreas: II. Effects of oxygen on long-term entrapped betaTC3 cell cultures.* Biotechnol Bioeng, 1999. **66**(4): p. 231-7.

200. Gross, J.D., I. Constantinidis, and A. Sambanis, *Modeling of encapsulated cell systems.* J Theor Biol, 2007. **244**(3): p. 500-10.

201. Hoesli, C.A., et al., *Reversal of diabetes by betaTC3 cells encapsulated in alginate beads generated by emulsion and internal gelation.* J Biomed Mater Res B Appl Biomater, 2012. **100**(4): p. 1017-28.

202. Ngoc, P.K., et al., *Improving the efficacy of type 1 diabetes therapy by transplantation of immunoisolated insulin-producing cells.* Hum Cell, 2011. **24**(2): p. 86-95.

203. O'Shea, G.M., G.M. F., and A.M. Sun, *Prolonged survival of transplanted islets of Langerhans encapsulated in a biocompatible membrane.* Biochim Biophys Acta, 1984. **804**(1): p. 133-136.

204. Shao, S., et al., *Correction of hyperglycemia in type 1 diabetic models by transplantation of encapsulated insulin-producing cells derived from mouse embryo progenitor.* J Endocrinol, 2011. **208**(3): p. 245-55.

205. Landázuri, N., et al., *Alginate microencapsulation of human mesenchymal stem cells as a strategy to enhance paracrine-mediated vascular recovery after hindlimb ischaemia.* J Tissue Eng Regen Med., 2012.

206. Hernandez, L. and E. Briese, *Analysis of diabetic hyperphagia and polydipsia.* Physiol Behav, 1972. **9**(5): p. 741-746.

207. Mizuno, T.M., et al., *Fasting regulates hypothalamic neuropeptide Y, agouti-related peptide, and proopiomelanocortin in diabetic mice independent of changes in leptin or insulin.* Endocrinology, 1999. **140**(10): p. 4551-4557.

208. Thorsteinsson, B., *Kinetic models for insulin disappearance from plasma in man.* Dan Med Bull, 1990. **37**(2): p. 143-153.

209. Koschorreck, M. and E.D. Gilles, *Mathematical modeling and analysis of insulin clearance in vivo.* BMC Syst Biol, 2008. **2**(43).

210. Casesnoves, A., et al., *Influence of anti-insulin antibodies on insulin immunoassays in the autoimmune insulin syndrome.* Ann Clin Biochem, 1998. **35**(Pt 6): p. 768-774.

211. Ottesen, J.L., et al., *The potential immunogenicity of human insulin and insulin analogues evaluated in a transgenic mouse model.* Diabetologia, 1994. **37**(12): p. 1178-1185.

212. Pepper, A.R., et al., *Diabetic rats and mice are resistant to porcine and human insulin: flawed experimental models for testing islet xenografts.* Xenotransplantation, 2009. **16**(6): p. 502-510.

213. Schneider, S., et al., *Long-term graft function of adult rat and human islets encapsulated in novel alginate-based microcapsules after transplantation in immunocompetent diabetic mice.* Diabetes, 2005. **54**(3): p. 687-693.

214. Skiles, M.L., S. Shai, and J.O. Blanchette, *Tracking hypoxic signaling within encapsulated cell aggregates.* J Vis Exp, 2011. **16**(58).

215. Skiles, M.L., et al., *Correlating hypoxia with insulin secretion using a fluorescent hypoxia detection system.* J Biomed Mater Res B Appl Biomater, 2011. **97**(1): p. 148-155.

216. Parker, H.E., et al., *Predominant role of active versus facilitative glucose transport for glucagon-like peptide-1 secretion.* Diabetologia, 2012. **55**(9): p. 2445-2455.

217. Cantley, J., et al., *The hypoxia response pathway and β-cell function.* Diabetes Obes Metab, 2010. **12**(Suppl. 2): p. 159-167.

218. Johnstone, R.W., *Histone-deacetylase inhibitors: novel drugs for the treatment of cancer.* Nat Rev Drug Discov, 2002. **1**(4): p. 287-299.

219. Damholt, A.B., et al., *Proglucagon processing profile in canine L cells expressing endogenous prohormone convertase 1/3 and prohormone convertase 2.* Endocrinology, 1999. **140**(10): p. 4800-8.

220. Yongye, A.B., et al., *Identification of a small molecule that selectively inhibits mouse PC2 over mouse PC1/3: a computational and experimental study.* PLoS One, 2013. **8**(2): p. e56957.

221. Savino, T.M., et al., *Nucleolar assembly of the rRNA processing machinery in living cells.* J Cell Biol, 2001. **153**(5): p. 1097-1110.

222. Hock, R.A., A.D. Miller, and W.R. Osborne, *Expression of human adenosine deaminase from various strong promoters after gene transfer into human hematopoietic cell lines.* Blood, 1989. **74**(2): p. 876-881.

223. Nikoulina, S.E., et al., *A Primary Colonic Crypt Model Enriched in Enteroendocrine Cells Facilitates a Peptidomic Survey of Regulated Hormone Secretion.* Mol Cell Proteomics, 2010. **9**(4): p. 728-741.

224. Dame, M.K., et al., *Human colonic crypts in culture: segregation of immunochemical markers in normal versus adenoma-derived.* Lab Invest, 2014. **94**(2): p. 222-34.

225. Matsumoto, E., et al., *Time of Day and Nutrients in Feeding Govern Daily Expression Rhythms of the Gene for Sterol Regulatory Element-binding Protein (SREBP)-1 in the Mouse Liver.* J Biol Chem, 2010. **285**(43): p. 33028-36.

226. Thule´, P.M., et al., *Hepatic insulin gene therapy prevents deterioration of vascular function and improves adipocytokine profile in STZ-diabetic rats.* Am J Physiol Endocrinol Metab, 2006. **290**(1): p. E114-E122.

227. Mansha, M., et al., *Problems encountered in bicistronic IRES-GFP expression vectors employed in functional analyses of GC-induced genes.* Mol Biol Rep, 2012. **39**(12): p. 10227-10234.

228. Rondas, D., et al., *Novel mechanistic link between focal adhesion remodeling and glucose-stimulated insulin secretion.* J Biol Chem, 2012. **287**(4): p. 2423-2436.

229. Kiernan, R., et al., *Post-activation turn-off of NF-kappa B-dependent transcription is regulated by acetylation of p65.* J Biol Chem, 2003. **278**(4): p. 2758-2766.

230. Heimberg, H., et al., *Inhibition of cytokine-induced NF-kappaB activation by adenovirus-mediated expression of a NF-kappaB super-repressor prevents beta-cell apoptosis.* Diabetes, 2001. **50**(10): p. 2219-2224.

231. Larsen, L., et al., *Inhibition of histone deacetylases prevents cytokine-induced toxicity in beta cells.* Diabetologia, 2007. **50**(4): p. 779-789.

232. Lundh, M., et al., *Lysine deacetylases are produced in pancreatic beta cells and are differentially regulated by proinflammatory cytokines.* Diabetologia, 2010. **53**(12): p. 2569-2578.

233. Skov, S., et al., *Histone deacetylase inhibitors: a new class of immunosuppressors targeting a novel signal pathway essential for CD154 expression.* Blood, 2003. **101**: p. 1430-1438.

234. Takigawa-Imamura, H., et al., *Stimulation of glucose uptake in muscle cells by prolonged treatment with scriptide, a histone deacetylase inhibitor.* Biosci Biotechnol Biochem, 2003. **67**(7): p. 1499-1506.

235. Kaiser, C. and S.R. James, *Acetylation of insulin receptor substrate-1 is permissive for tyrosine phosphorylation.* BMC Biol, 2004. **2**(23).

236. Christensen, D.P., et al., *Histone deacetylase (HDAC) inhibition as a novel treatment for diabetes mellitus.* Mol Med, 2011. **17**(5-6): p. 378-390.

237. Richon, V.M., et al., *A class of hybrid polar inducers of transformed cell differentiation inhibits histone deacetylases.* Proc Natl Acad Sci U S A, 1998. **95**(6): p. 3003-3007.

238. Del Prete, M.J., et al., *Degradation of cellular mRNA is a general early apoptosis-induced event.* FASEB J, 2003. **16**(14): p. 2003-2005.

239. Luczak, M.W. and P.P. Jagodzinski, *Trichostatin A down-regulates CYP19 transcript and protein levels in MCF-7 breast cancer cells.* Biomed Pharmacother, 2009. **63**(4): p. 262-266.

240. Xu, W.S., R.B. Parmigiani, and P.A. Marks, *Histone deacetylase inhibitors: molecular mechanisms of action.* Oncogene, 2007. **26**(37): p. 5541-5552.

241. Kim, S.J., C. Nian, and C.H. McIntosh, *Glucose-dependent insulinotropic polypeptide and glucagon-like peptide-1 modulate beta-cell chromatin structure.* J Biol Chem, 2009. **284**(19): p. 12896-12904.